
Image: Carl Knox, OzGrav-Swinburne University of Technology

Gravitational waves

Soichiro Morisaki
ICRR/University of Tokyo

Mar. 26, 2024.

“SYNERGIES AT NEW FRONTIERS”, Kashiwa, Japan.

Gravitational-wave observatories

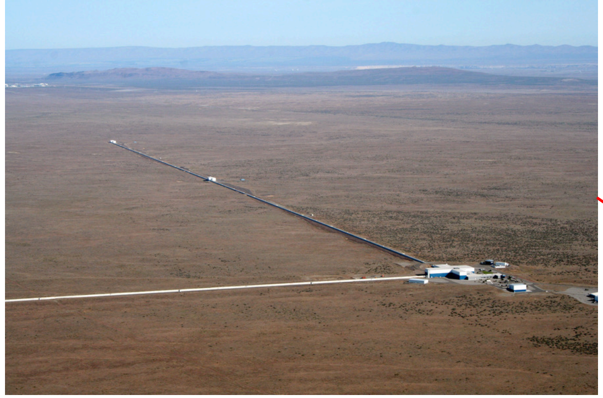

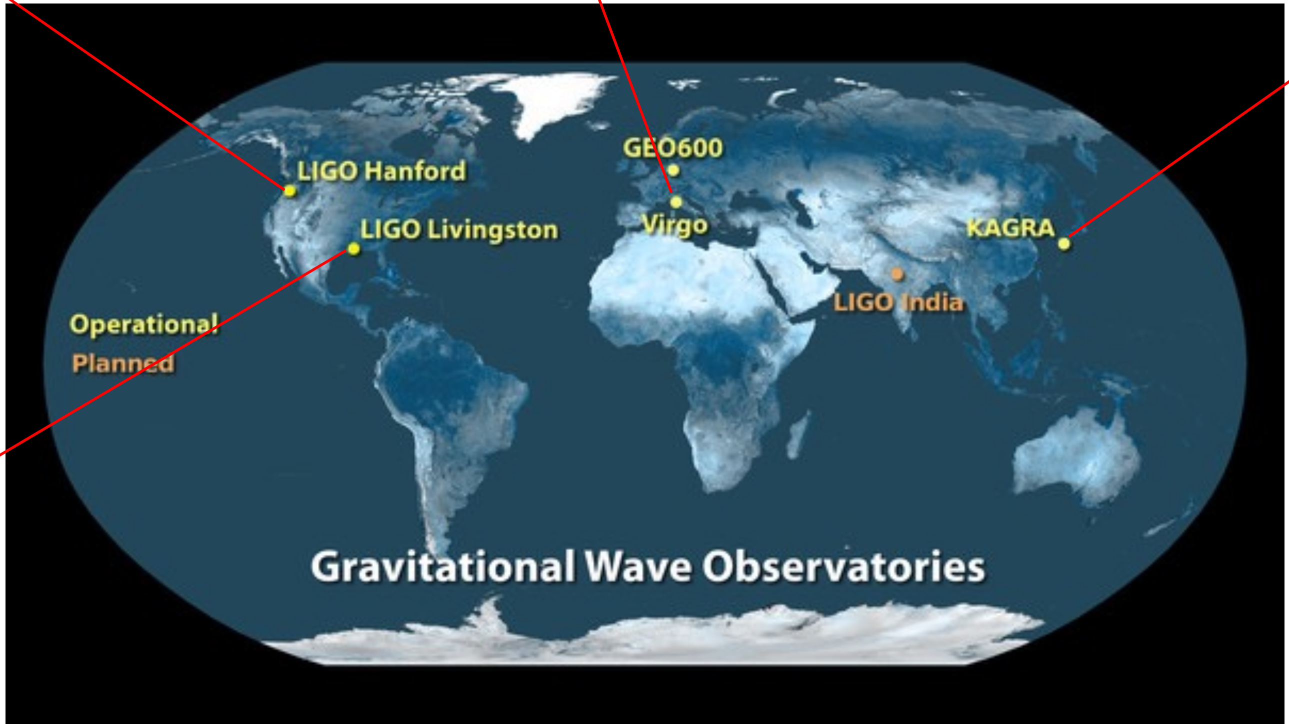

LIGO-Virgo-KAGRA (LVK) collaboration

Figure credit:
Caltech/MIT/LIGO Lab/ICRR

Observing timeline

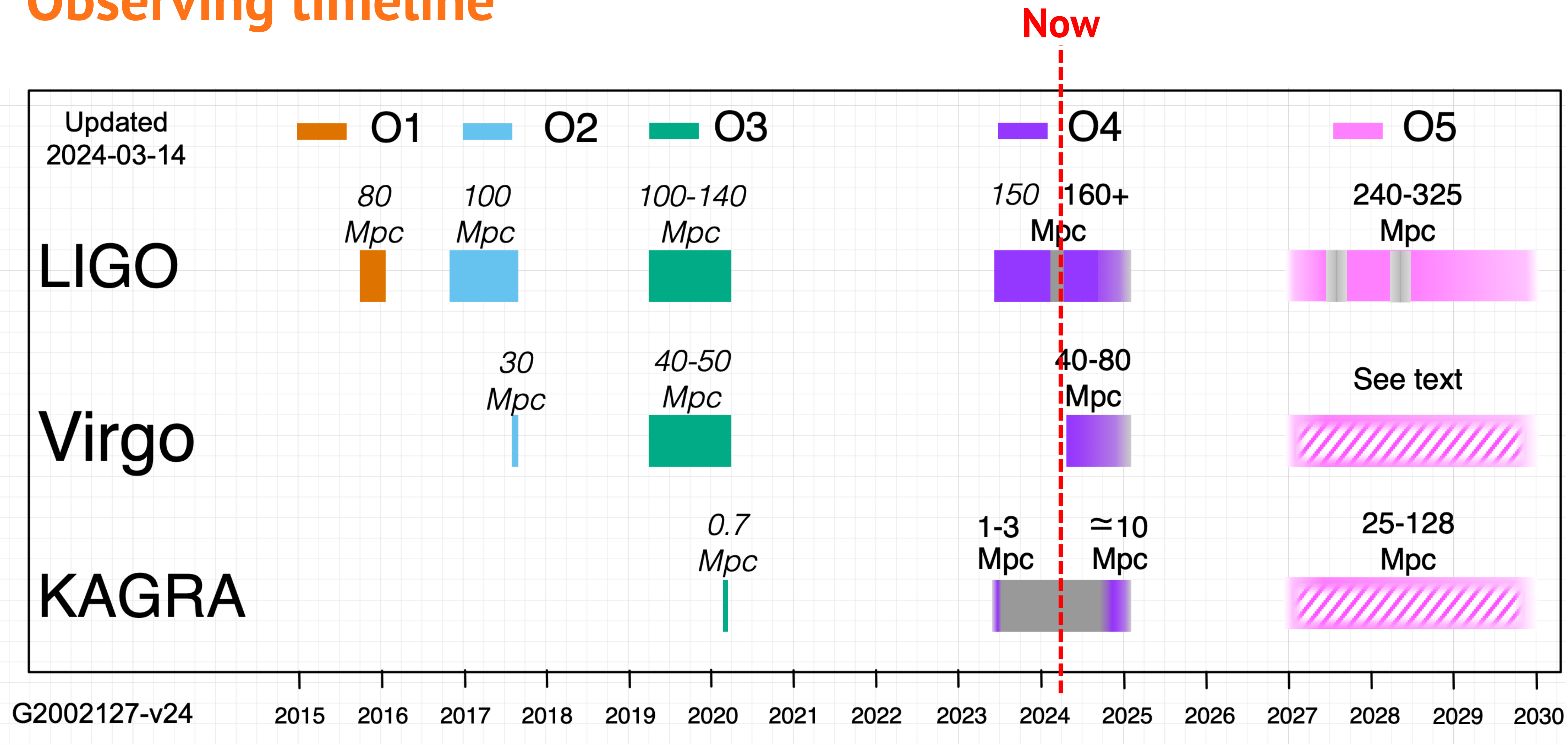

Figure: Observing plan (https://observing.docs.ligo.org/plan/)

Compact binary coalescence (CBC)

Credit: Vijay Varma et al., Binary Black Hole Explorer

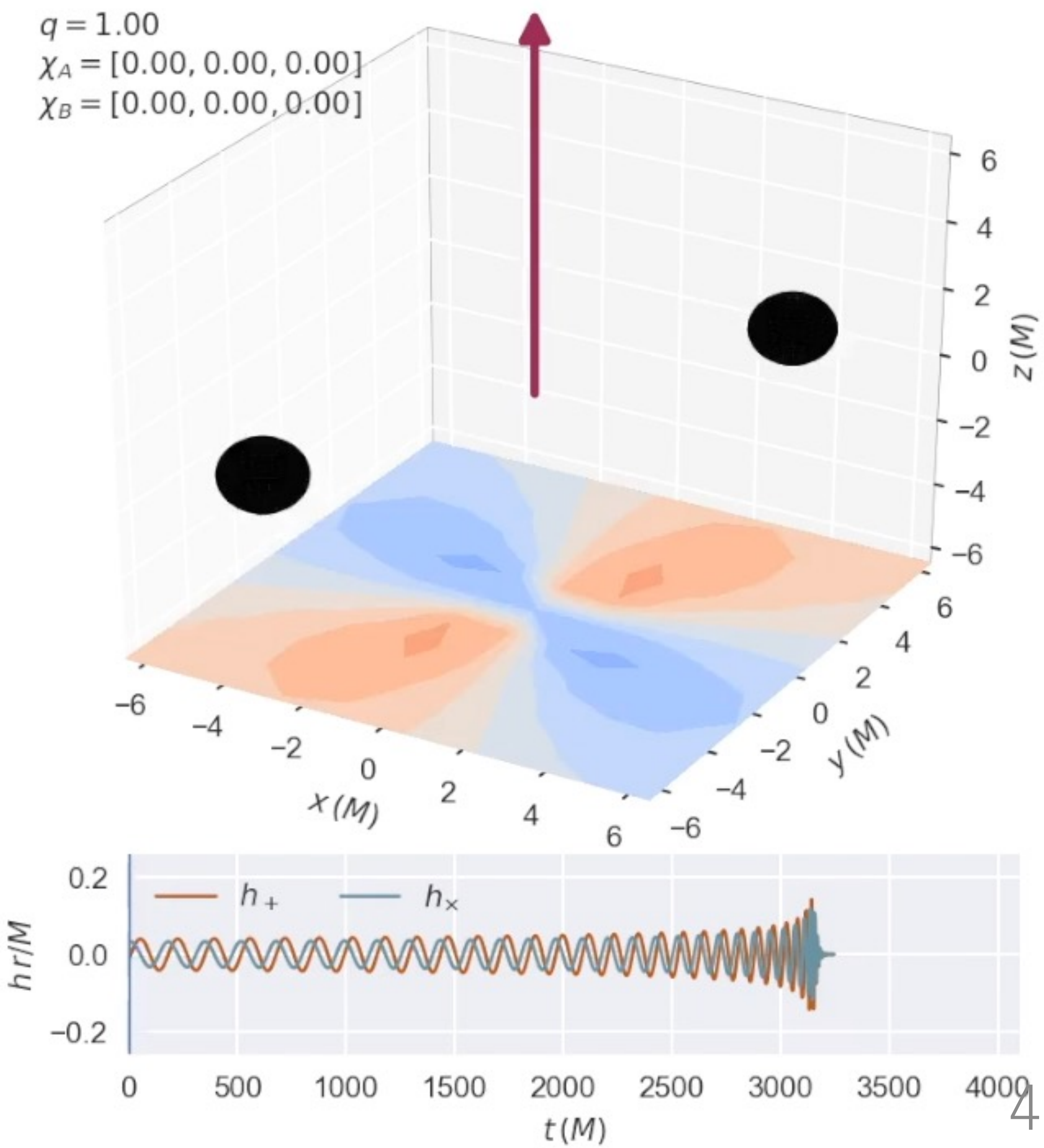

- A pair of merging black holes (BHs) or neutron stars (NSs).
- Increasing frequency ("Chirp signal").
- Characterized by masses, spins, and tidal deformation of colliding objects.

Credit: Abbott+, PRL **116**, no.6, 061102 (2016).

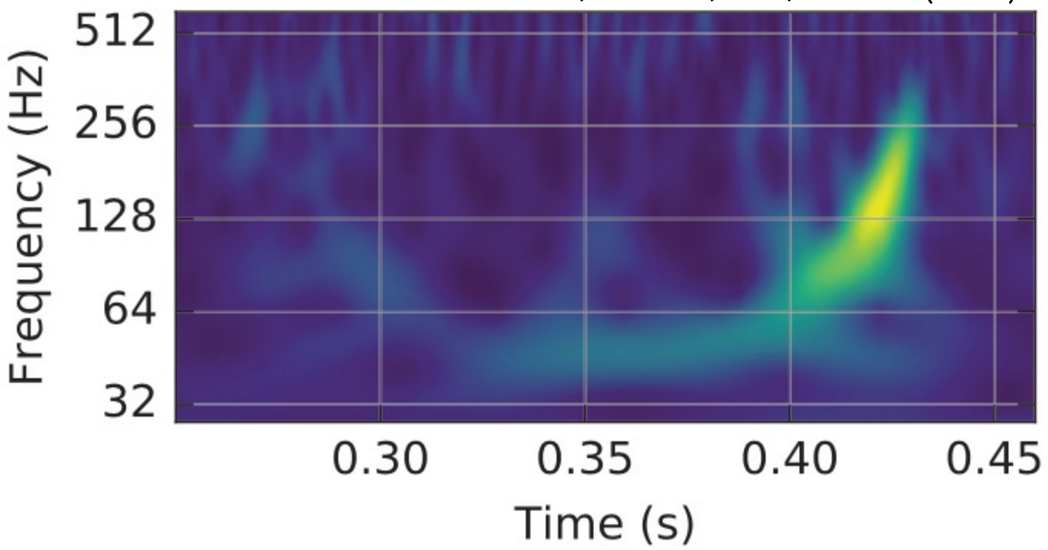

Gravitational-Wave Transient Catalog

Detections from 2015-2020 of compact binaries with black holes & neutron stars

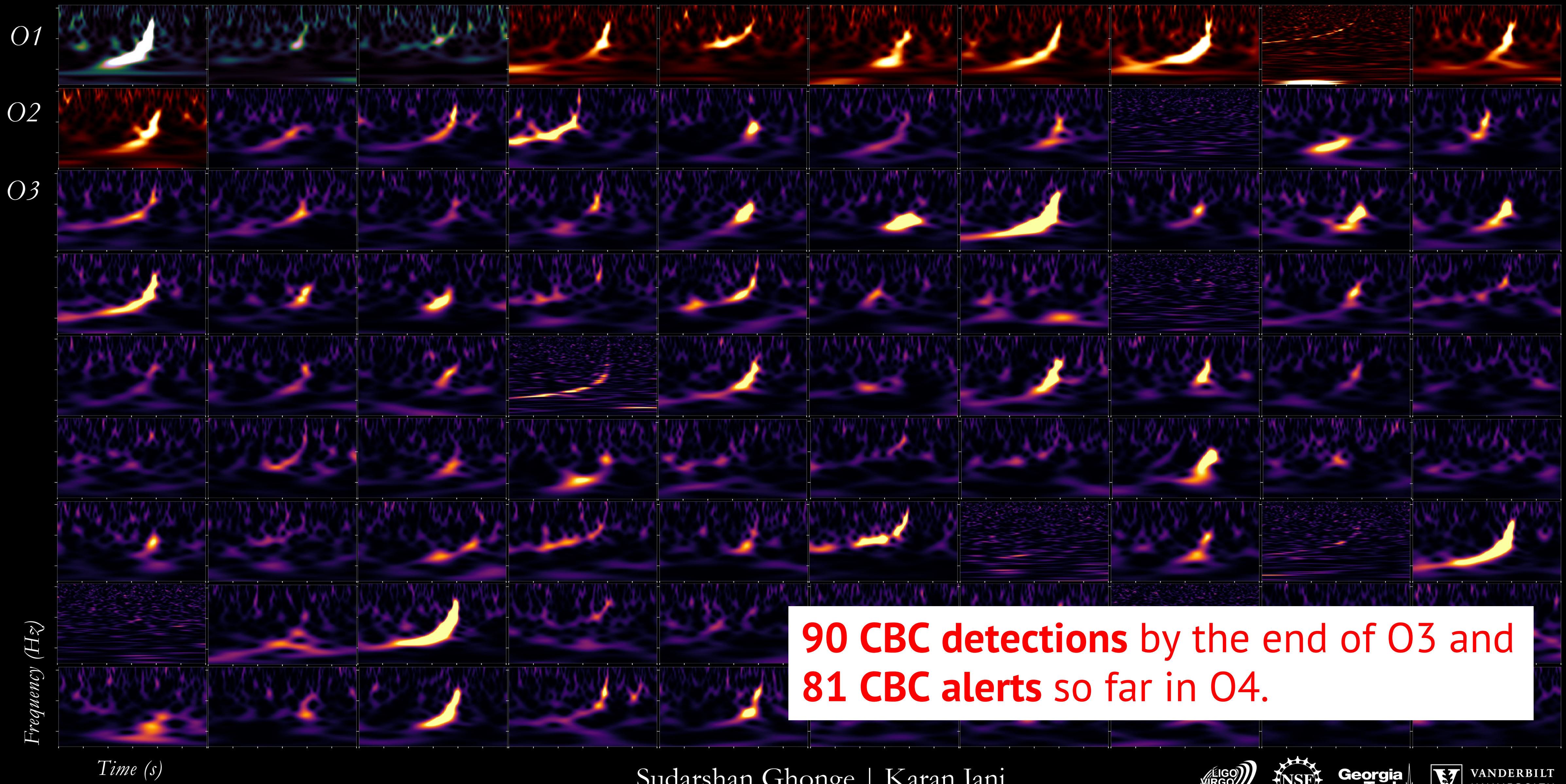

90 CBC detections by the end of O3 and **81 CBC alerts** so far in O4.

Sudarshan Ghonge | Karan Jani

Figure credit: Abbott+, PRL **125**, no.10, 101102 (2020).

Binary black holes (BBHs)

Most ($> 90\%$) of the CBCs were consistent with BBHs.

<u>Exceptional events</u>

- **GW190412:** Unequal masses ($30.1^{+4.6}_{-5.3}M_{\odot}$, $8.3^{+1.6}_{-0.9}M_{\odot}$), a higher-order GW moment detected.
- **GW190814:** Unequal masses $\left(\frac{m_2}{m_1} = 0.112^{+0.008}_{-0.009}\right)$, the secondary can be a NS ($m_2 = 2.59^{+0.08}_{-0.09}M_{\odot}$).
- **GW190521:** Heavy BHs $\left(85^{+21}_{-14}M_{\odot}, 66^{+17}_{-18}M_{\odot}\right)$ merging into an IMBH $\left(M_f = 142^{+28}_{-16}M_{\odot}\right)$.

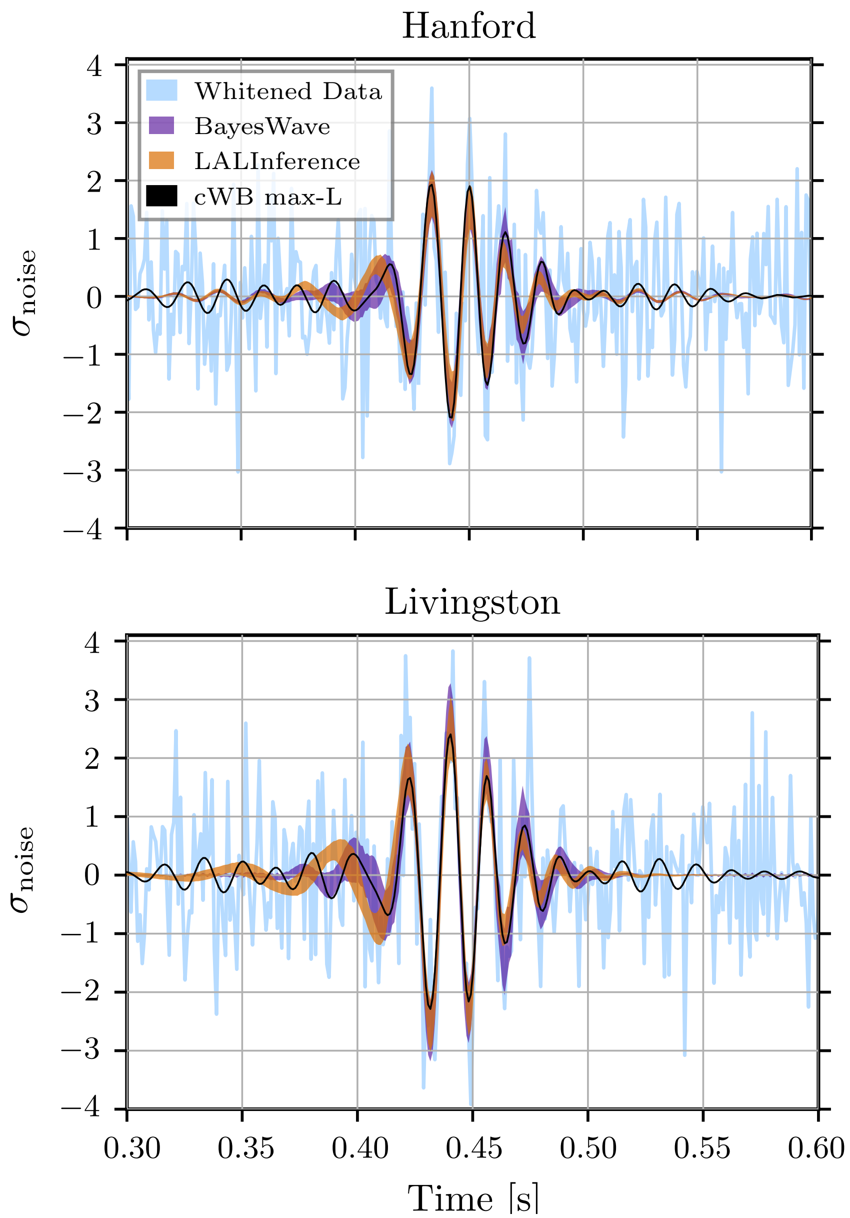

Figure: GW190521

Population properties of BBHs

Masses

- Local maxima at $\sim 10 M_\odot$ and $\sim 35 M_\odot$ ($> 99\%$ credibility).
- Inconclusive evidence for pair-instability mass gap ($65 - 120 M_\odot$).

Spins

- Spins generally small ($\chi \lesssim 0.4$), but nonvanishing.
- Tilt angle has broad distribution

Redshift

- Merger rate increases with redshift (at 99.6%).

Figure credit: Abbott+, PRX **13**, 011048 (2023).

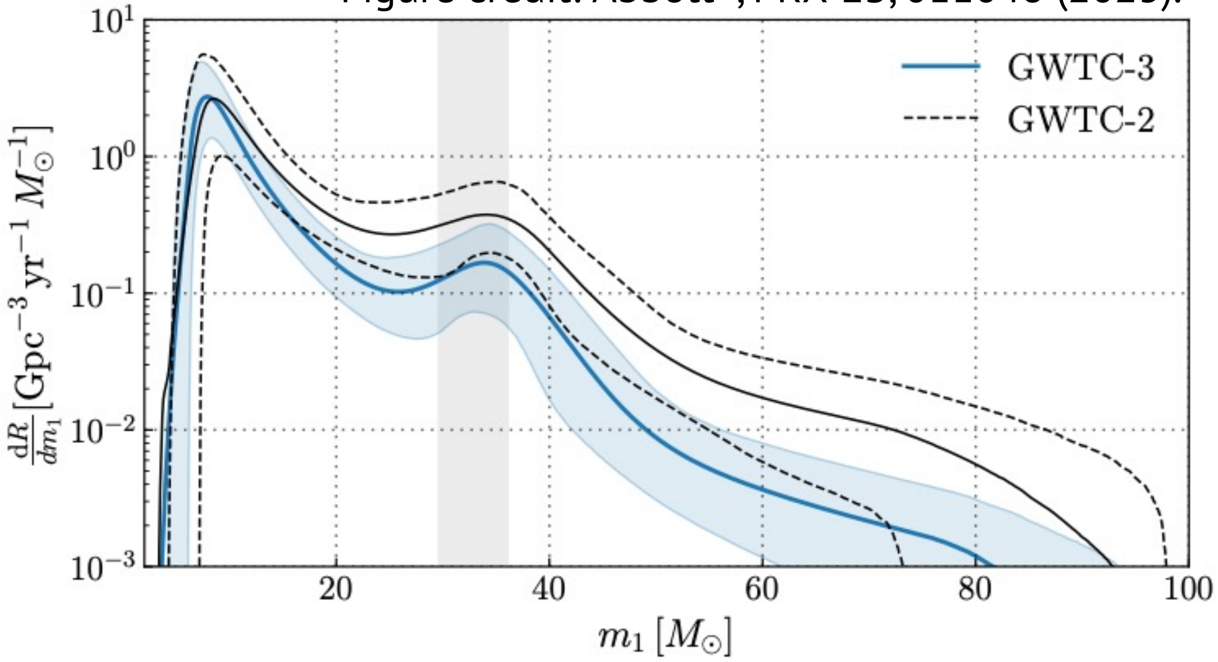

Figure: Recovered BBH mass distribution

Tests of general relativity (GR)

Figure credit:
Abbott+, PRL **116**, no. 22, 221101 (2016),
Abbott+, PRL **116**, no.6, 061102 (2016).

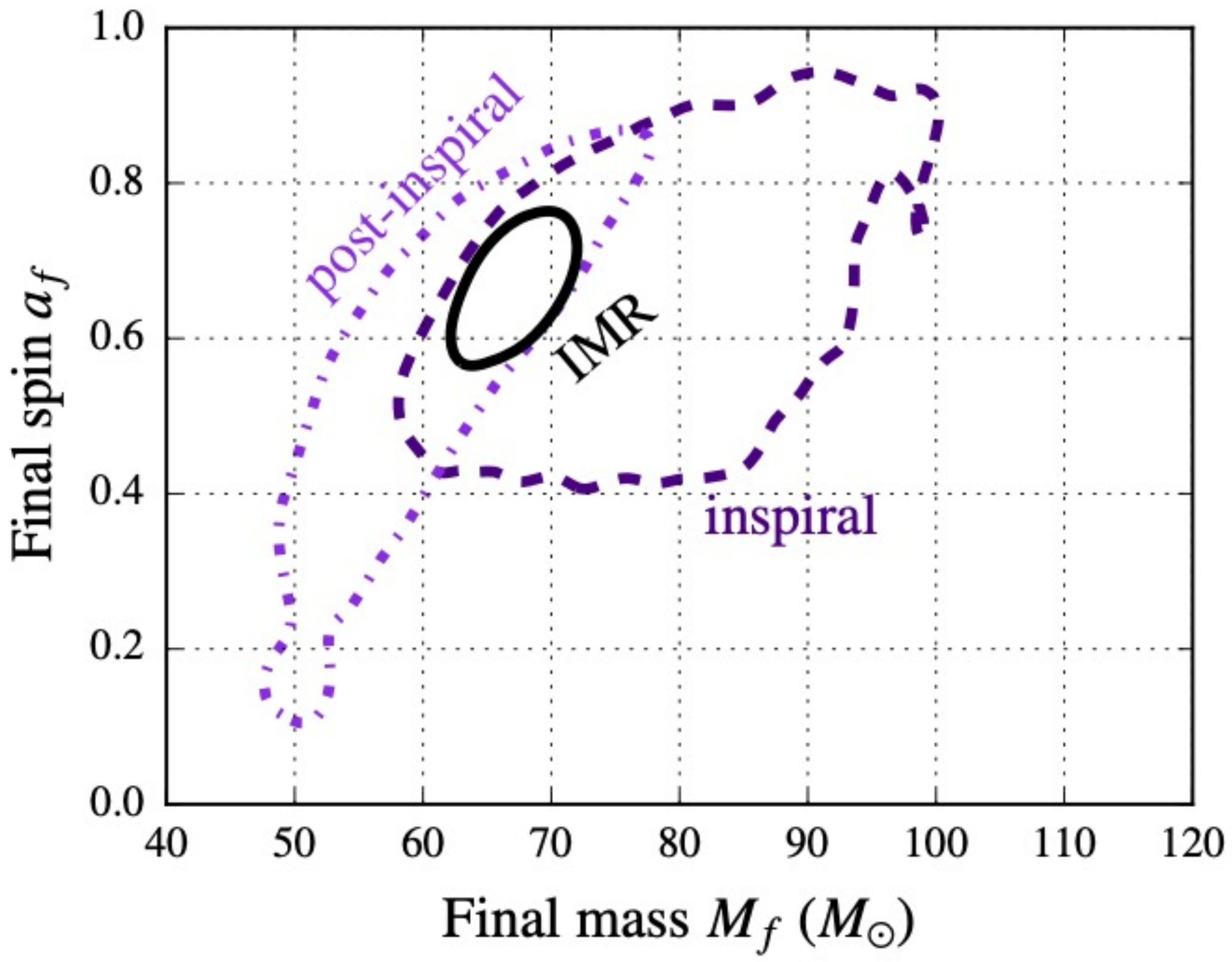

Figure: Consistency between inspiral and ringdown from GW150914

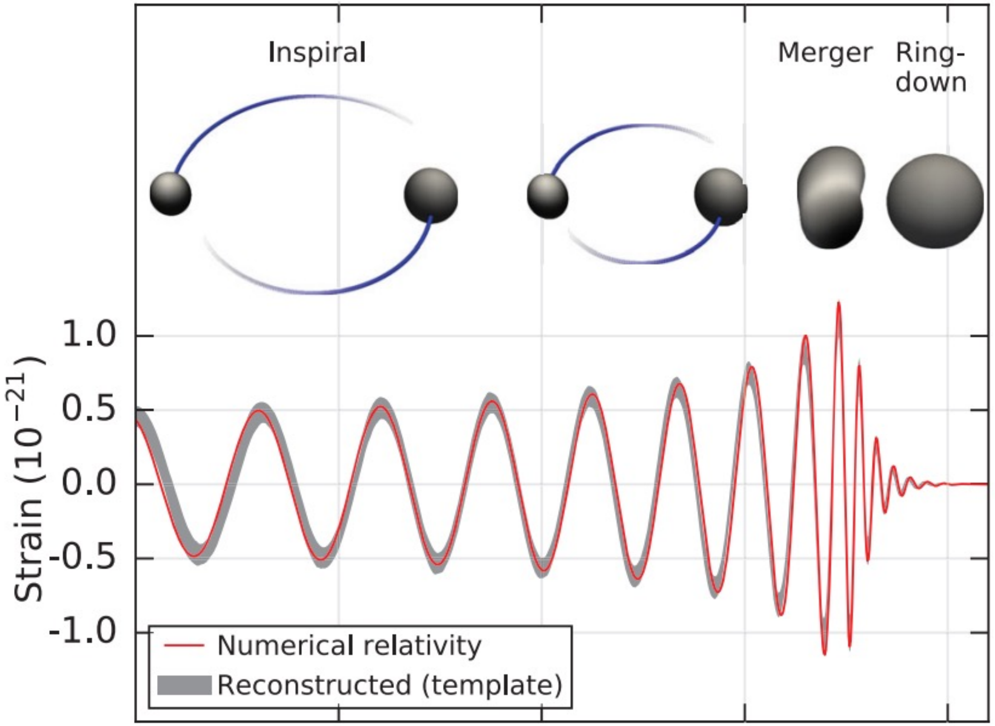

Various tests of GR have been performed and passed so far.

GW170817: multi-messenger observation

Figure credit:
Abbott+, ApJL **848**, no.2, L12 (2017).

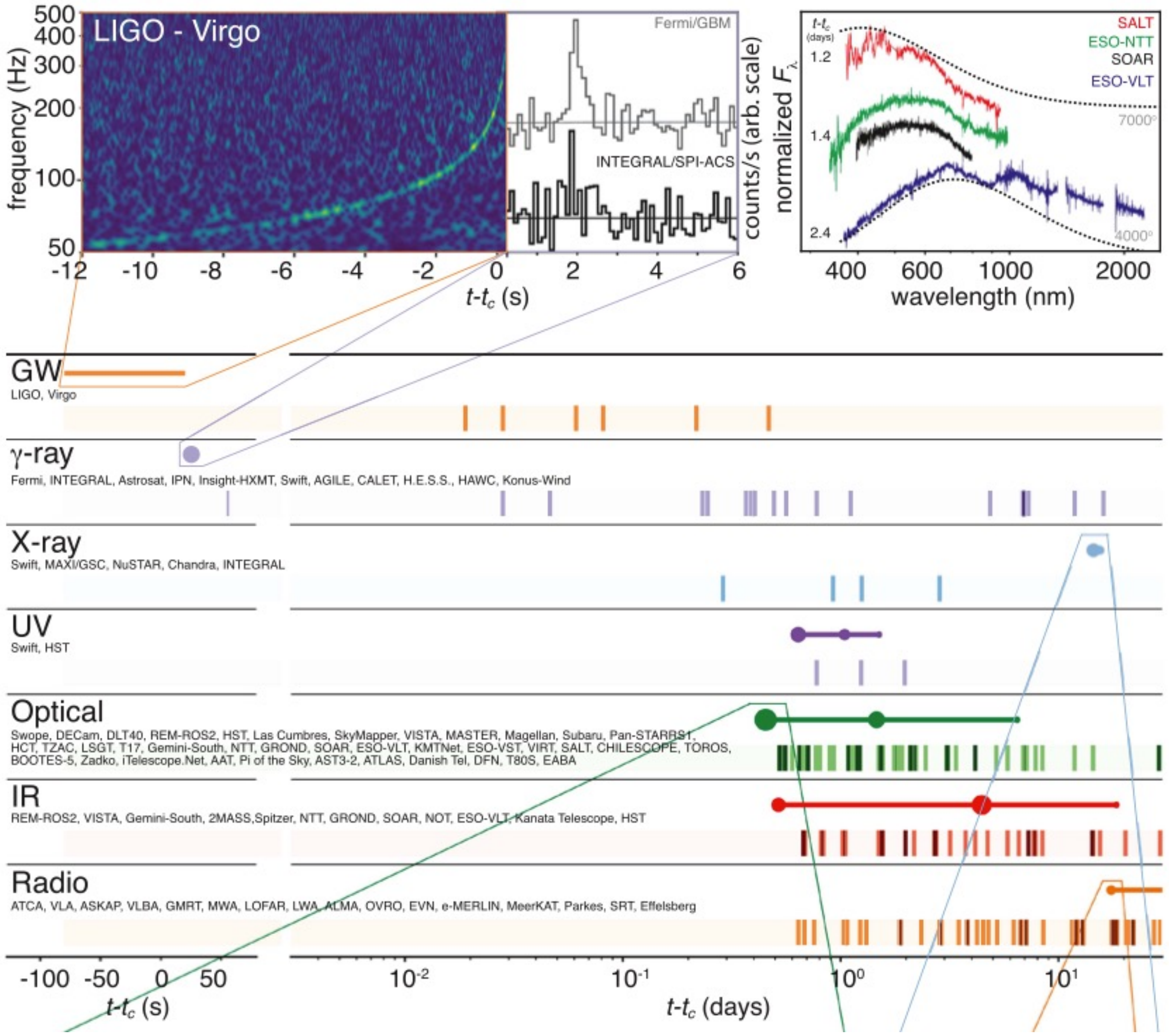

Figure: Multi-messenger observations of GW170817

The first detection of
binary neutron star (BNS) with GWs

GRB observed 1.7s after the merger

- Jet formation by the merger
- $|v_{GW} - v_{EM}|/v_{EM} \leq O(10^{-15})$

Observed optical/IR emissions were consistent with kilonova.
→ Origin of r-processss elements

Independent measurement of Hubble constant: $H_0 = 70.0^{+12.0}_{-8.0}\ \mathrm{km\ s^{-1}\ Mpc^{-1}}$.

GW170817: constraints on properties of dense matter

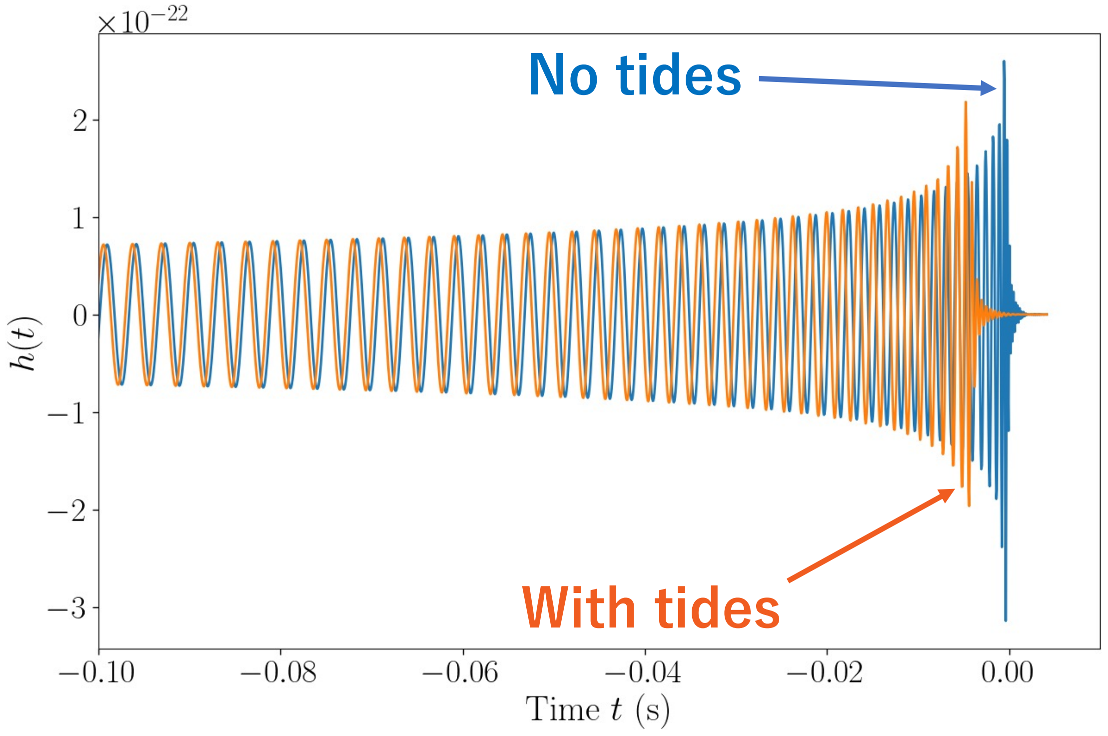

Figure credit: Abbott+, PRL **119**, no.16, 161101 (2017).

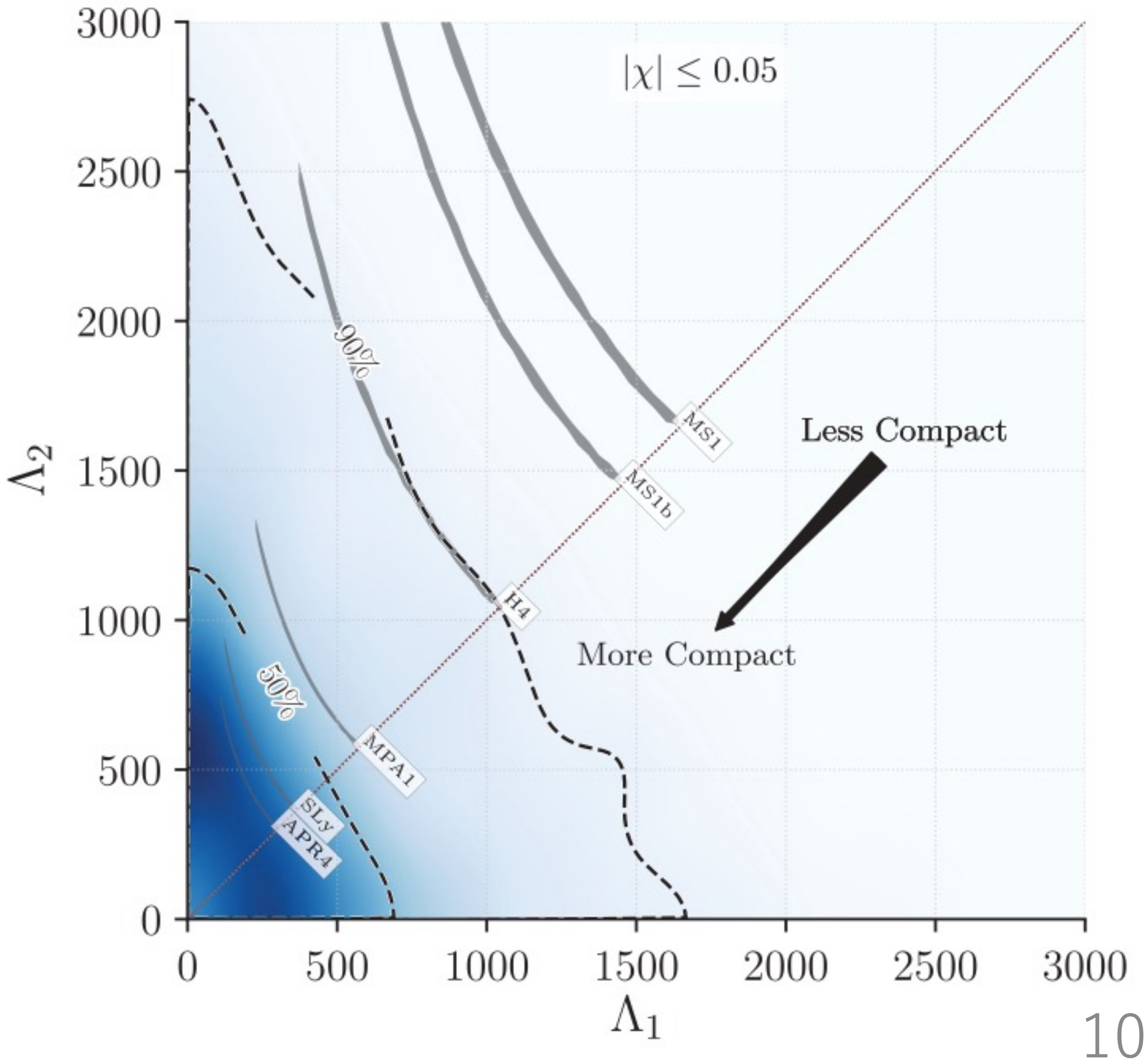

- Obtained upper bounds on tidal deformability parameters, Λ_1 and Λ_2.

- Excluded stiff equations of state (MS1, MS1b, …), which result in large radii.

GW190425: Heavy BNS

- Heavier than galactic BNSs:

$$m_1 = (1.61\text{—}2.52)\ M_\odot,$$
$$m_2 = (1.12\text{—}1.68)\ M_\odot.$$

- LIGO-Hanford was not observing.
  → Large localization uncertainties
  (~ 16% of the whole sky)

- The source is also distant, (90— 230) Mpc.

- No EM or neutrino counterparts.

Figure credit: Abbott+, ApJL **892**, no.1, L3 (2020).

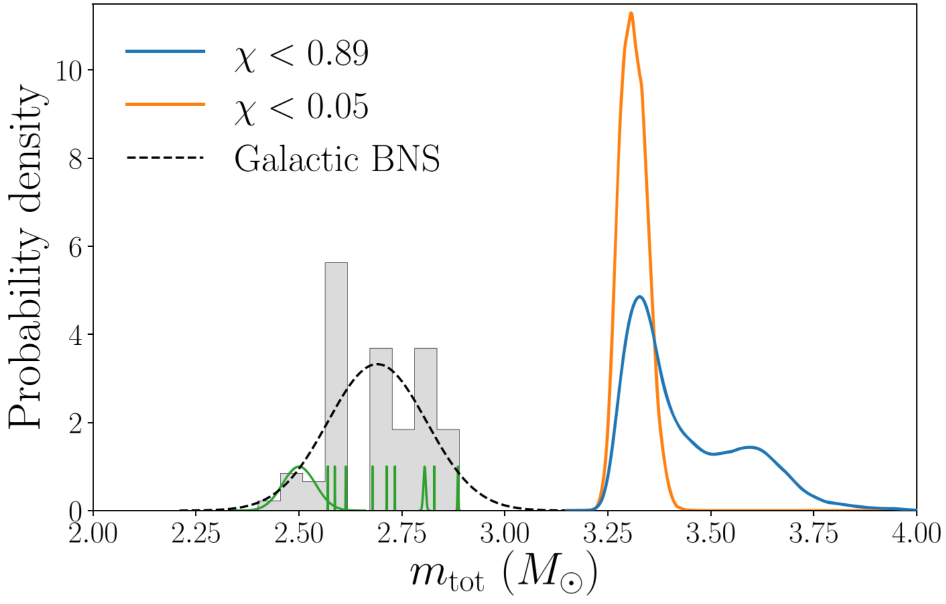

Figure: Total masses of GW190425 (orange, blue) and galactic merging binary neutron stars (gray)

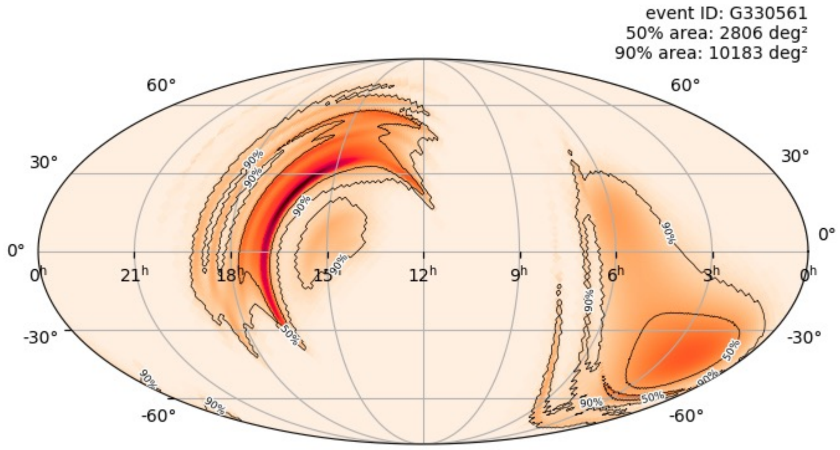

Figure: 2D Localization of GW190425

NSBH event candidates

Reference: Abbott+, ApJL **915**, no.1, L5 (2021).

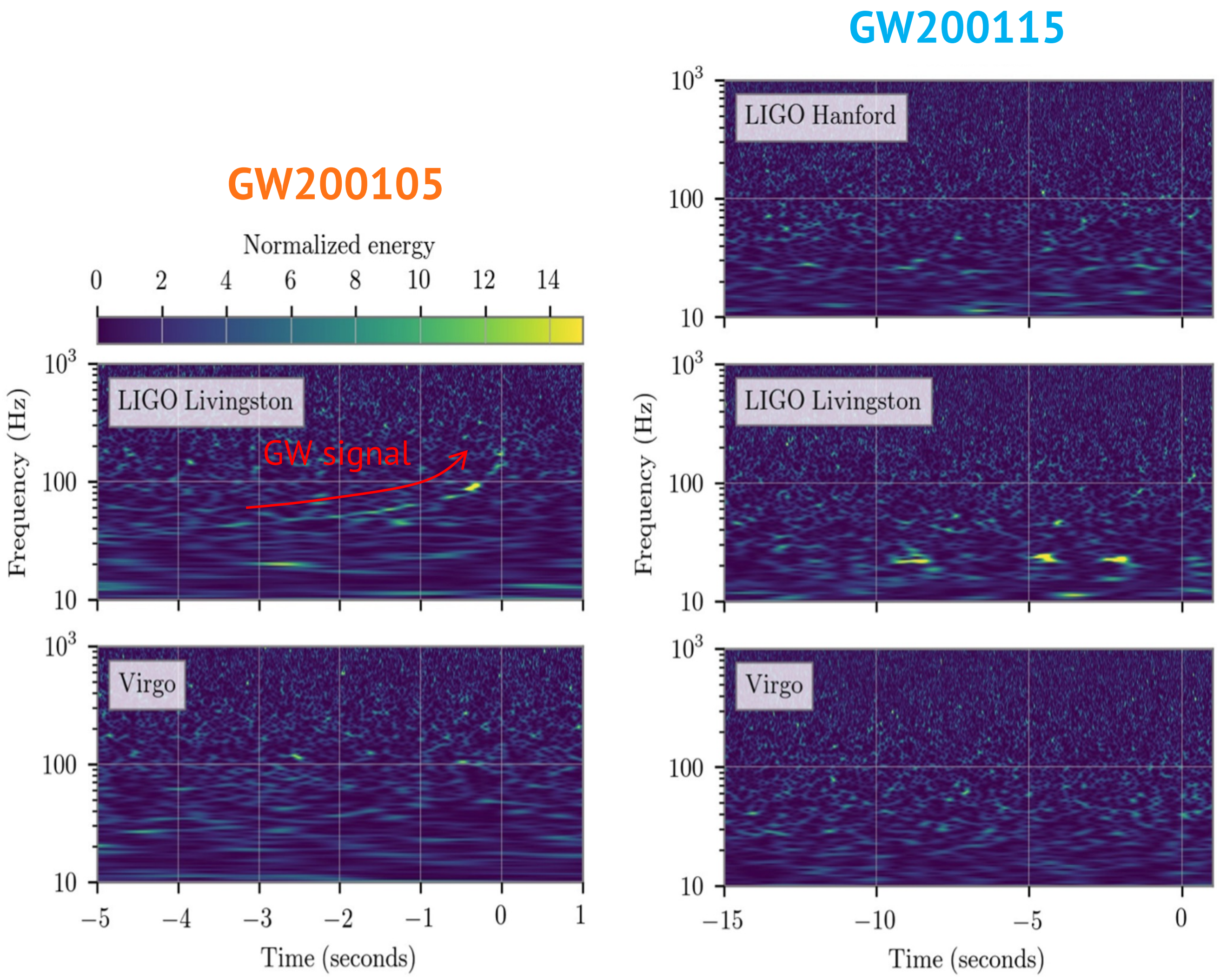

Time-frequency maps of data containing GW200105 (left) and GW200115 (right)

	m_1	m_2
GW200105	$8.9^{+1.2}_{-1.5} M_\odot$	$1.9^{+0.3}_{-0.2} M_\odot$
GW200115	$5.7^{+1.8}_{-2.1} M_\odot$	$1.5^{+0.7}_{-0.3} M_\odot$

- Masses consistent with neutron star-black hole (NSBH)
- No direct evidence of secondary objects being neutron stars (No EM counterparts, no tidal information)

Observing timeline

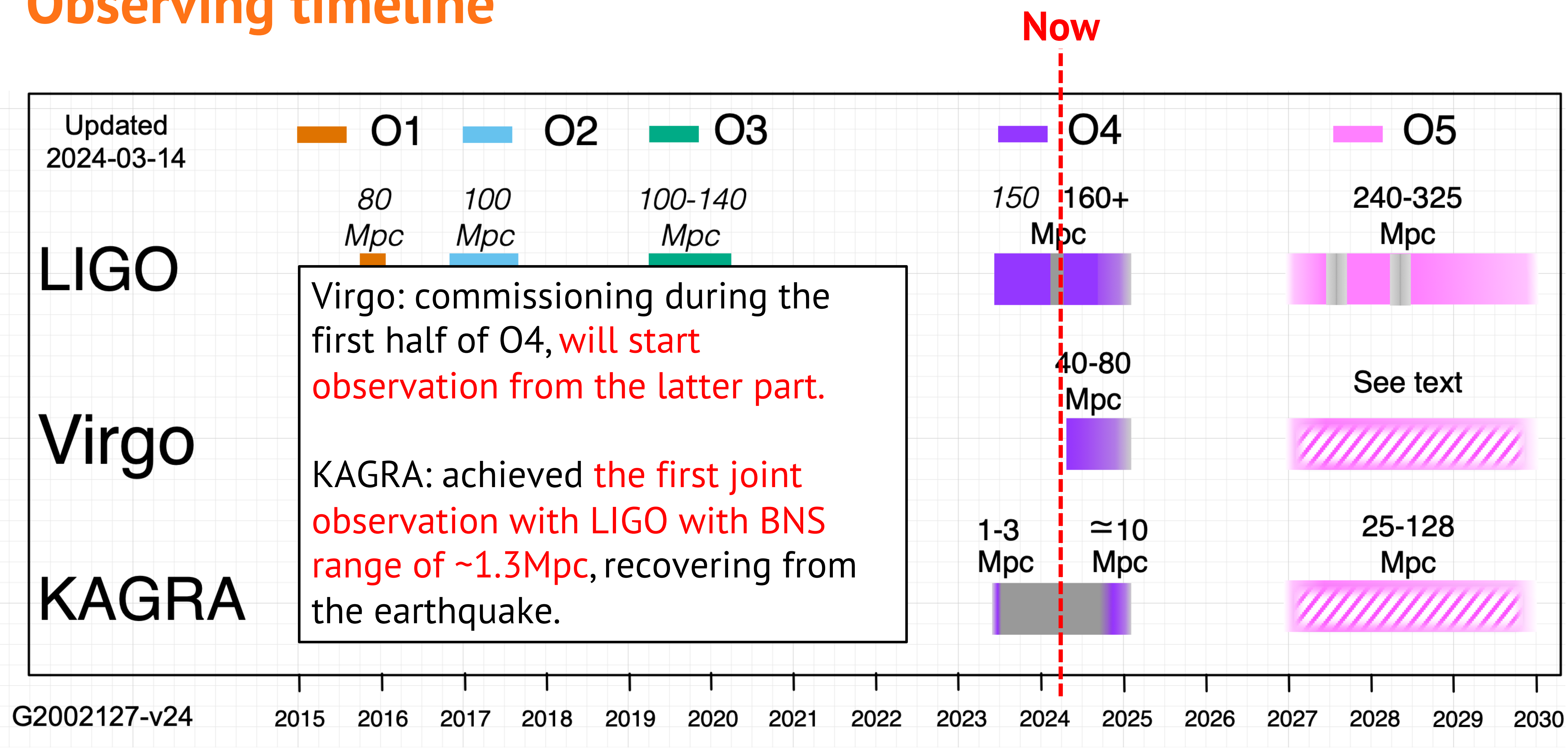

Virgo: commissioning during the first half of O4, will start observation from the latter part.

KAGRA: achieved the first joint observation with LIGO with BNS range of ~1.3Mpc, recovering from the earthquake.

Figure: Observing plan (https://observing.docs.ligo.org/plan/)

LIGO sensitivity in O4

https://online.igwn.org

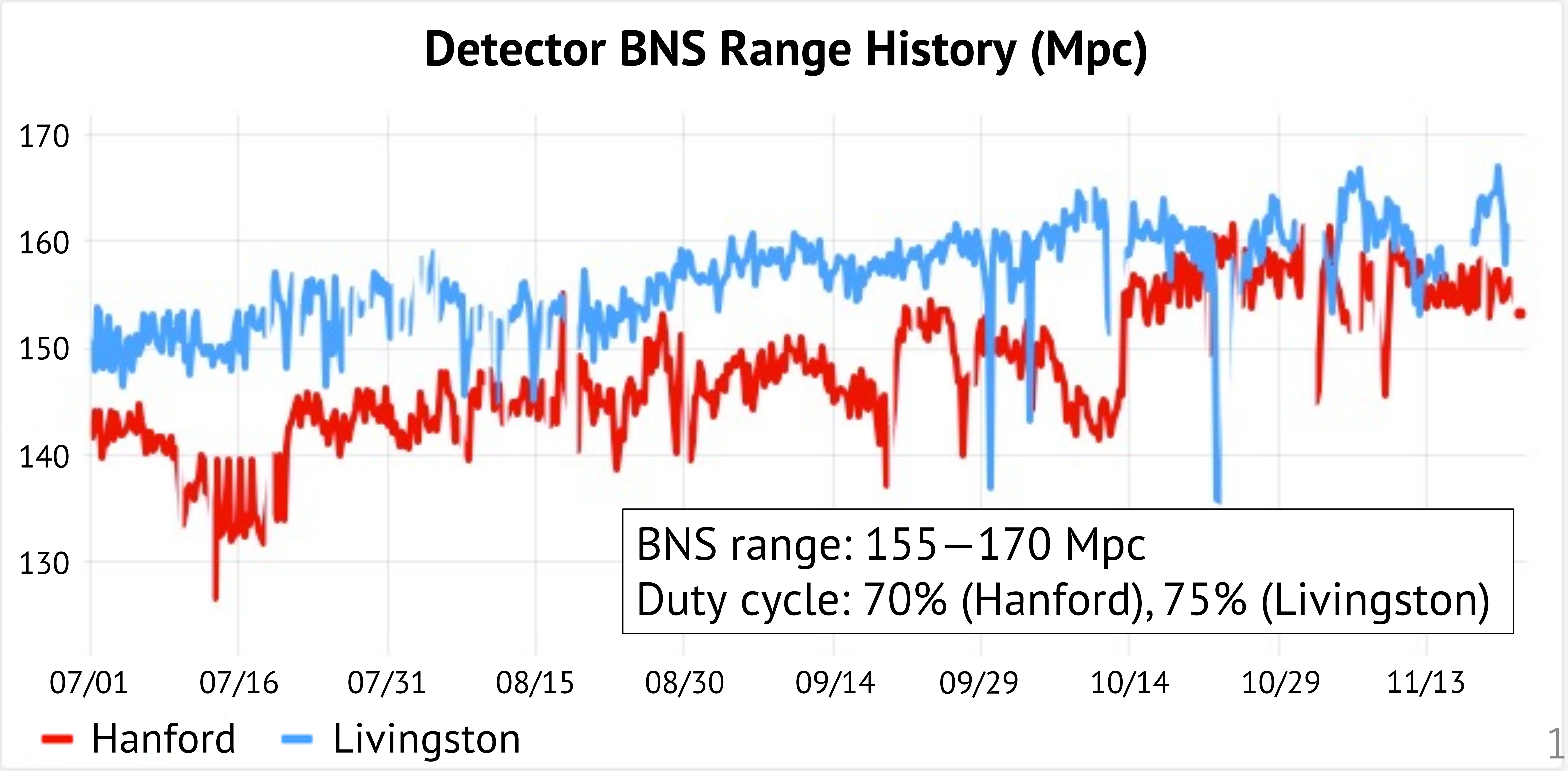

O4 alert timescale

Credit: LIGO/Virgo/KAGRA Public Alerts User Guide (https://emfollow.docs.ligo.org/userguide/index.html)

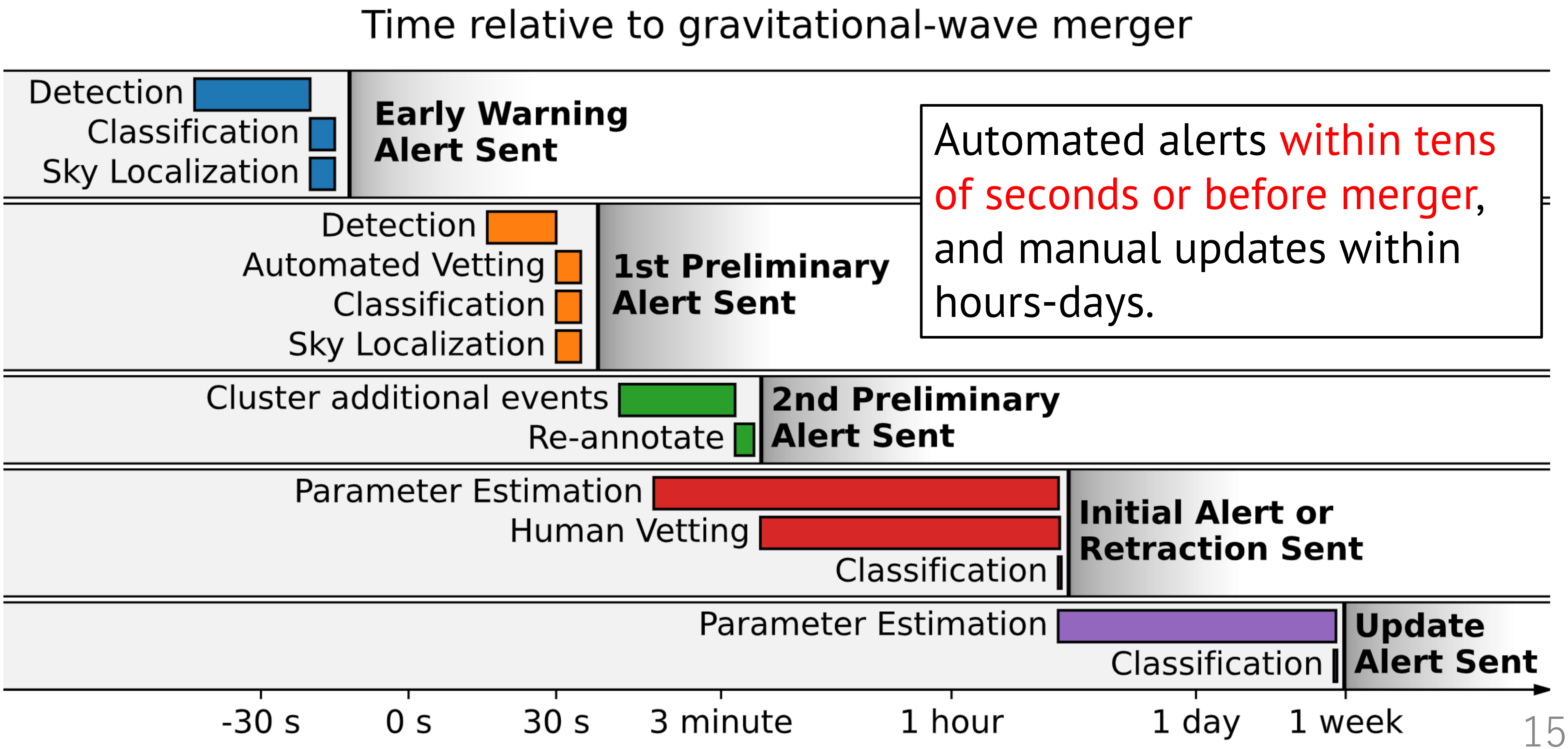

Automated alerts within tens of seconds or before merger, and manual updates within hours-days.

* All the figures are taken from [S230627c](S230627c).

Public data products

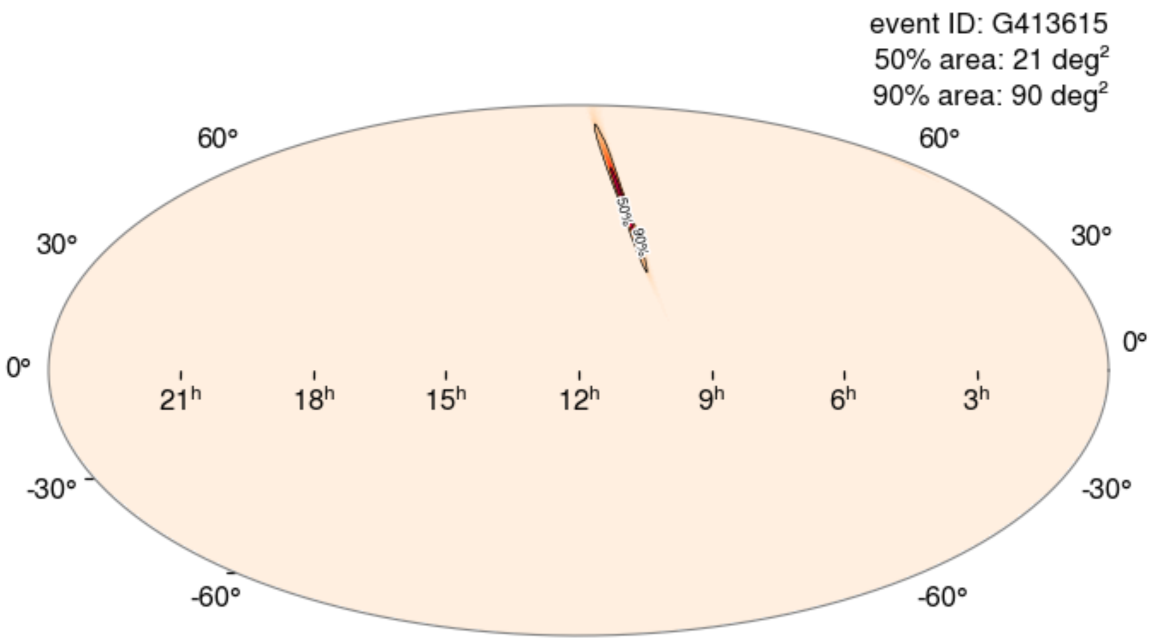

Figure: source localization

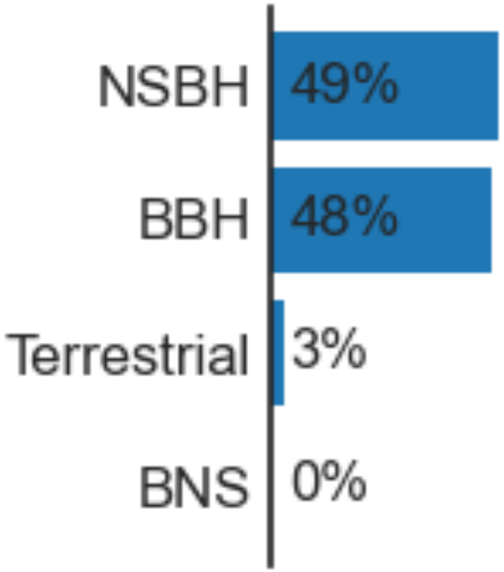

Figure: source classification

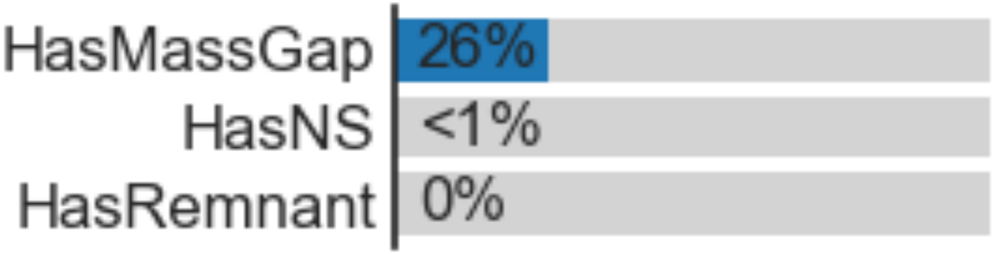

Figure: EM-Bright probabilities

Updates with detailed parameter estimation

GCN Circular 34087

Subject
LIGO/Virgo/KAGRA S230627c: Updated Sky localization and EM Bright Classification
Date
2023-06-27T04:37:12Z (3 months ago)
From
jgolomb@caltech.edu

The LIGO Scientific Collaboration, the Virgo Collaboration, and the KAGRA Collaboration report:

We have conducted further analysis of the LIGO Hanford Observatory (H1) and LIGO Livingston Observatory (L1) data around the time of the compact binary merger (CBC) candidate S230627c (GCN Circular 34086). Parameter estimation has been performed using Bilby [1] and a new sky map, Bilby.multiorder.fits,0, distributed via GCN Notice, is available for retrieval from the GraceDB event page:

Update GCN circular for S230627c
https://gcn.nasa.gov/circulars/34087

Localization and mass-spin information is updated by parameter estimation exploring broader space with Bilby (Ashton+ 2019, Romero-Shaw+ 2020).

The analysis is accelerated with **focused reduced order quadrature** (**Morisaki** and Raymond 2020, **Morisaki**+ 2023).

ex) For S230627c, updated skymap was sent ~2 hours after detection (c.f. it took ~60 hours at median in O3), reducing the 90% credible area: $90\ \mathrm{deg}^2 \rightarrow 82\ \mathrm{deg}^2$.

S230529ay

- FAR: 1/(160.44 years)
- NSBH or BNS
- Hanford was off → Livingston-only detection
- Distance: 197 ± 62 Mpc

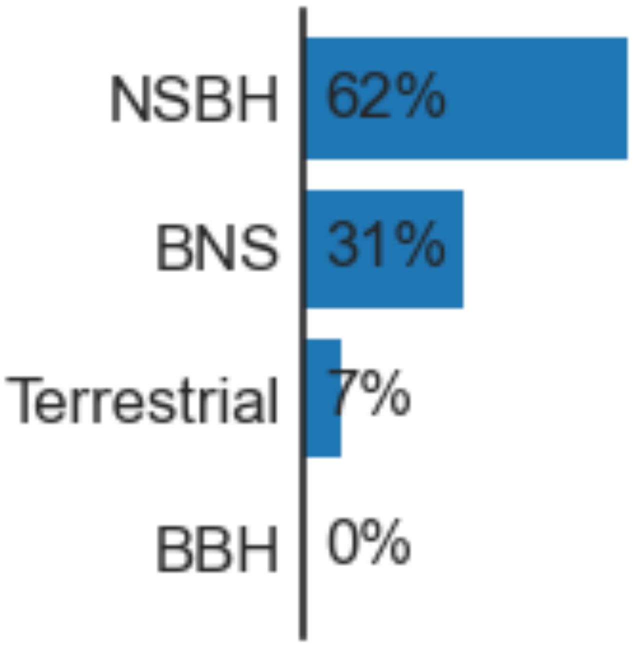

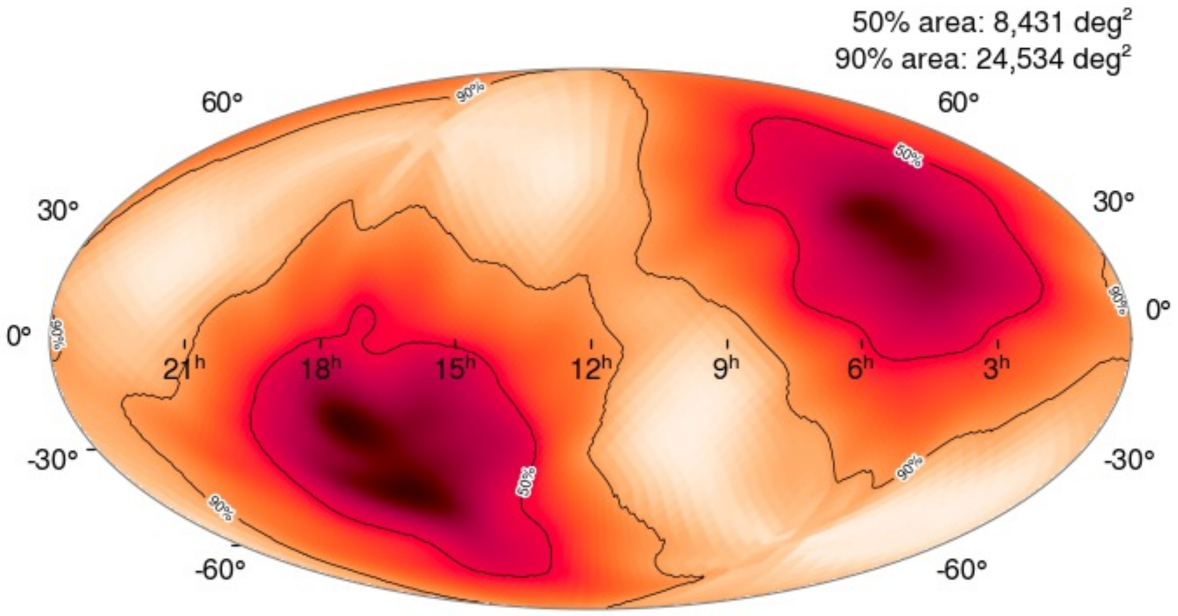

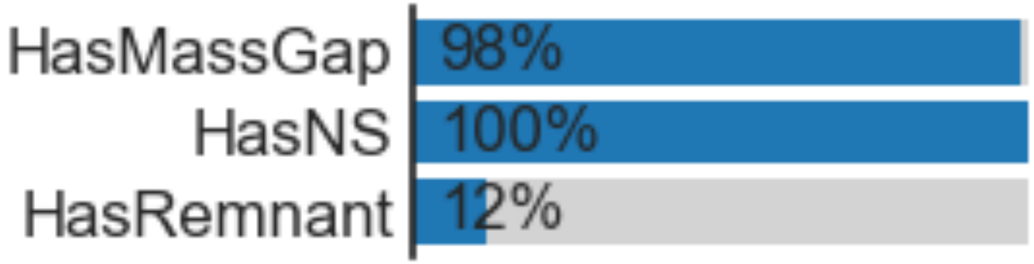

S230627c

- FAR: 1/(100.04 years)
- BBH or NSBH
- The best localized event in O4: 82 deg^2 (90%)
- Distance: 291 ± 64 Mpc

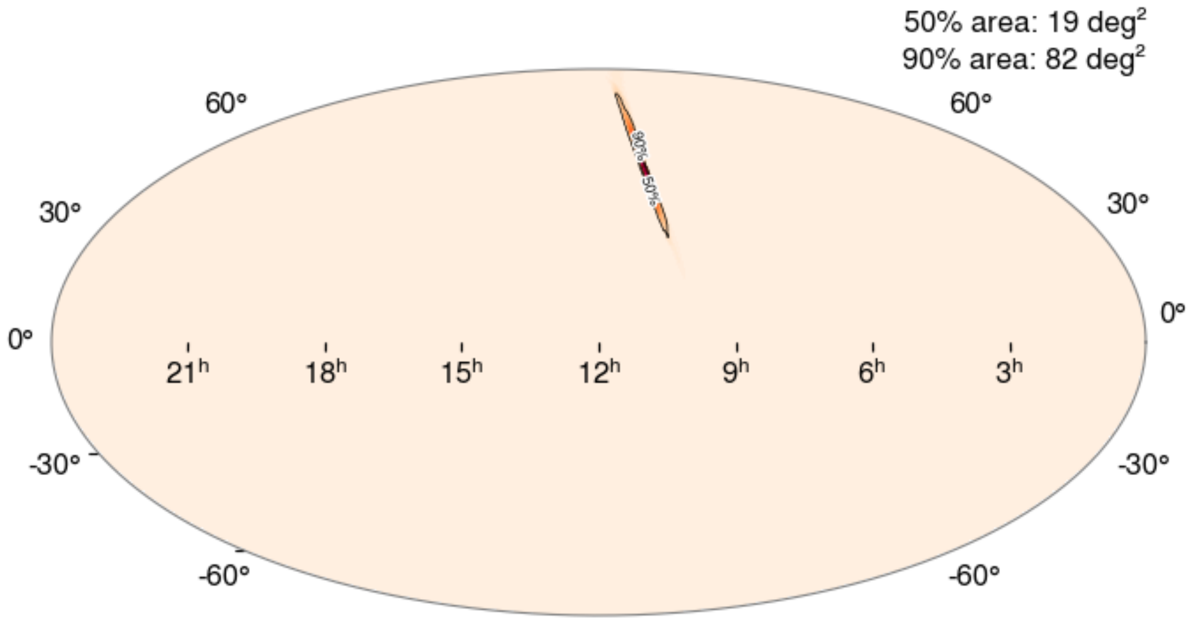

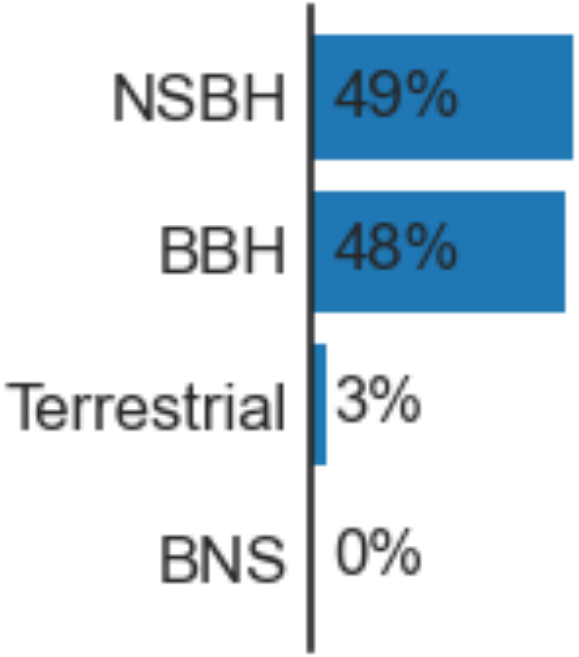

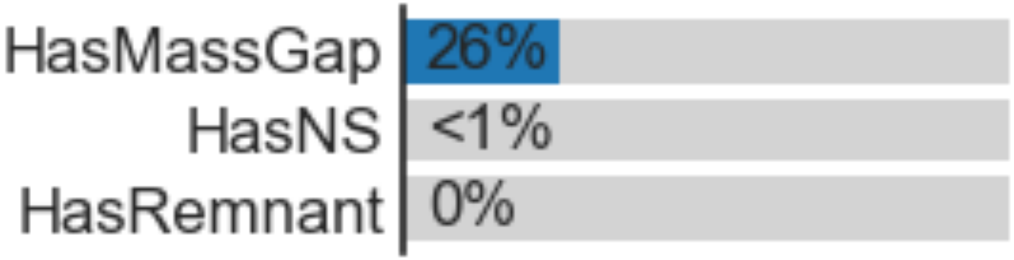

Localization errors

Credit: Ajisha Sajayan, Kaustubh Jha (IIT Kanpur) & Kunal Mooley
http://www.tauceti.caltech.edu/kunal/O4.html

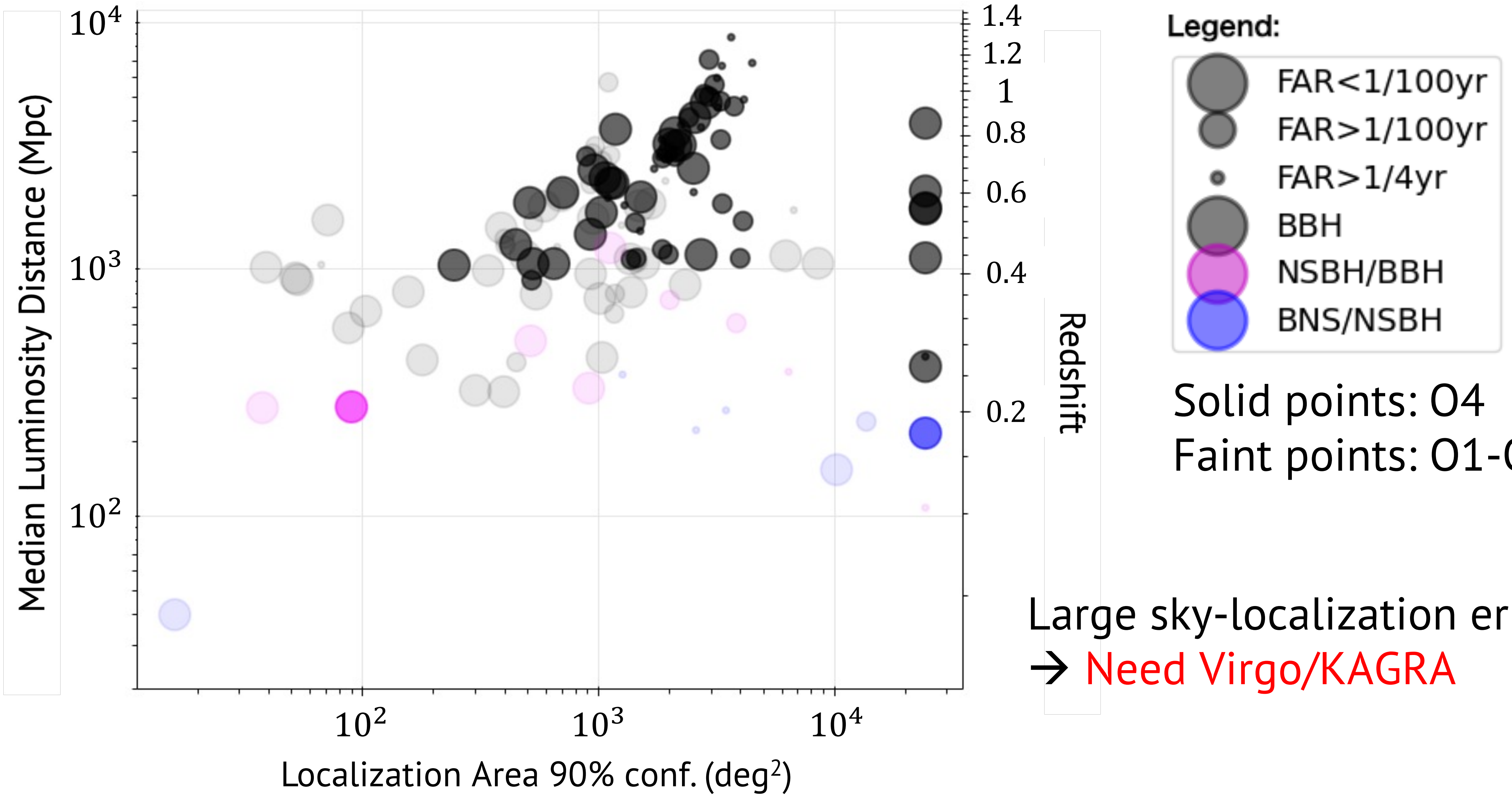

Solid points: O4
Faint points: O1-O3

Large sky-localization errors
→ Need Virgo/KAGRA

GRB 231115A

Short GRB at the position consistent with the galaxy M82 (~3.5 Mpc) (See GCN Circular 35035 and 35036).

$$\sqrt{F_+^2 + F_\times^2} = 0.9$$

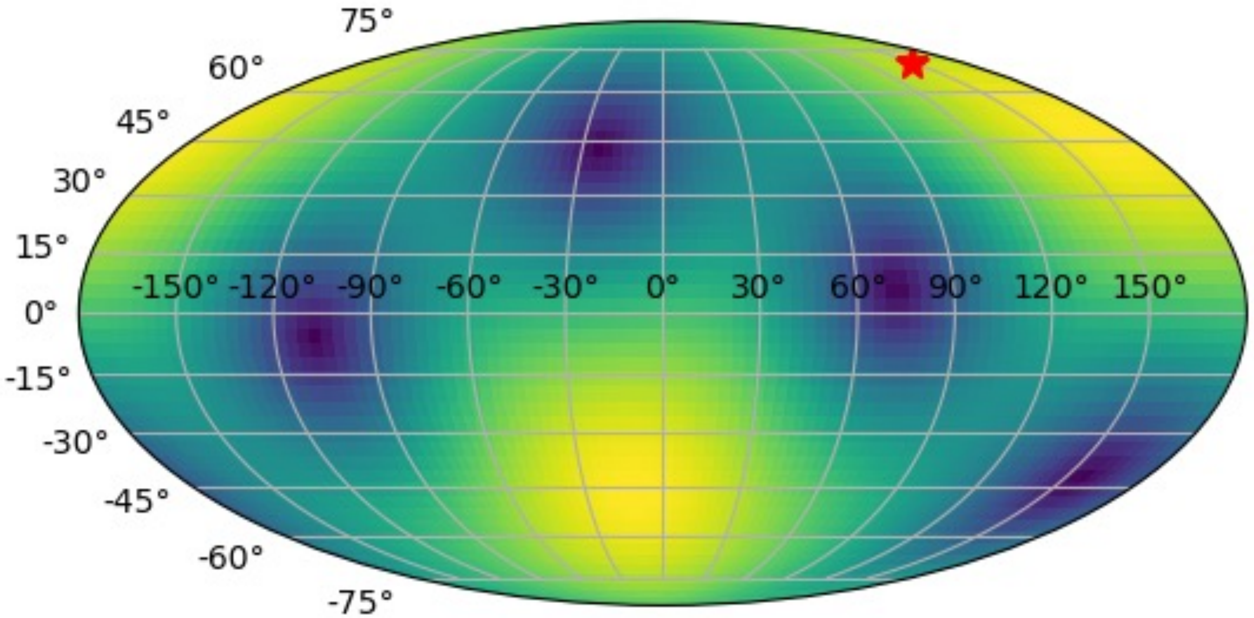

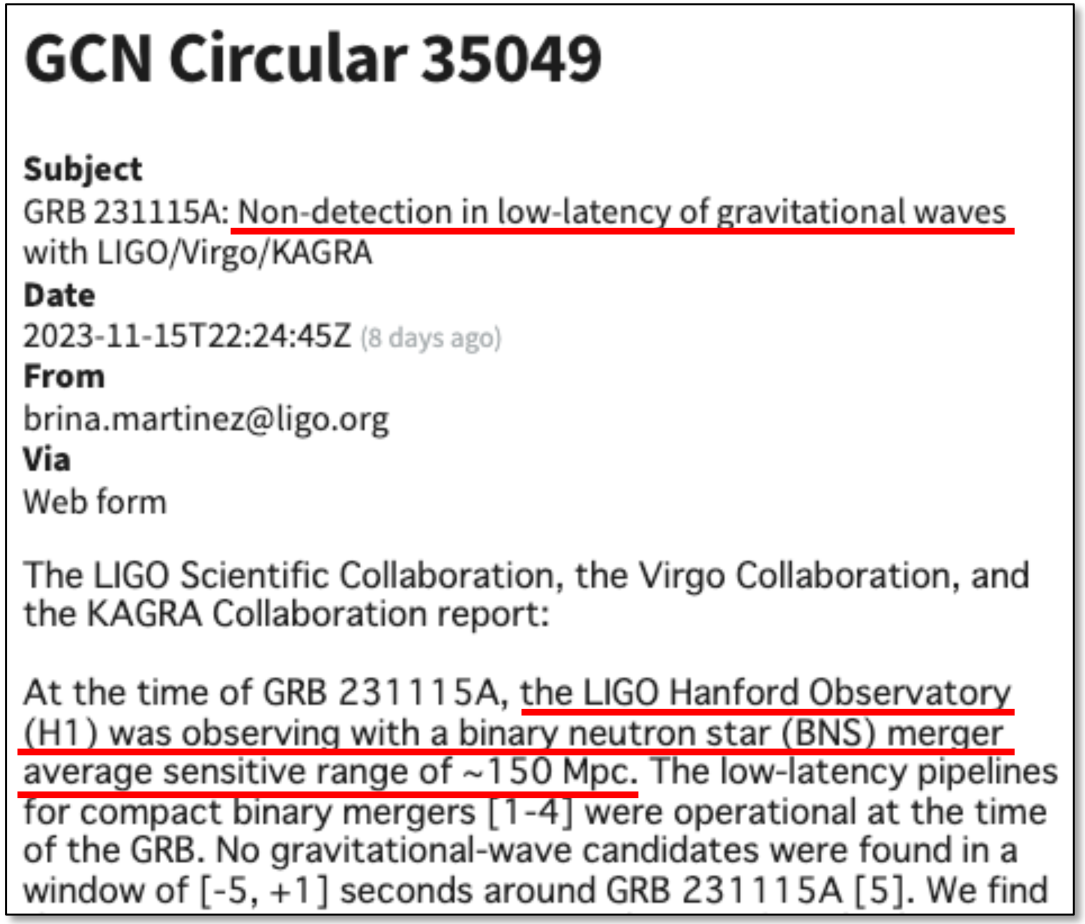

GCN Circular 35049

Subject
GRB 231115A: Non-detection in low-latency of gravitational waves with LIGO/Virgo/KAGRA
Date
2023-11-15T22:24:45Z (8 days ago)
From
brina.martinez@ligo.org
Via
Web form

The LIGO Scientific Collaboration, the Virgo Collaboration, and the KAGRA Collaboration report:

At the time of GRB 231115A, the LIGO Hanford Observatory (H1) was observing with a binary neutron star (BNS) merger average sensitive range of ~150 Mpc. The low-latency pipelines for compact binary mergers [1-4] were operational at the time of the GRB. No gravitational-wave candidates were found in a window of [-5, +1] seconds around GRB 231115A [5]. We find

https://gcn.nasa.gov/circulars/35049

LIGO, VIRGO AND KAGRA OBSERVING RUN PLANS

https://observing.docs.ligo.org/plan/

ER16: The engineering run (ER16) will start on 20 March 2024 at 15:00 UTC and last for 2 weeks. Most of these 2 weeks will be focused on gathering multiple-interferometer observation time so

O4b: The LIGO Hanford (LHO), LIGO Livingston (LLO), and Virgo detectors plan to commence observing run O4b at 15:00 UTC on 3 April 2024. O4b will run until February 2025 (specific date TBD), with no planned breaks in observing.

The recent commissioning activities have allowed the Virgo detector to routinely achieve a BNS range around 55 Mpc. The plan for the forthcoming weeks aims at improving stability to optimize

nine of twenty mirror suspension systems in KAGRA needed repair. The recovery work for them is ongoing. We hope to finish this recovery work as soon as possible and restart commissioning, then join O4b before the end of O4 with a BNS range of around 10 Mpc.

Summary

- 90 compact binary coalescences were detected by the end of O3.
    - Population properties of binary black holes
    - Tests of GR
    - GW + EM observation of binary neutron star
    - Neutron star-black holes

- O4 is currently ongoing.
    - 81 alerts in the first half of O4
    - A few NSBH/BNS event candidates
    - Large localization errors due to the lack of a third detector
    - We will resume observation in ~a week with Virgo.

Basic

CBC parameters

- Frequency evolution → $m_1, m_2, \chi_{1\parallel}, \chi_{2\parallel}$ (and tidal deformability for BNS, NSBH)
- Amplitude modulation → $\chi_{1\perp}, \chi_{2\perp}$

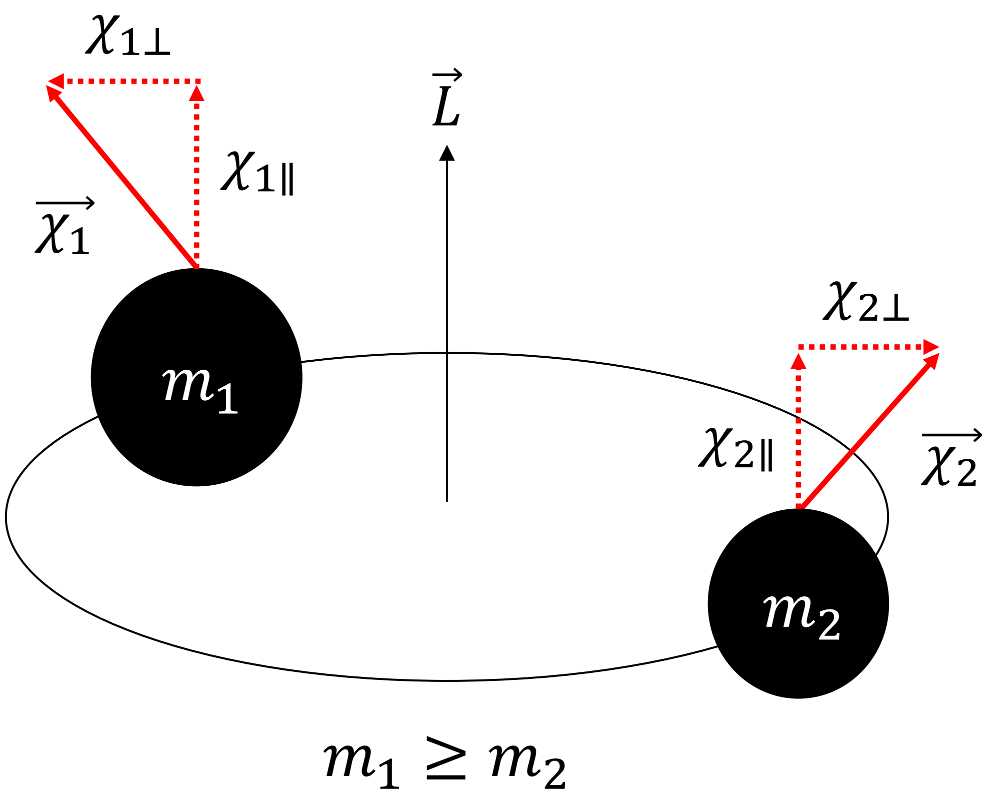

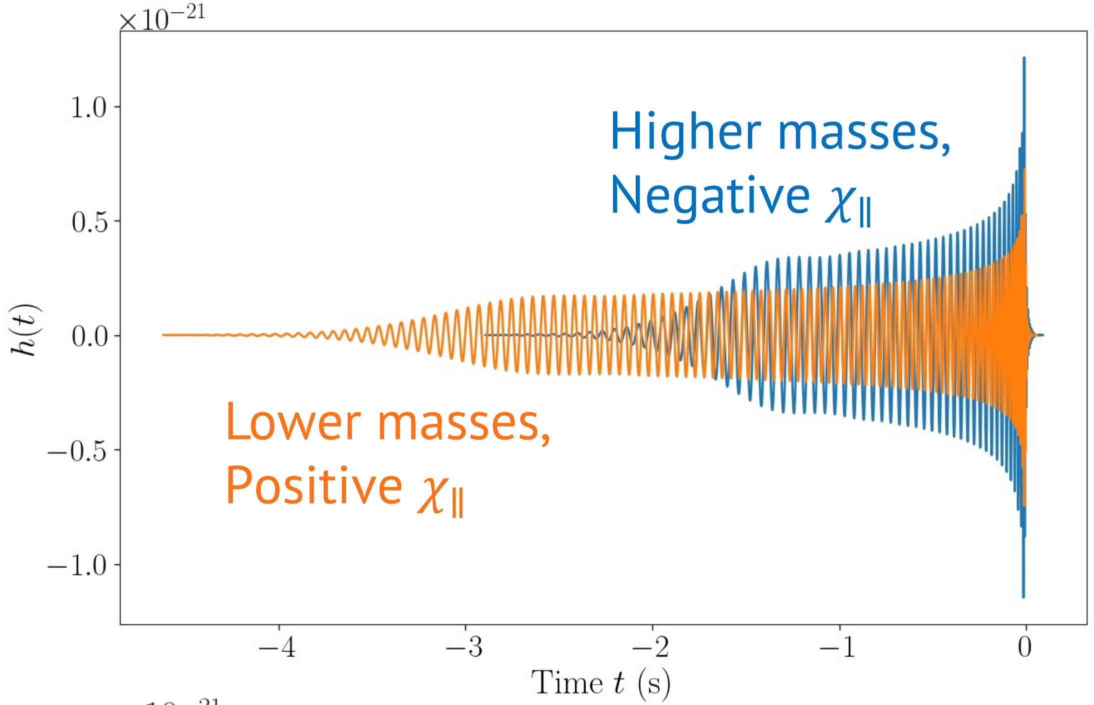

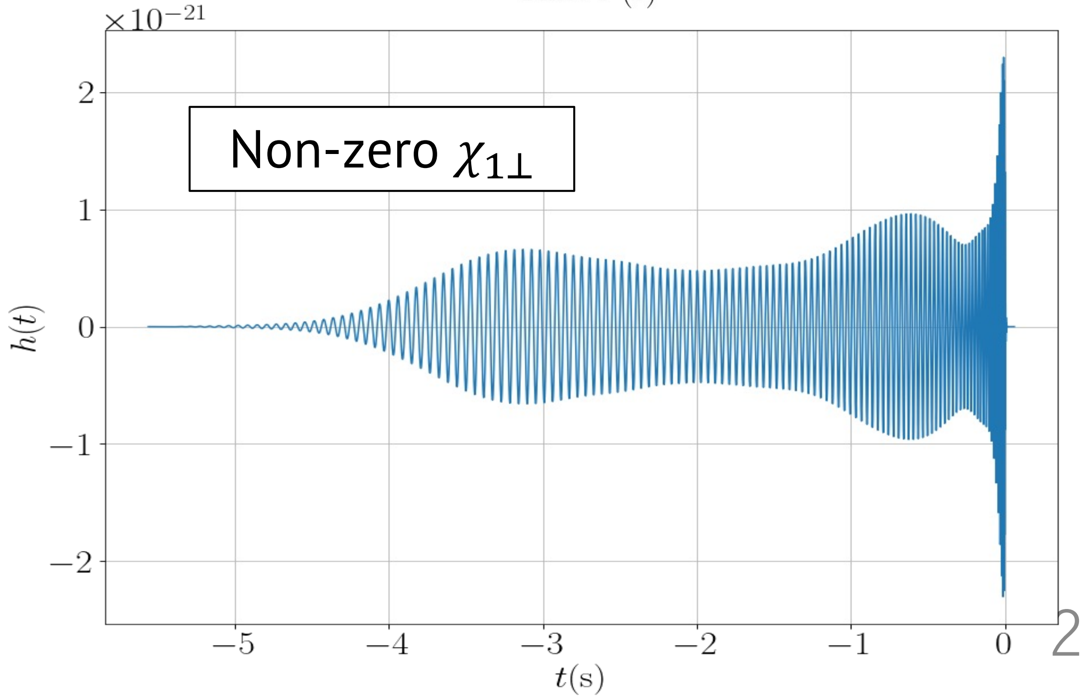

Matched filtering

Credit: Ryan Magee

Correlate expected waveform (*template*) with data to optimally extract signal.

The output is referred to as *signal-to-noise ratio (SNR) time series.*

SNR is normalized so that its expectation value is unity if no signal.

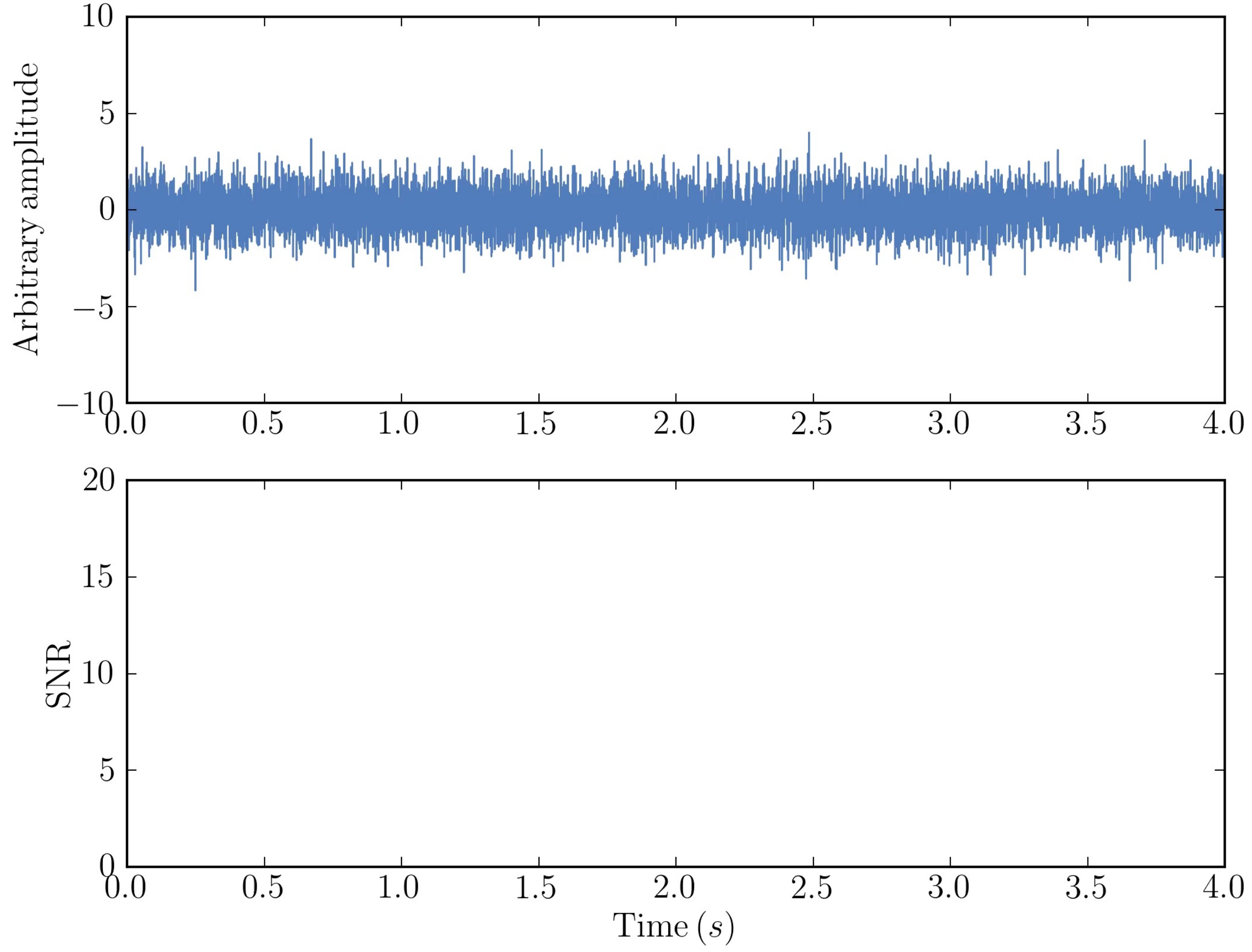

Figure: Demonstration of matched filtering

Matched filtering

$$\rho(t) = 4\left|\int_0^\infty \frac{\boxed{\tilde{d}(f)}\,\boxed{\tilde{h}^*(f)}}{\boxed{S(f)}} e^{2\pi i f t}\,\mathrm{d}f\right|$$

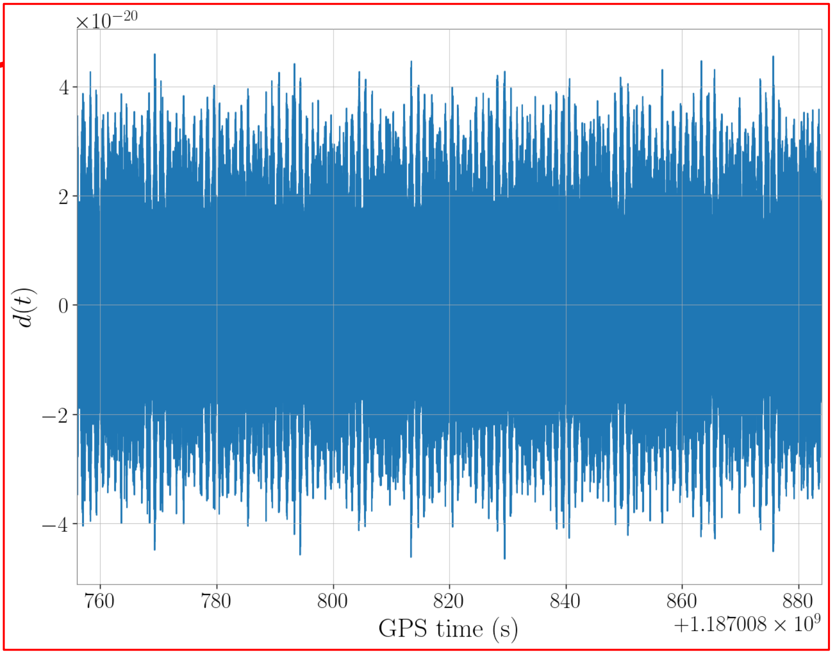

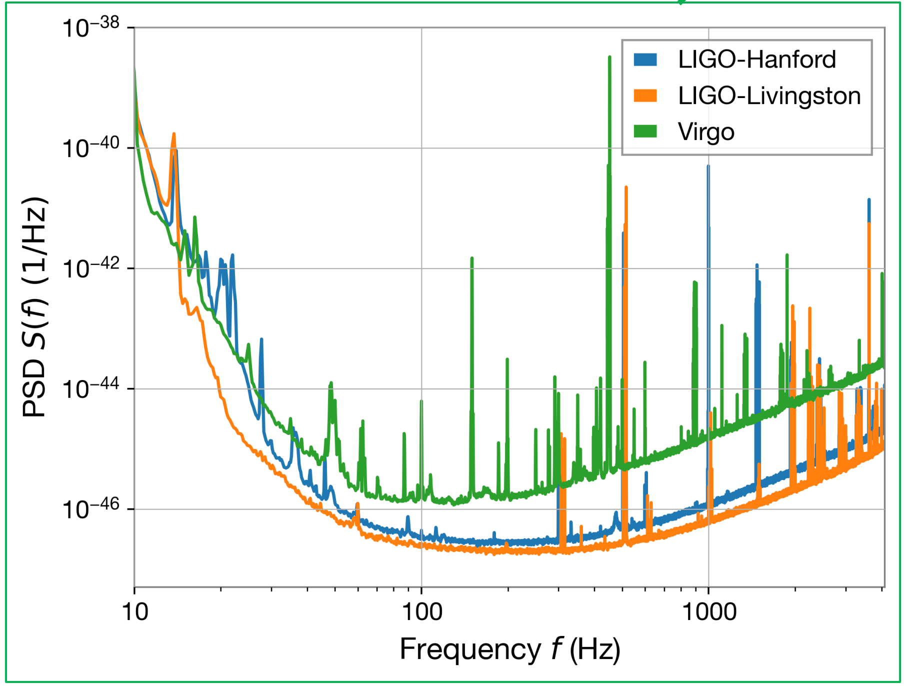

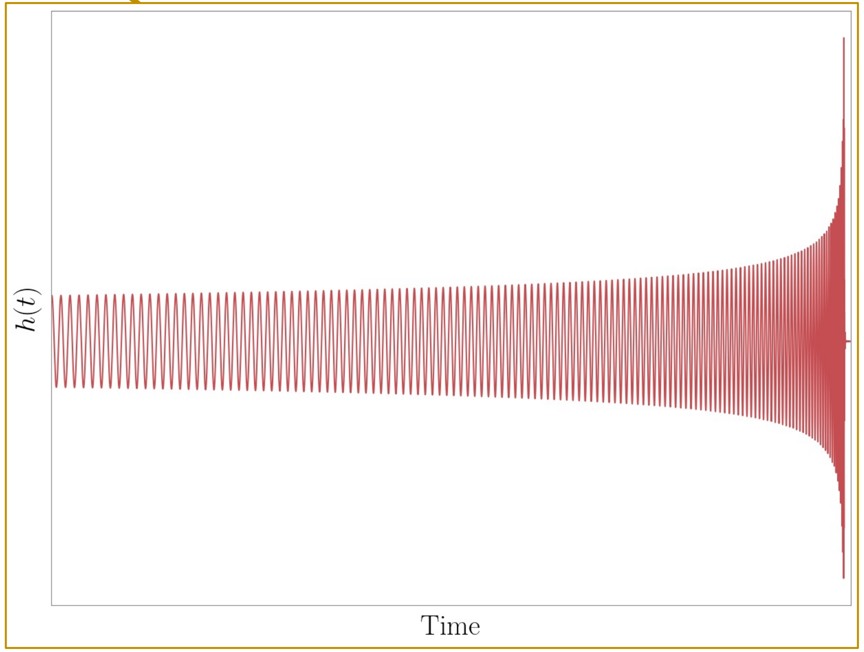

Matched filtering

$$\rho(t) = 4\left|\int_0^\infty \frac{\tilde{d}(f)\tilde{h}^*(f)}{\boxed{S(f)}} e^{2\pi i f t}\mathrm{d}f\right|$$

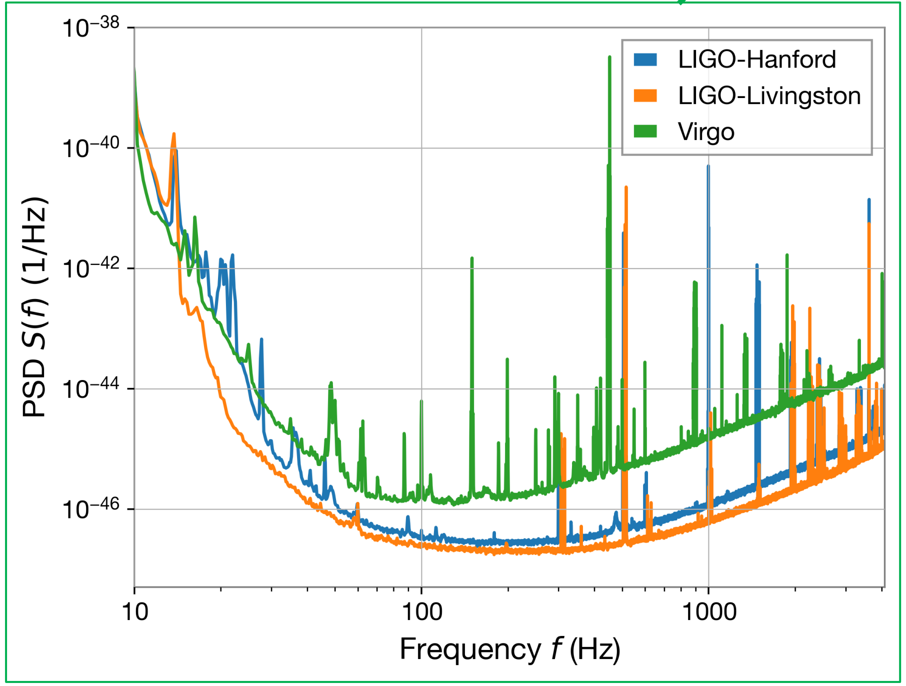

Power spectral density (PSD) of noise:

$$S(f) = \frac{2}{T}\langle|\tilde{n}(f)|^2\rangle.$$

$\tilde{n}(f)$: Fourier transform of noise T: data duration

- It is estimated as an average of off-source data segments.
- It characterizes noise power at each frequency.

Template bank

Data are filtered with a set of templates (*template bank*) parameterized by the 4 parameters, $(m_1, m_2, \chi_{1z}, \chi_{2z})$.

Credit: Mukherjee *et al.*, PRD **103**, 084047 (2021).

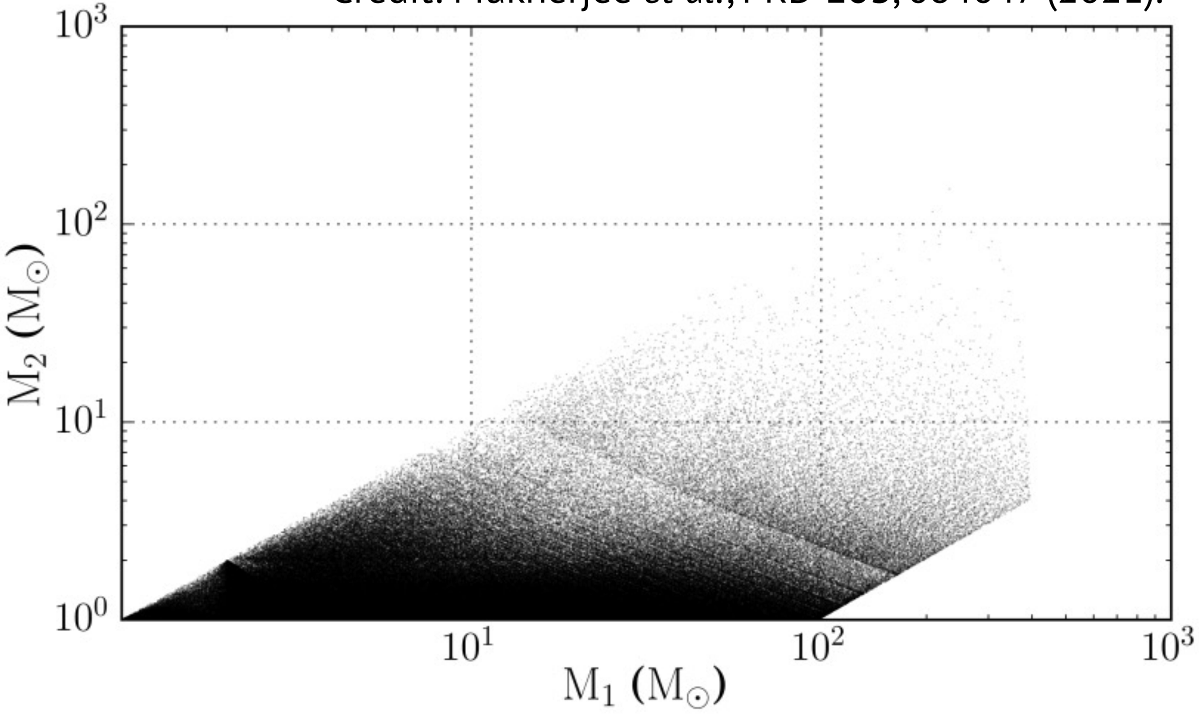

Figure: Template bank used by GstLAL in O2 (661,335 templates in total)

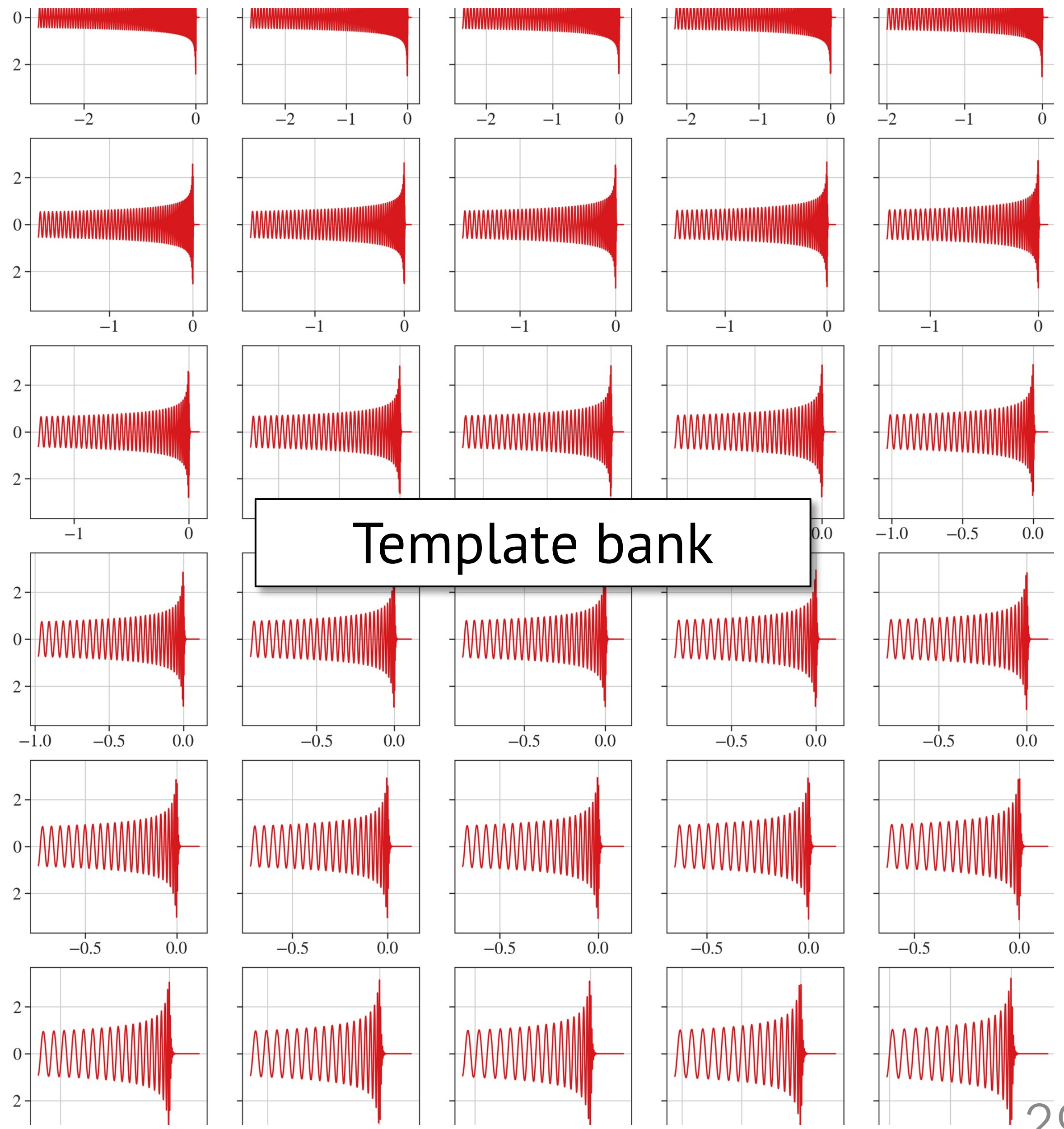

Source localization

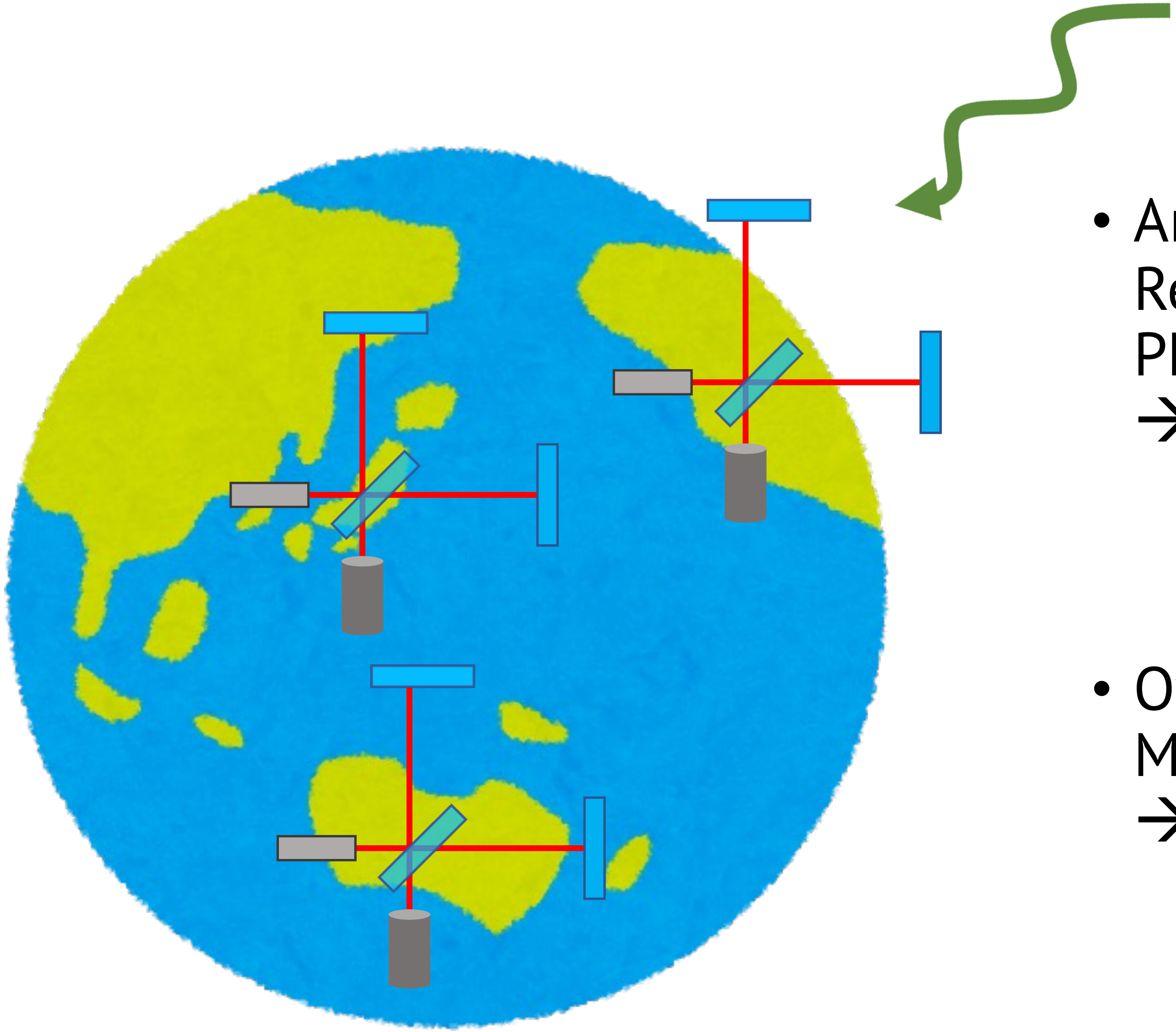

- Arrival time differences,
  Relative amplitudes,
  Phase differences.
  → The direction to the source

- Overall signal amplitude,
  Masses from frequency evolution.
  → Luminosity distance to the source

Source localization

Bayestar (Singer & Price, 2016) uses SNR time series to quickly localize a GW source.

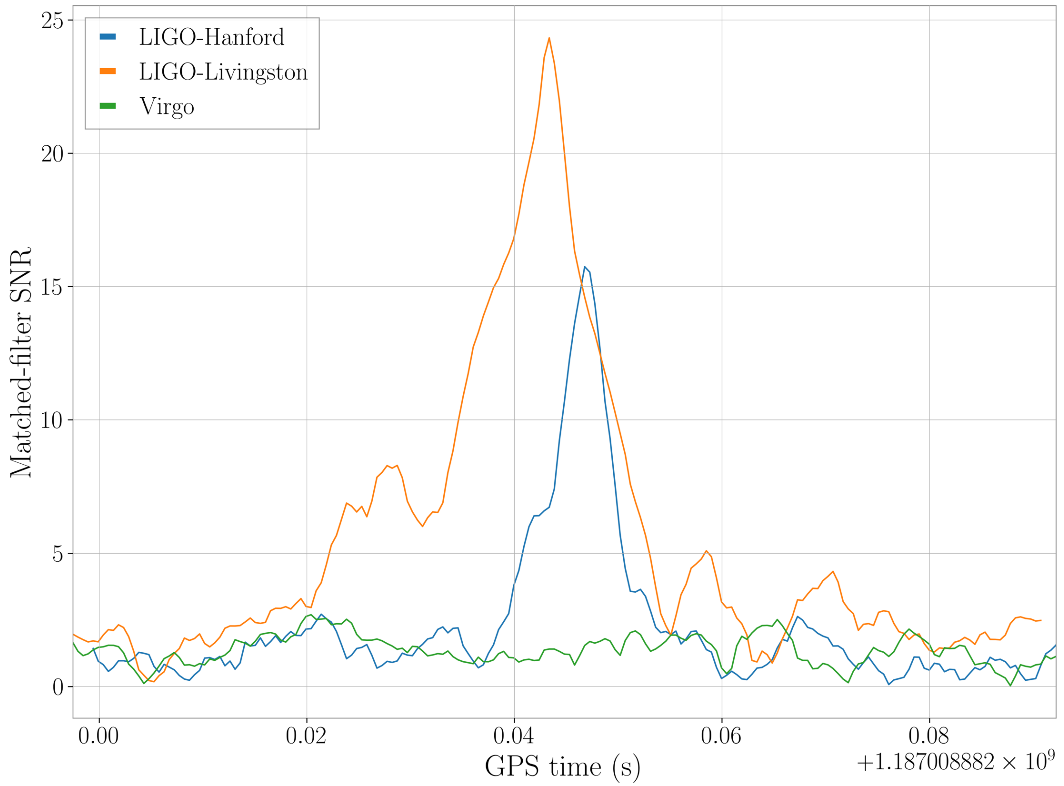

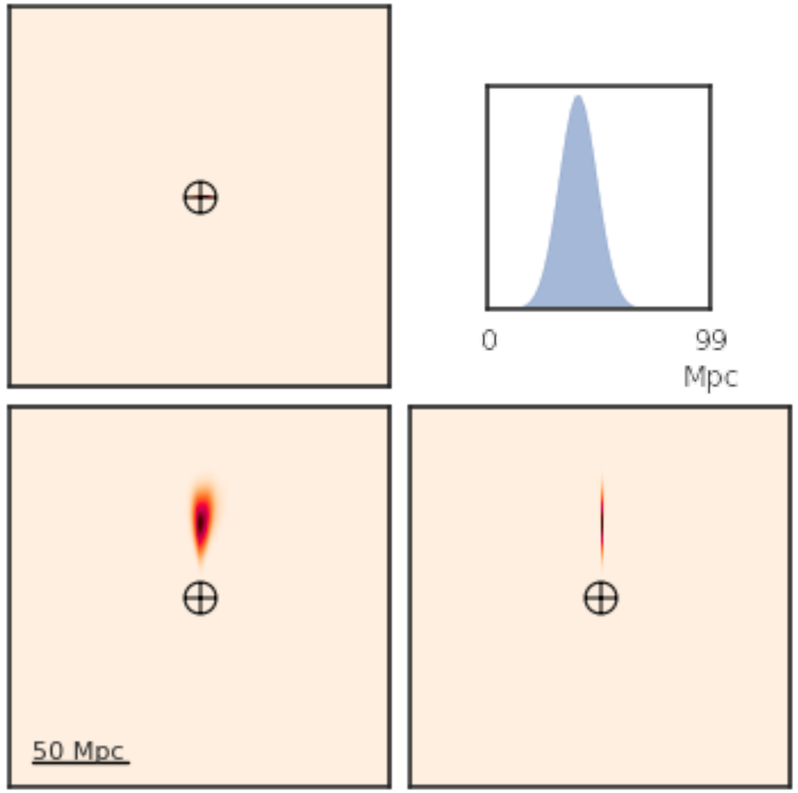

GW170817 was localized within $31\ \mathrm{deg}^2$ and $(40 \pm 8)\ \mathrm{Mpc}$ (90% credible level), the sky map was sent ~4 hours after the detection.

Bayesian inference

$$p(\theta|d) \propto p(d|\theta)p(\theta)$$

Posterior **Likelihood** **Prior**

θ: source parameters

d: data

Bayesian inference

$$p(\theta|d) \propto p(d|\theta)p(\theta)$$

Posterior **Likelihood** **Prior**

Data model: $d(t) = h(t;\theta) + n(t)$, noise is assumed to be stationary and Gaussian,

$$p(d|\theta) \propto \exp\left[-\frac{2}{T}\sum_{l}\frac{|\tilde{n}(f_l)|^2}{S(f_l)}\right] = \exp\left[-\frac{2}{T}\sum_{l}\frac{\left|\tilde{d}(f_l) - \tilde{h}(f_l;\theta)\right|^2}{S(f_l)}\right].$$

Generalization to data from multiple detectors: $d_1, d_2, \ldots,$

$$p(\{d_I\}_I|\theta) \propto \prod_I \exp\left[-\frac{2}{T}\sum_{l}\frac{\left|\tilde{d}_I(f_l) - \tilde{h}_I(f_l;\theta)\right|^2}{S_I(f_l)}\right].$$

Bayesian inference

$$p(\theta|d) \propto p(d|\theta)p(\theta)$$

Posterior **Likelihood** **Prior**

- Right ascension and declination are fixed to those of the host galaxy, NGC 4993.
- Two priors on spin magnitude:
  - Low-spin prior: $\chi < 0.05$ (consistent with the observed binary pulsars)
  - High-spin prior: $\chi < 0.89$
- Uninformative priors
  - Uniform in $m_{1,2}$, $|\overrightarrow{\chi_{1,2}}|$, $\Lambda_{1,2}$, ϕ_c, and t_c. Range of t_c is ± 0.1s around the trigger time.
  - Isotropic for spin directions and binary orientation.
  - Distance prior $\propto D_L^2$.

Stochastic sampling

We want probability density function of selected parameters…

→ Draw samples from posterior and make their histograms!

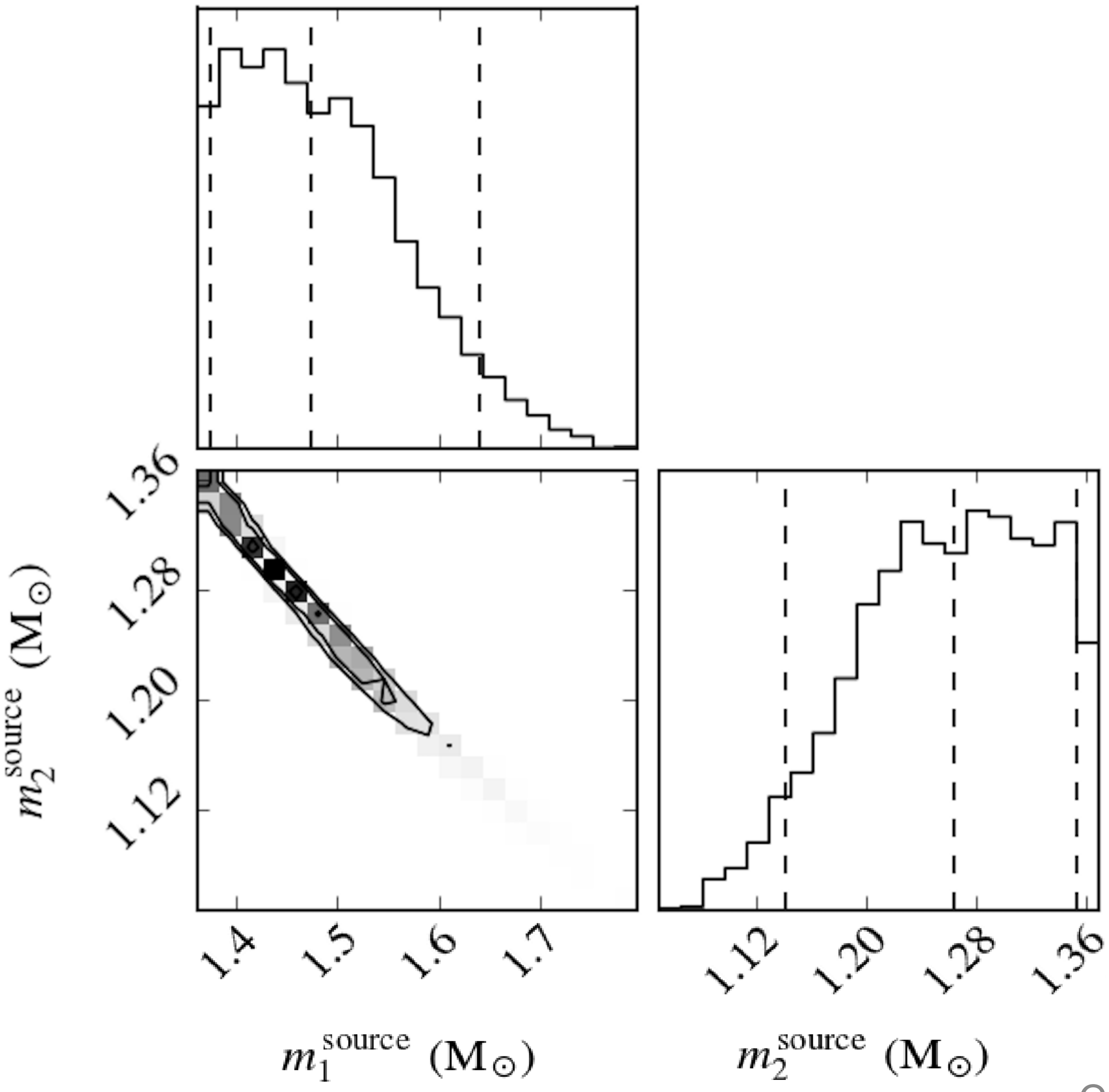

Various efficient algorithms for sampling

- Markov-chain Monte Carlo (MCMC)
- Nested sampling

Reduced Order Quadrature (ROQ)

References:
Canizares+ PRL **114**, 071104 (2015),
Smith+, PRD **94**, 044031 (2016).

- Dominant cost = generation of frequency-domain waveform $\tilde{h}(f_l)$
- Its cost is proportional to L , the number of frequency points $\{f_l\}_{l=1}^{L}$.
- Interpolate waveform values at $K \ll L$ interpolation nodes $\{F_k\}_{k=1}^{K}$,

$$\tilde{h}(f_l) \simeq \sum_{k=1}^{K} \tilde{h}(F_k)\underbrace{B_k(f_l)}_{\text{ROQ basis}}. \quad (l = 1,2,\dots,L)$$

→ Speed-up by L/K

- ROQ basis $B_k(f_l)$ and interpolation nodes $\{F_k\}_{k=1}^{K}$ are constructed for target mass-spin space and waveform model.

Results from 01—03

On 14 September 2015,
LIGO observed gravitational waves.

Image credit: Caltech/MIT/LIGO Lab

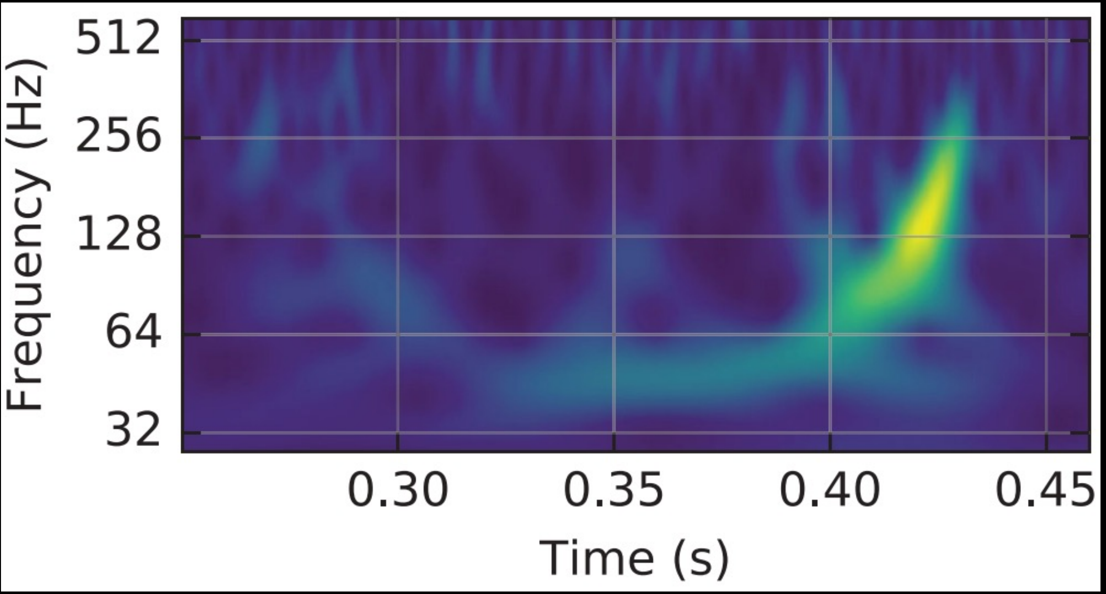

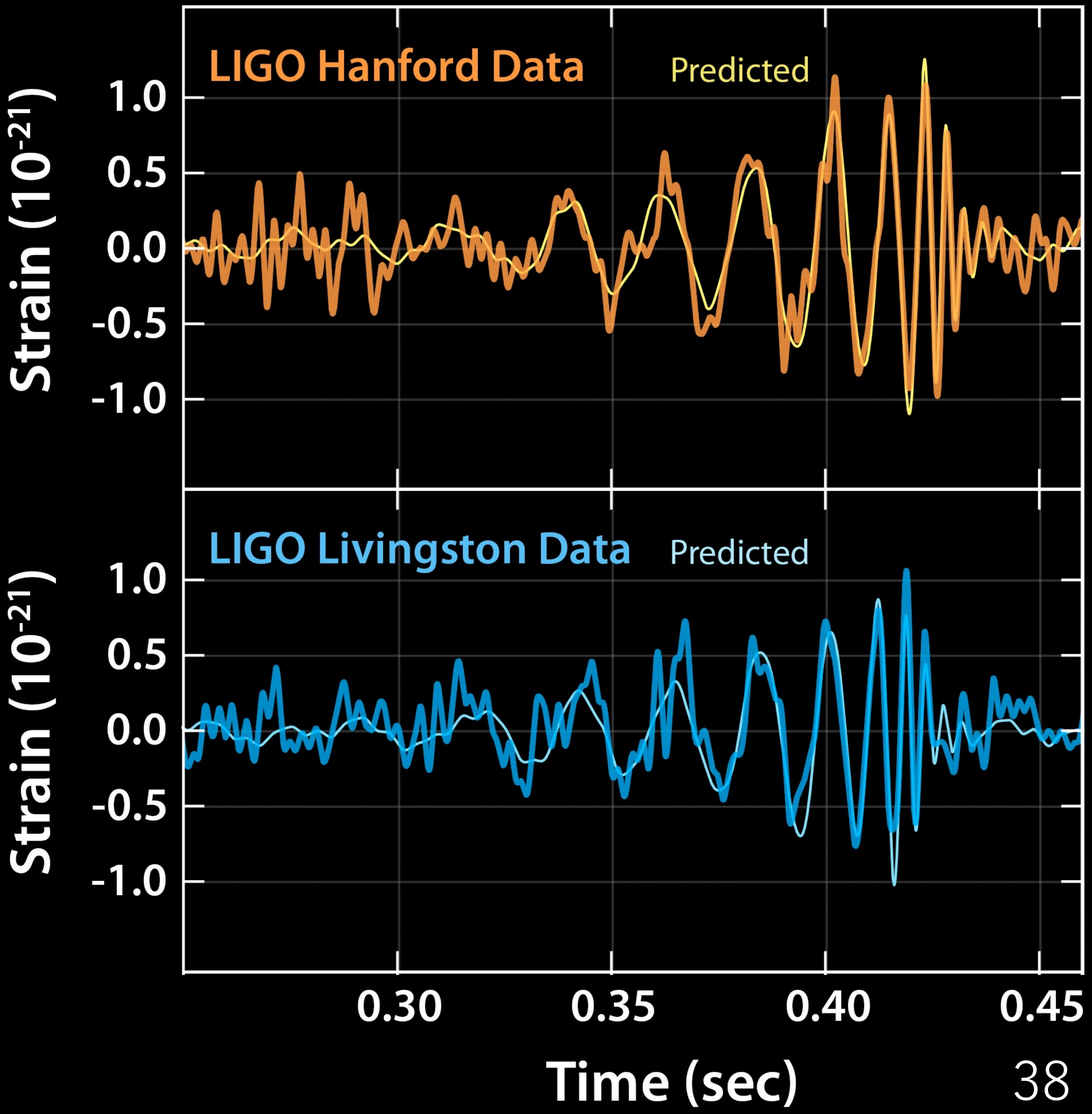

Unequal-mass binaries

Reference: Abbott+, PRD **102**, no. 4, 043015 (2020), Abbott+, ApJL **896**, no.2, L44 (2020).

GW190412

- $m_1 = 30.1^{+4.6}_{-5.3} M_{\odot}$, $m_2 = 8.3^{+1.6}_{-0.9} M_{\odot}$.
- Strong evidence of higher GW harmonics ($p \leq 6 \times 10^{-4}$).

GW190814

- $m_1 = 23.2^{+1.1}_{-1.0} M_{\odot}$, $m_2 = 2.59^{+0.08}_{-0.09} M_{\odot}$.
- Strong evidence of higher GW harmonics ($p \leq 2.5 \times 10^{-4}$).
- The secondary mass is in “mass gap” between NS and BH.

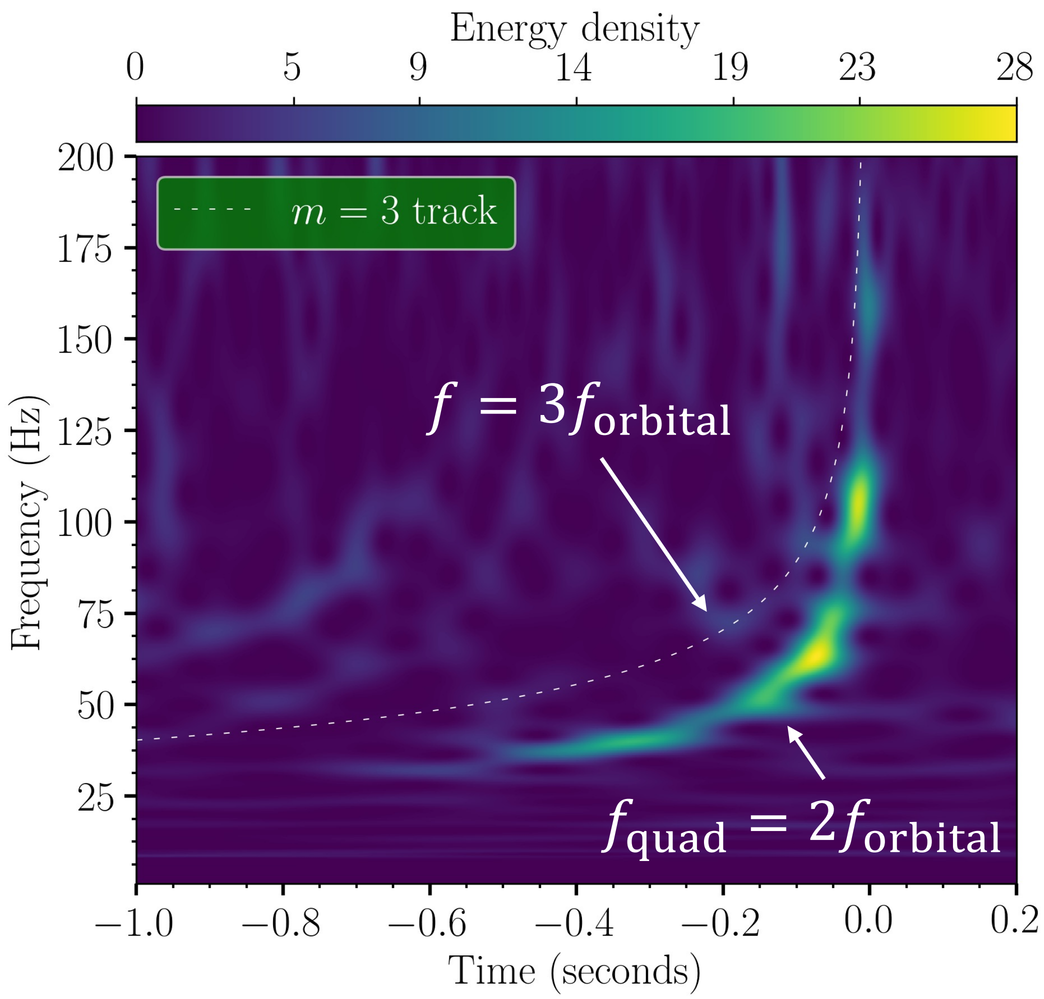

Figure: LIGO-Livingston data for GW190412

GW190521: the heaviest BBH

Reference: Abbott+, PRL **125**, no.10, 101102 (2020), Abbott+, ApJL **900**, no.1, L13 (2020).

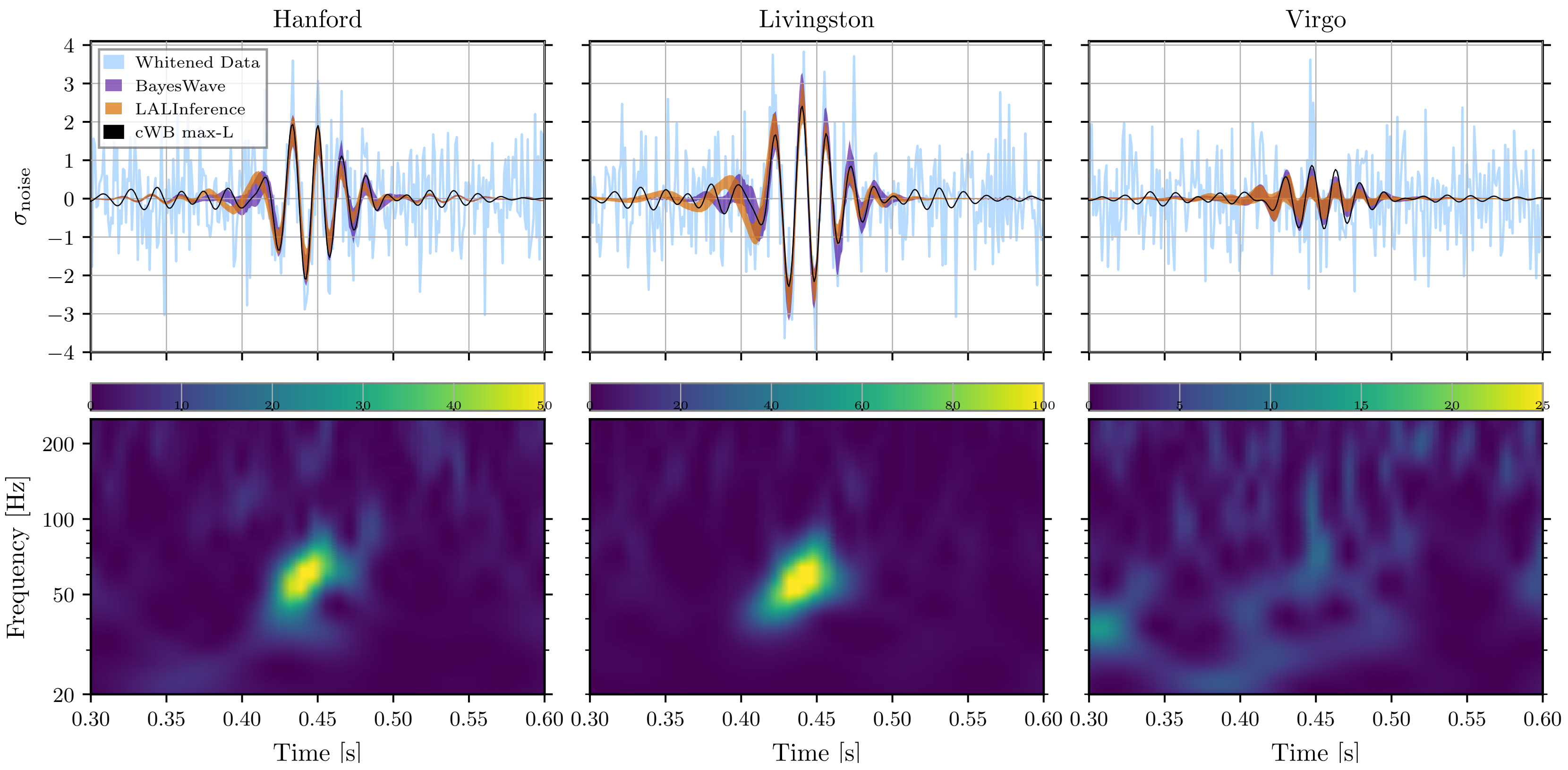

Figure: LIGO-Virgo data for GW190521

GW190521:

$m_1 = 85^{+21}_{-14} M_\odot$,

$m_2 = 66^{+17}_{-18} M_\odot$.

- The primary mass m_1 is in the pair-instability mass gap, $(65 - 120) M_\odot$.
- The remnant is an intermediate mass black hole: $M_f = 142^{+28}_{-16} M_\odot$.

BBH distribution: Mass

Figure credit: Abbott+, PRX **13**, 011048 (2023).

"Observed" distribution

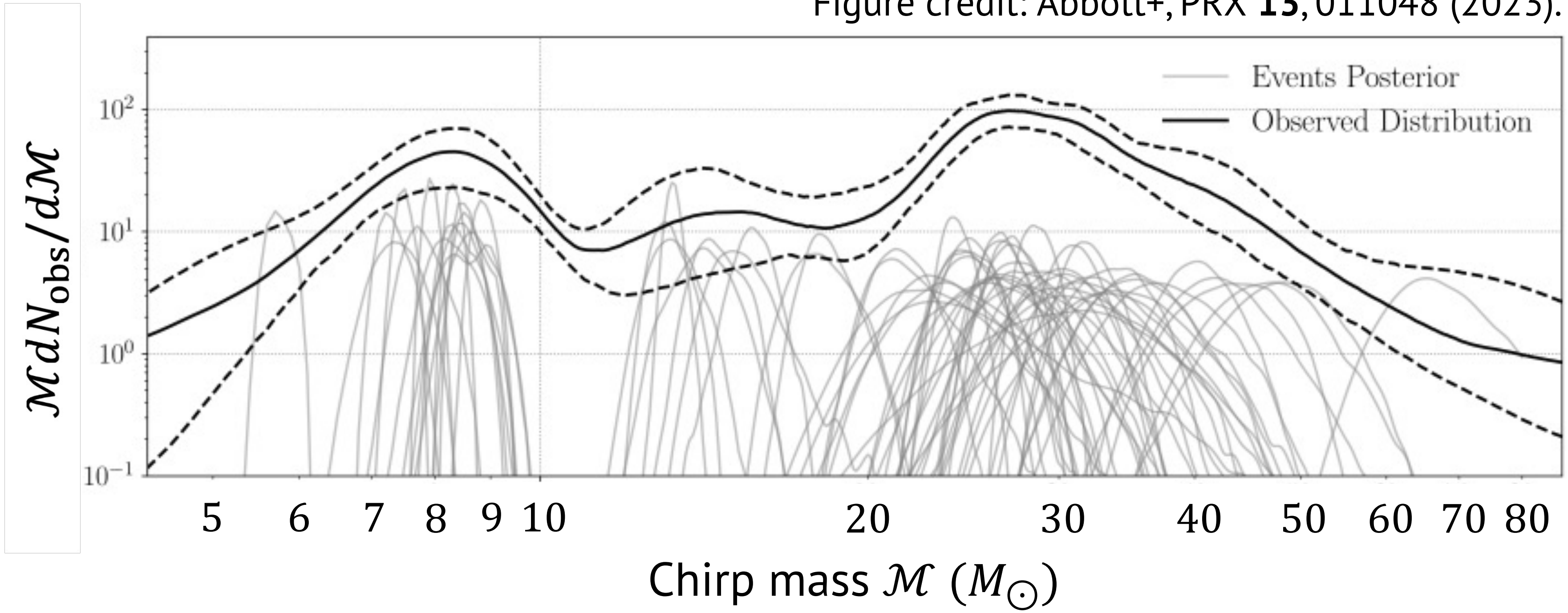

Chirp mass $\mathcal{M}$ is mass combination measured precisely with GWs:

$$\mathcal{M} = \frac{(m_1 m_2)^{\frac{3}{5}}}{(m_1+m_2)^{\frac{1}{5}}}.$$

BBH distribution: Mass

Figure credit: Abbott+, PRX **13**, 011048 (2023).

"Observed" distribution

After correcting observation bias

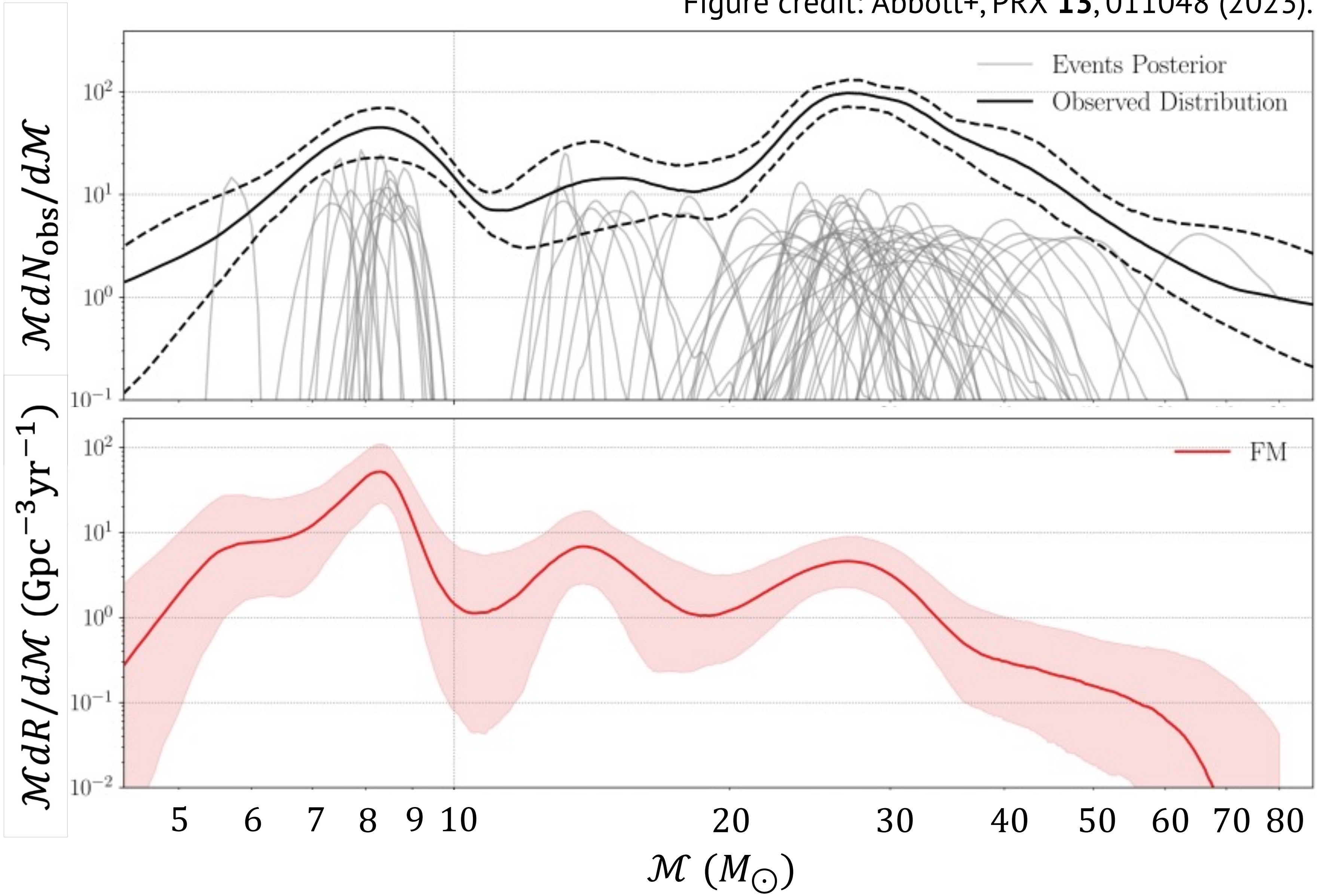

Population properties of binary black holes

R. Abbott et al., PRX **13**, 011048 (2023).

"Observed" population

After correcting observation bias

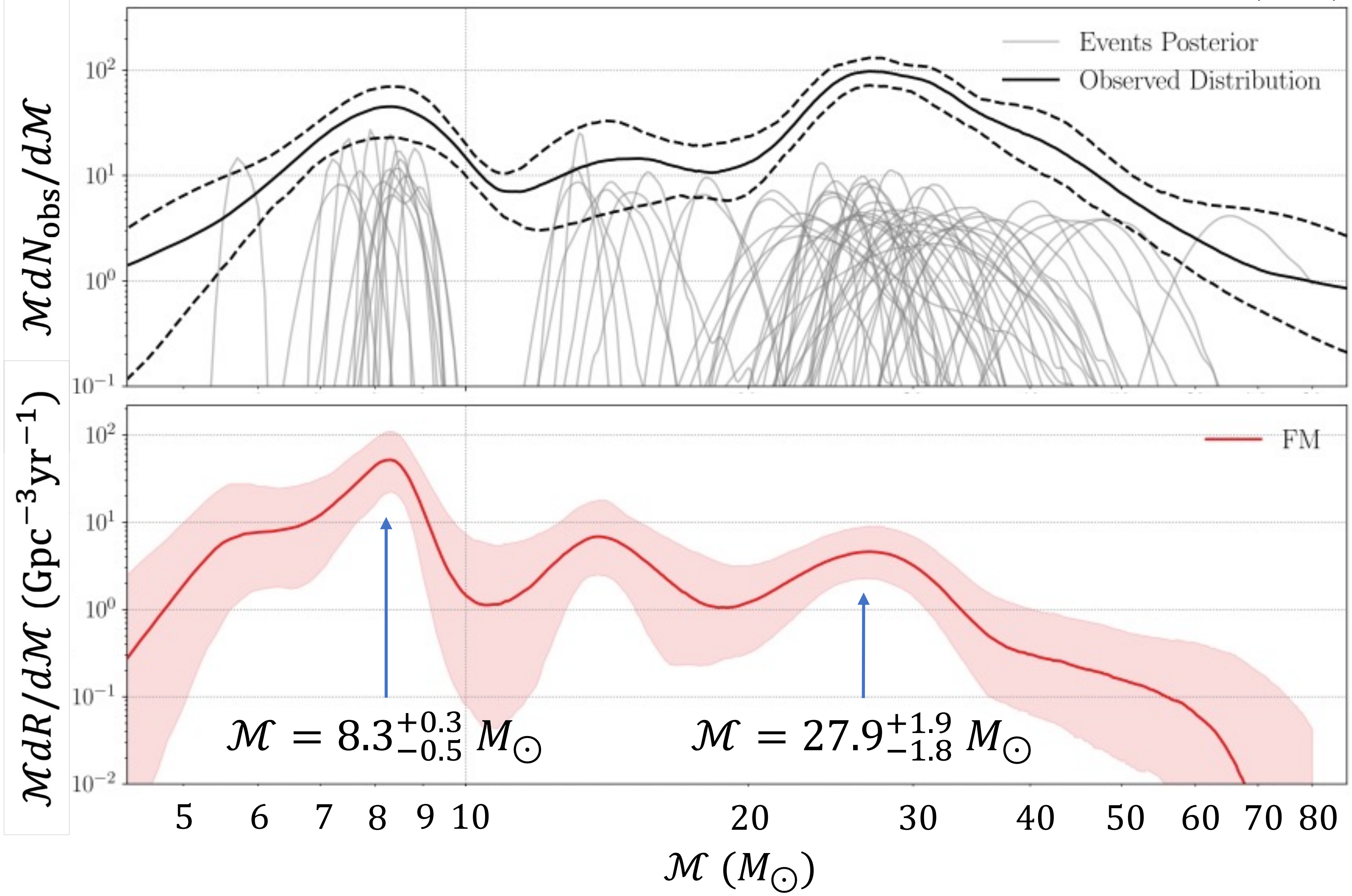

BBH population: Spin

e.g. Mandel and Farmer, arXiv: 1806.05820

Isolated field binaries

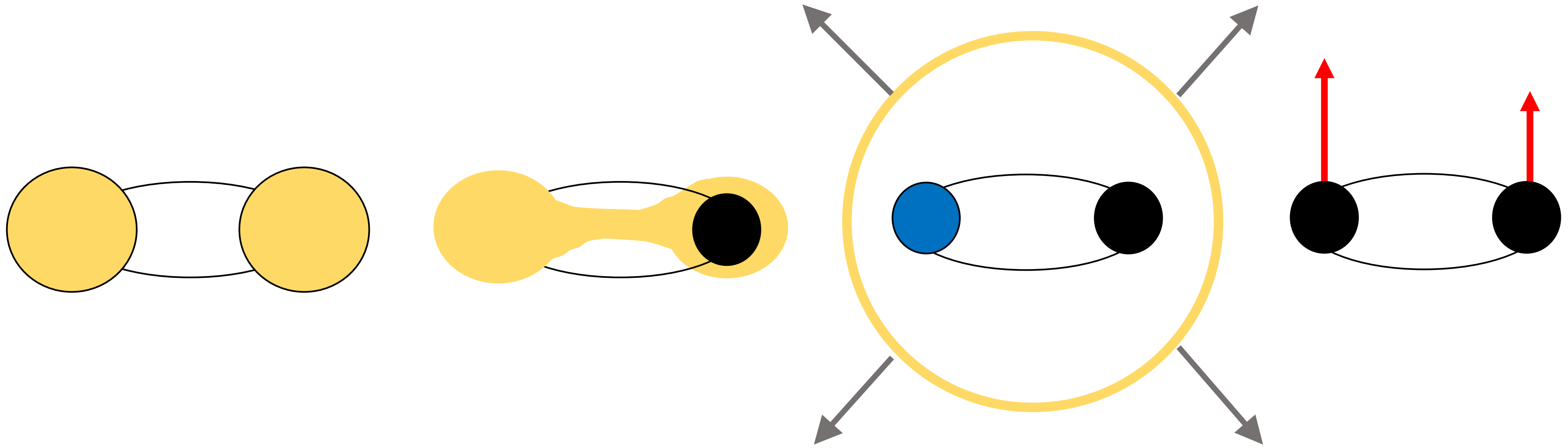

Dynamical formation

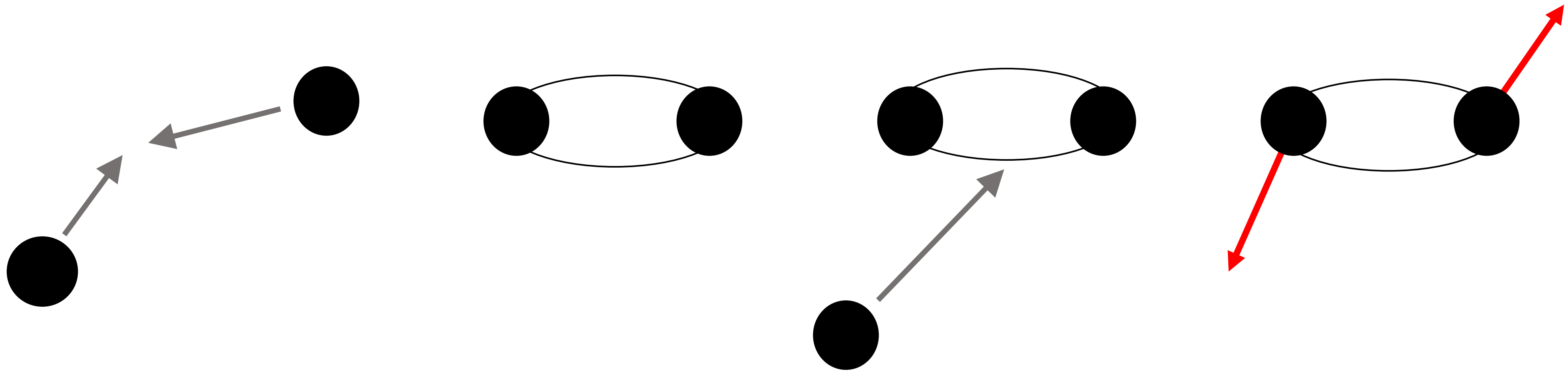

BBH distribution: Mass

Figure credit: Abbott+, PRX **13**, 011048 (2023).

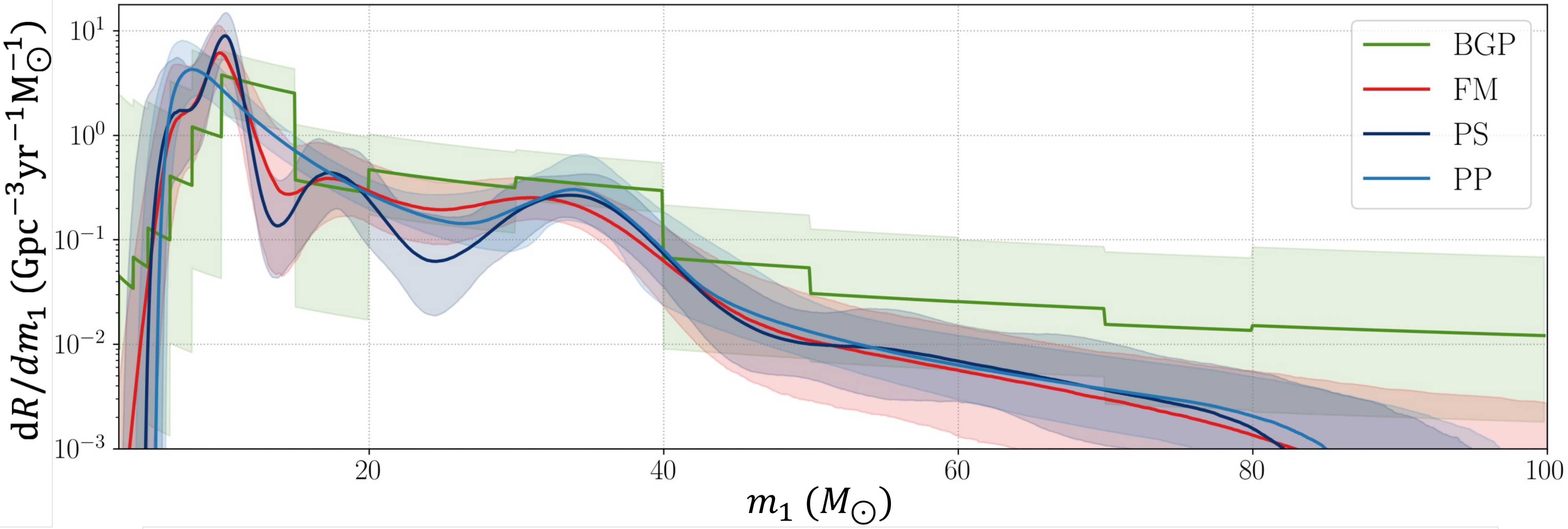

Figure: Differential merger rate, $\mathrm{d}R/dm_1$, from various distribution models

- Local maxima at $m_1 \sim 10M_\odot$ and $m_1 \sim 35M_\odot$ (> 99% credibility)
- A few massive BBHs e.g. GW190521 ($m_1 = 85^{+21}_{-14}M_\odot, m_2 = 66^{+17}_{-18}M_\odot$)
  → Inconclusive evidence for pair-instability mass gap ($65 - 120M_\odot$).

BBH distribution: Spin

Image credit: Abbott+, PRX **13**, 011048 (2023).

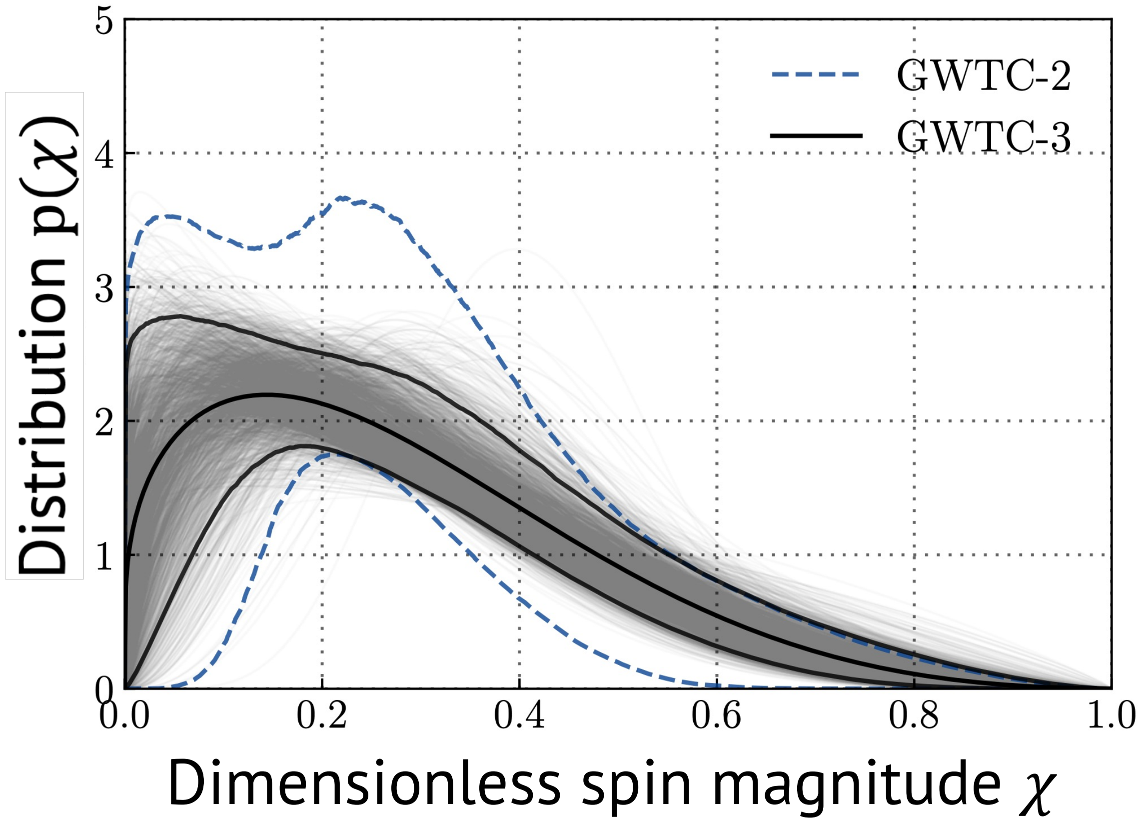

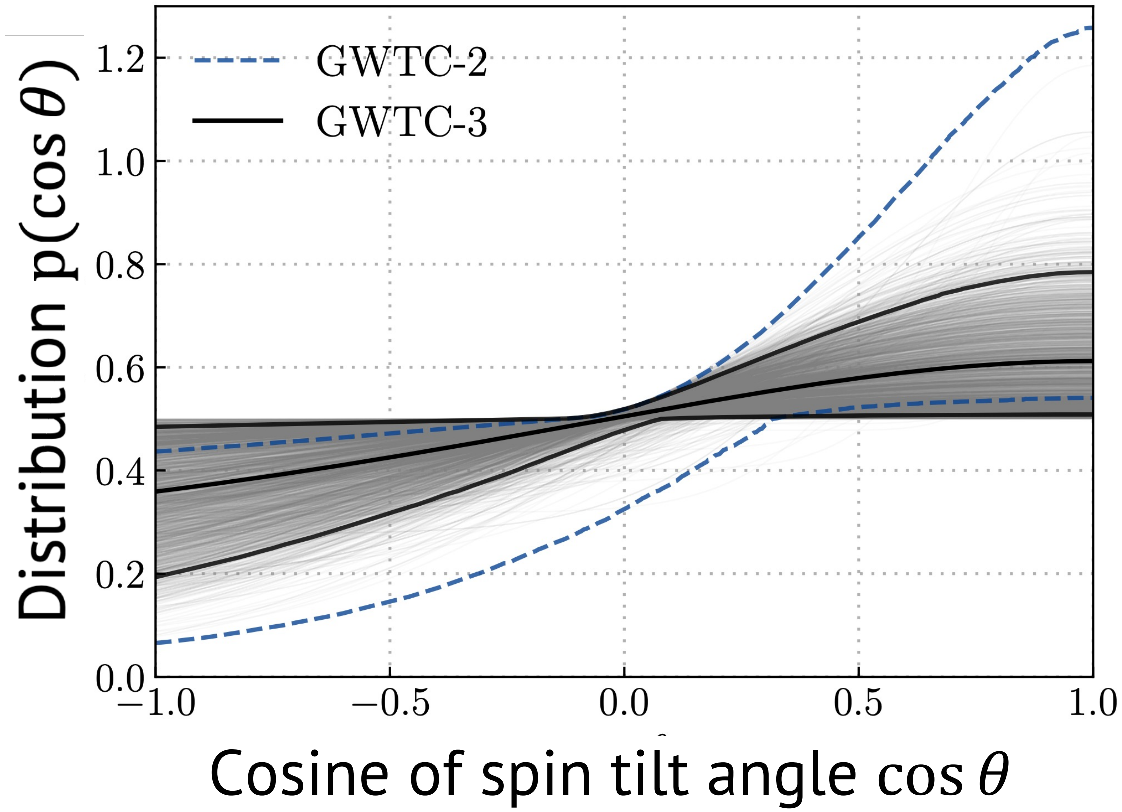

- Spin magnitude generally small ($\chi \lesssim 0.4$), but not-vanishing.
- Tilt angle has broad distribution, but $\cos\theta = 1$ preferred (But see Roulet+ 2021 about model dependence).

BBH distribution: Redshift

- Signal amplitude + masses
  → Luminosity distance
  → Redshift z

- Merger rate $\propto (1+z)^\kappa$, with $\kappa = 2.9^{+1.7}_{-1.8}$ (90% CI).

- Merger rate increases with redshift (at 99.6%).

- No evidence that mass distribution varies with redshift.

Image credit: Abbott+, PRX **13**, 011048 (2023).

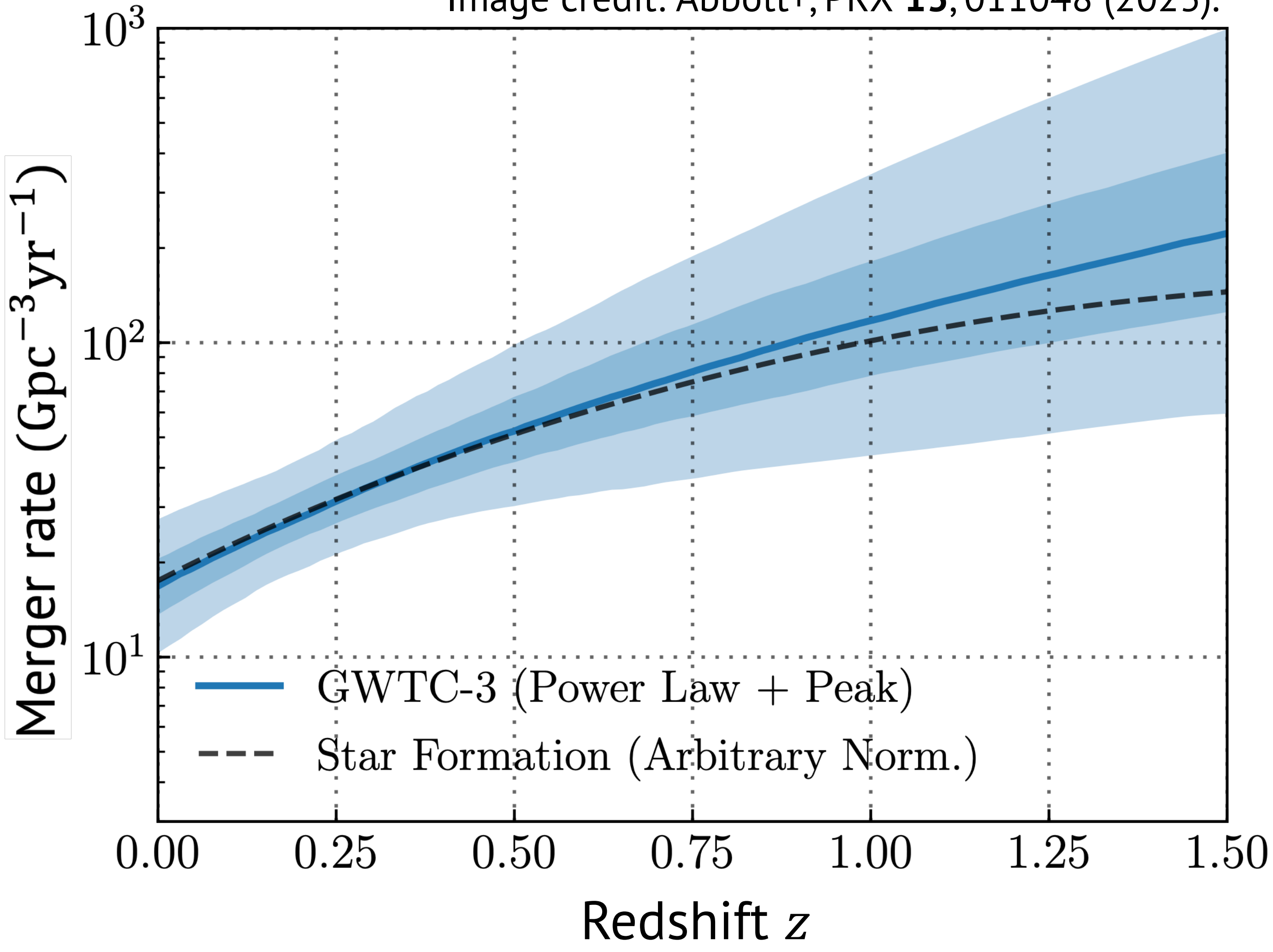

Figure: Redshift evolution of merger rate

Event rate

BNS:

$10\ \mathrm{Gpc^{-3}yr^{-1}}$ - $1700\ \mathrm{Gpc^{-3}yr^{-1}}$

NSBH:

$7.8\ \mathrm{Gpc^{-3}yr^{-1}} - 140\ \mathrm{Gpc^{-3}yr^{-1}}$

BBH (at $z = 0.2$):

$17.9\ \mathrm{Gpc^{-3}yr^{-1}}$ - $44\ \mathrm{Gpc^{-3}yr^{-1}}$

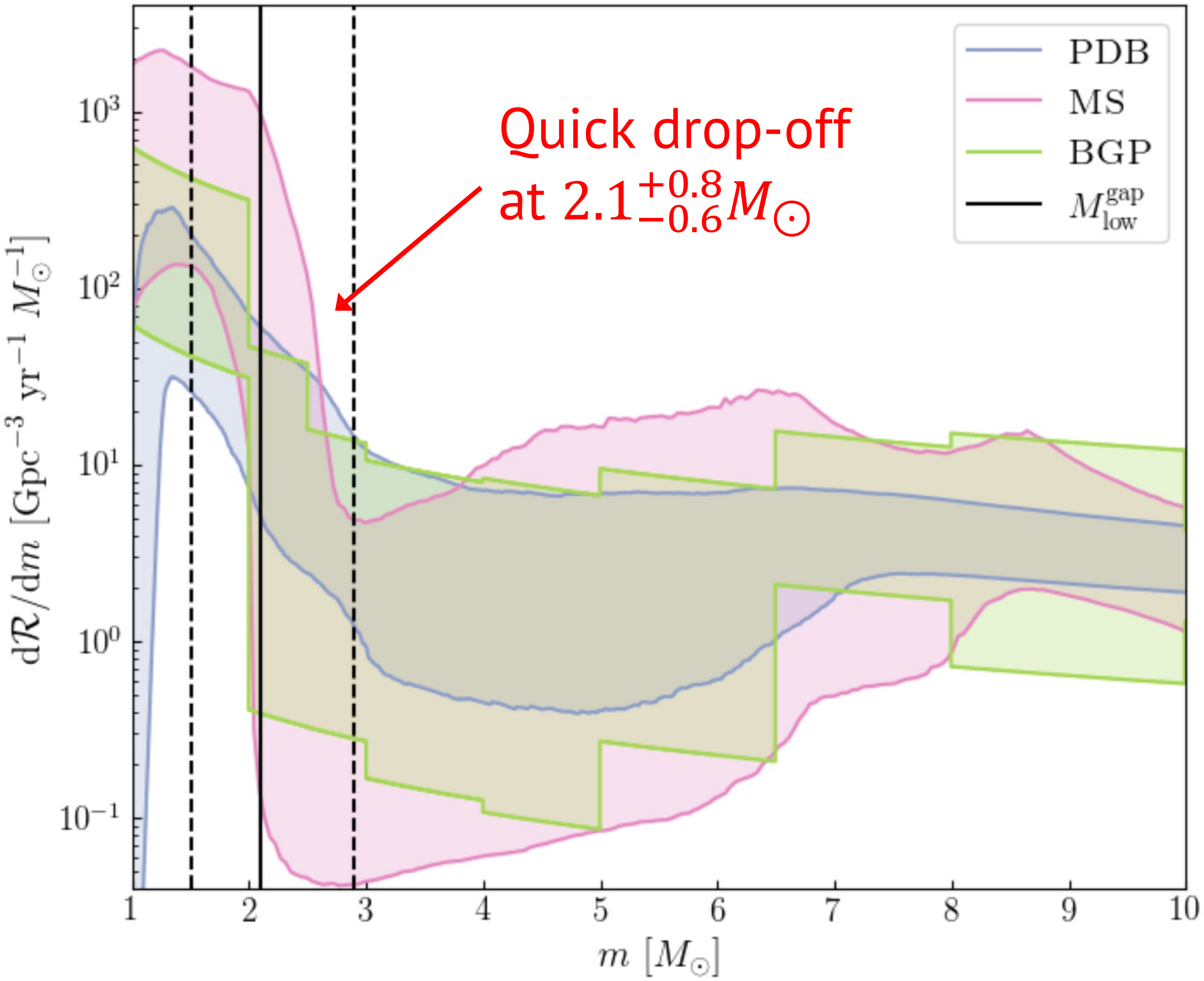

Figure: Differential merger rate as a function of component mass

GW170817: The first observed GWs from BNS

- Hubble constant measurement

$$cz = H_0 D_L$$

EM obs. GW obs.

$$H_0 = 70.0^{+12.0}_{-8.0}\ \mathrm{km\ s^{-1}\ Mpc^{-1}}$$
$$(68.3\%,\ 1\sigma)$$

- sGRB observed ~1.7s after GWs

→ Speed of GWs Abbott+ ApJL **848** L13 2017

$$\left|\frac{v_{\mathrm{GW}} - v_{\mathrm{EM}}}{v_{\mathrm{EM}}}\right| \leq O(10^{-15})$$

Figure credit: Abbott+, Nature **551**, 85 (2017).

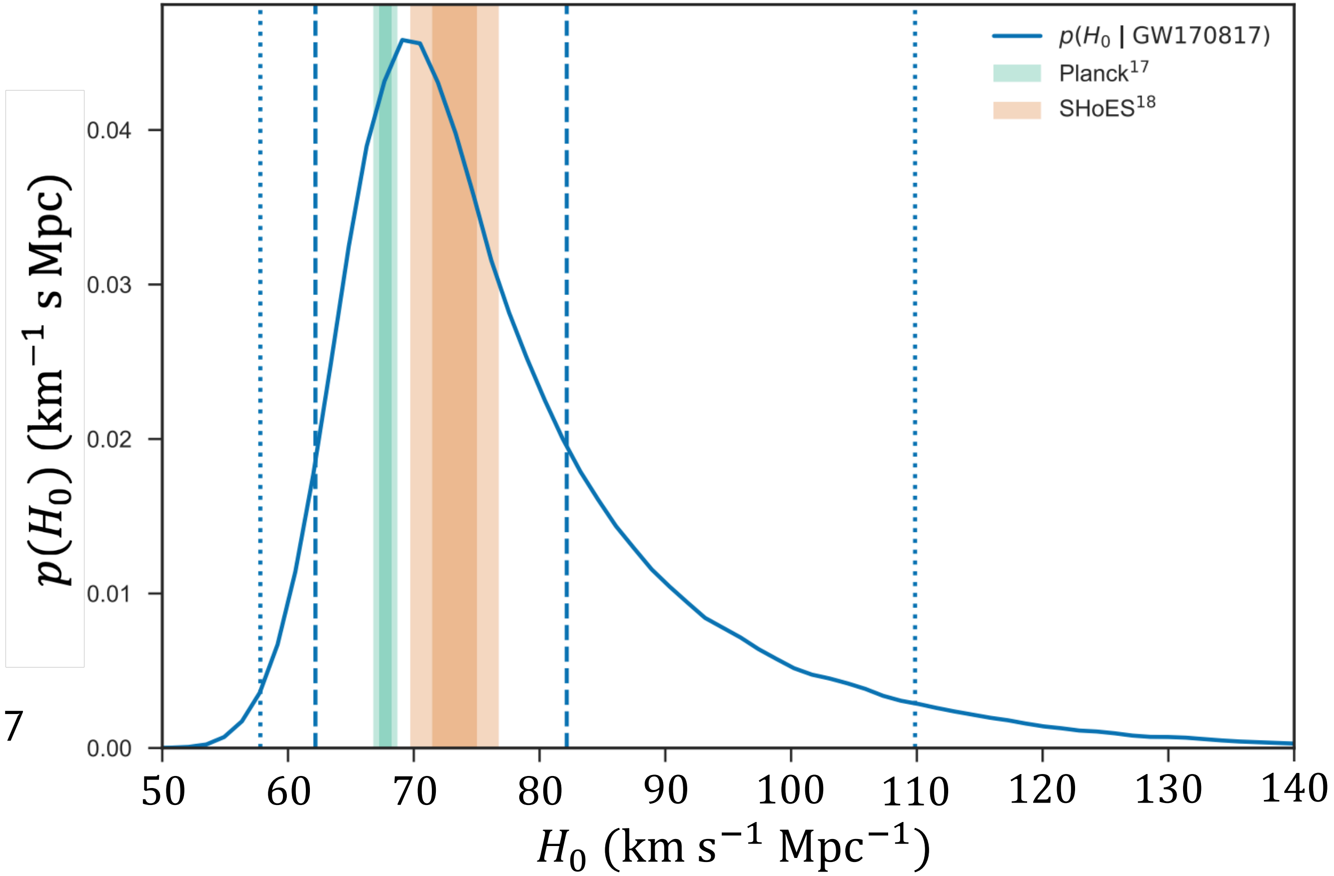

Figure: H_0 estimated with the joint observation of GW170817 and its electromagnetic counterpart

GW170817: The first observed GWs from BNS

Reference:
Abbott+, PRX **9**, 011001 (2019).

Constraints on tidal deformability from GWs

→ Constraints on the equation of state: $p = p(\rho)$.

→ Constraints on the radii:

$R_1 = 11.9^{+1.4}_{-1.4}$ km, $R_2 = 11.9^{+1.4}_{-1.4}$ km. (90% CL)

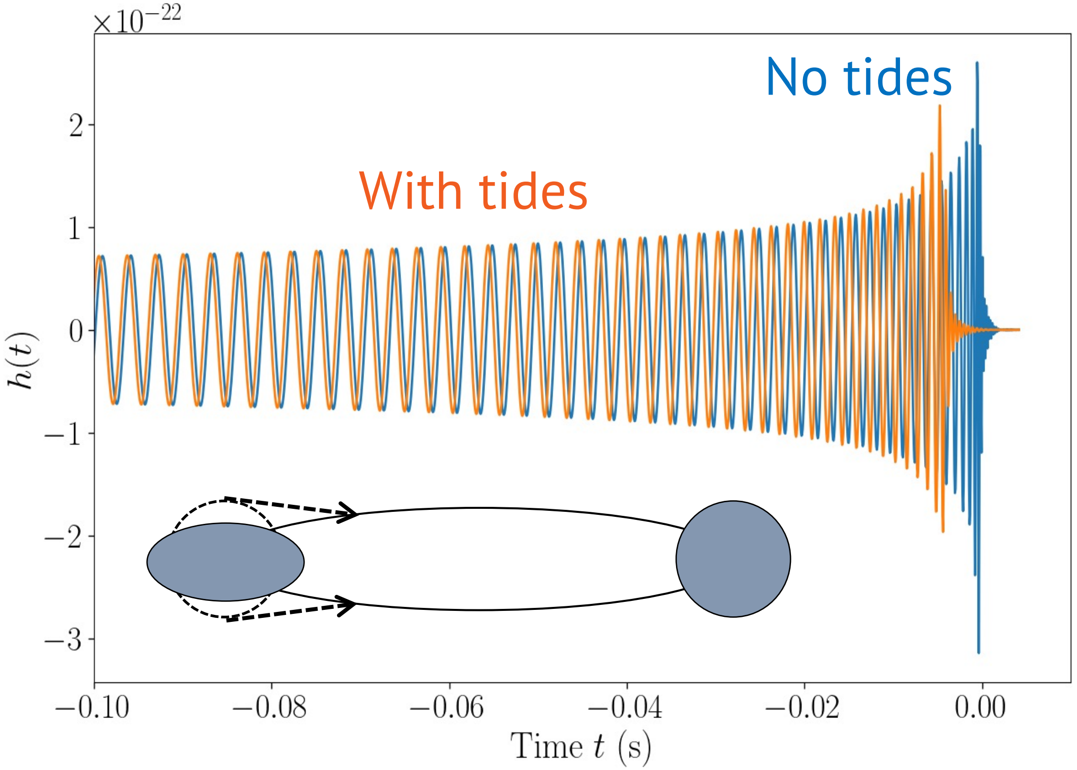

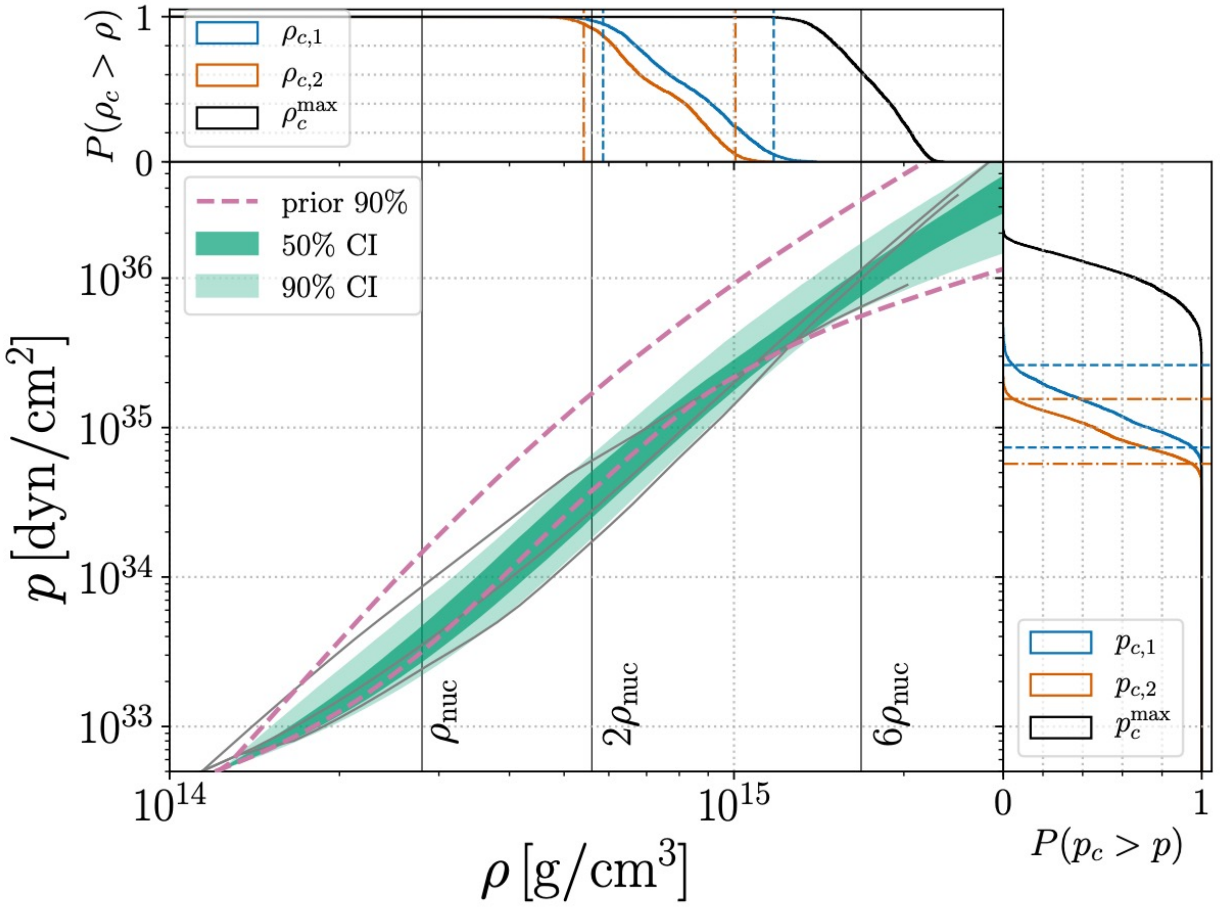

Figure: Recovered nuclear equation of state from GW170817

Discovery paper

THE ASTROPHYSICAL JOURNAL LETTERS, 915:L5 (24pp), 2021 July 1 https://doi.org/10.3847/2041-8213/ac082e

Observation of Gravitational Waves from Two Neutron Star–Black Hole Coalescences

Abstract

We report the observation of gravitational waves from two compact binary coalescences in LIGO's and Virgo's third observing run with properties consistent with neutron star–black hole (NSBH) binaries. The two events are named GW200105_162426 and GW200115_042309, abbreviated as GW200105 and GW200115; the first was observed by LIGO Livingston and Virgo and the second by all three LIGO–Virgo detectors. The source of GW200105 has component masses $8.9^{+1.2}_{-1.5}$ and $1.9^{+0.3}_{-0.2}\,M_\odot$, whereas the source of GW200115 has component masses $5.7^{+1.8}_{-2.1}$ and $1.5^{+0.7}_{-0.3}\,M_\odot$ (all measurements quoted at the 90% credible level). The probability that the secondary's mass is below the maximal mass of a neutron star is 89%–96% and 87%–98%, respectively, for GW200105 and GW200115, with the ranges arising from different astrophysical assumptions. The source luminosity distances are 280^{+110}_{-110} and 300^{+150}_{-100} Mpc, respectively. The magnitude of the primary spin of GW200105 is less than 0.23 at the 90% credible level, and its orientation is unconstrained. For GW200115, the primary spin has a negative spin projection onto the orbital angular momentum at 88% probability. We are unable to constrain the spin or tidal deformation of the secondary component for either event. We infer an NSBH merger rate density of 45^{+75}_{-33} Gpc^{-3} yr^{-1} when assuming that GW200105 and GW200115 are representative of the NSBH population or 130^{+112}_{-69} Gpc^{-3} yr^{-1} under the assumption of a broader distribution of component masses.

R. Abbott et al., 2021 ApJL **915** L5, arXiv: 2106.15163.

Detector network

- Detector ranges
  LIGO-Hanford: ~120 Mpc
  LIGO-Livingston: ~130-140 Mpc
  Virgo: ~50 Mpc

- LIGO-Hanford was not operating at the time of GW200105.

- Noise excess at ~20 Hz in Livingston for GW200115
  → exclude data below 25Hz in parameter estimation

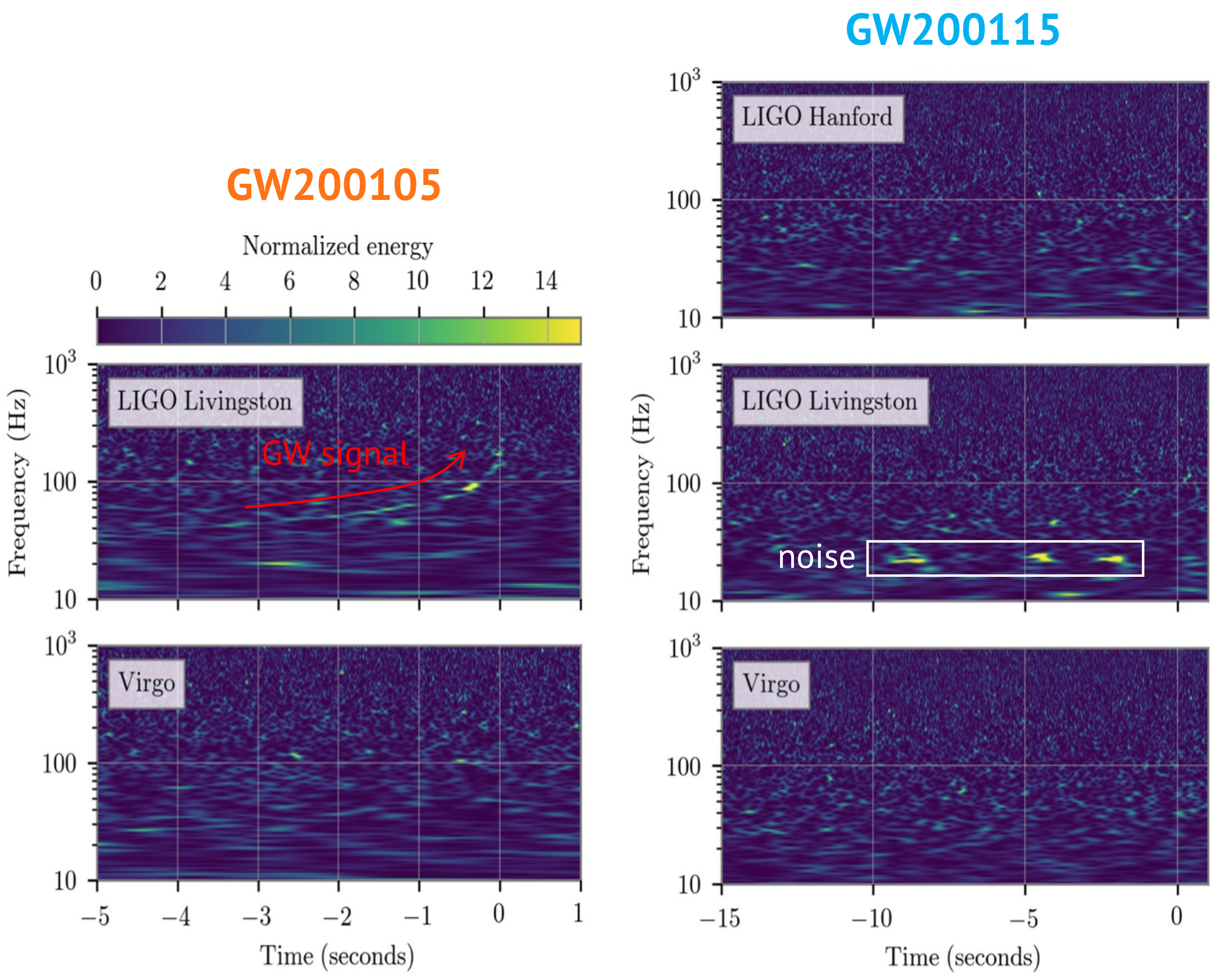

Time-frequency maps of data containing GW200105 (left) and GW200115 (right)

Detection summary

Event	GW200105	GW200115
Signal-to-Noise Ratio (H, L, V)	N/A, 13.6, 2.7 (Livingston-only)	6.9, 8.6, 2.9 (HL coincidence)
False Alarm Rate	low latency: 1/(15 days) offline: 1/(2.8 yr)	low latency: 1/(1513 yr) offline: From 1/(182 yr) to < 1/(10^5 yr)
GCN Notice Latency	More than 1 day	After 6 mins
Sky localization	7700 deg^2 (low latency) 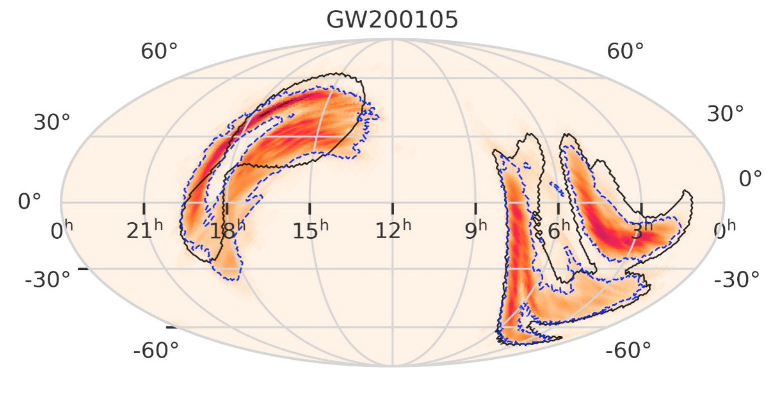 	900 deg^2 (low latency) 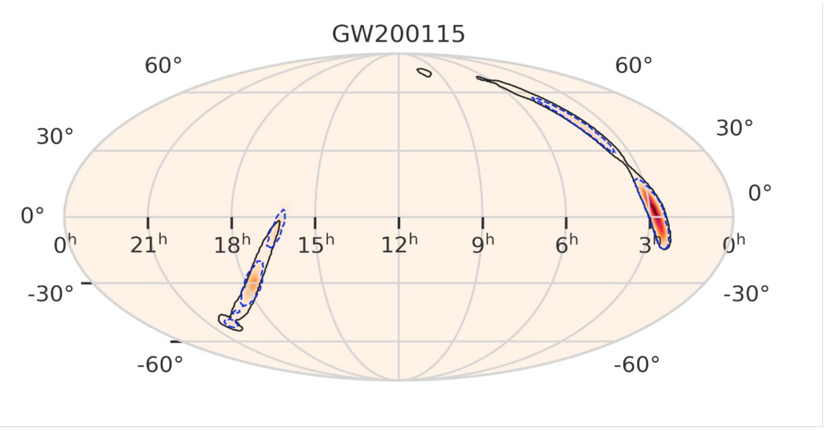
Distance	~265 Mpc (low latency)	~330 Mpc (low latency)
# Follow-up GCNs	21 (**No EM/neutrino counterparts**, e.g. [1])	31 (**No EM/neutrino counterparts**)

[1] S. Anand et al., Nature Astron. **5**, 46 (2021).

GW200105 & GW200115 R. Abbott et al., Astrophys. J. Lett. **915**, no.1, L5 (2021).

GW200105

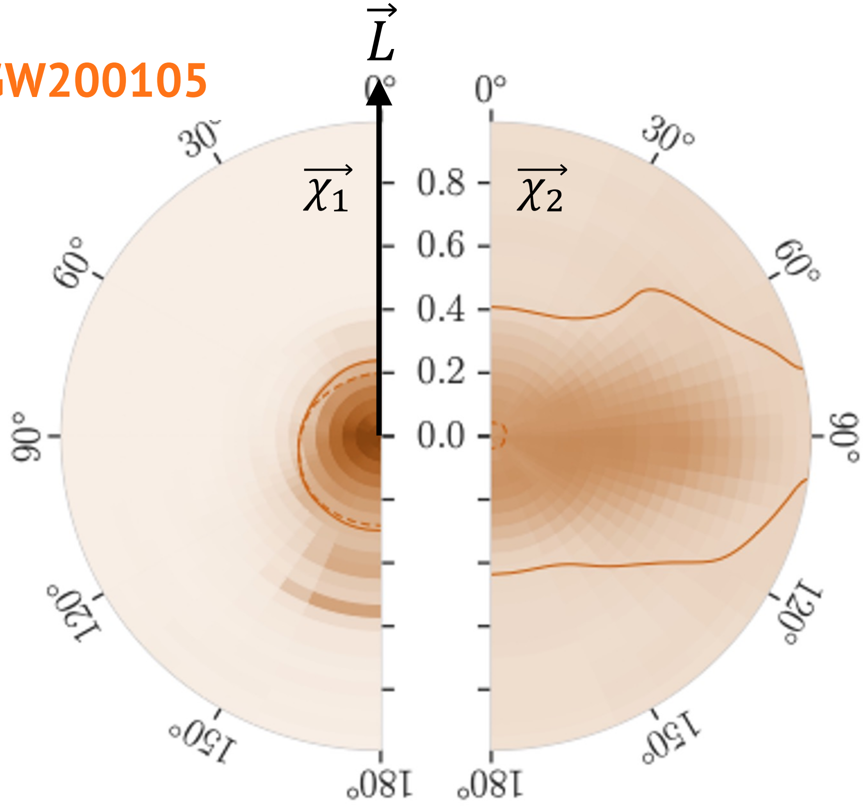

GW200115

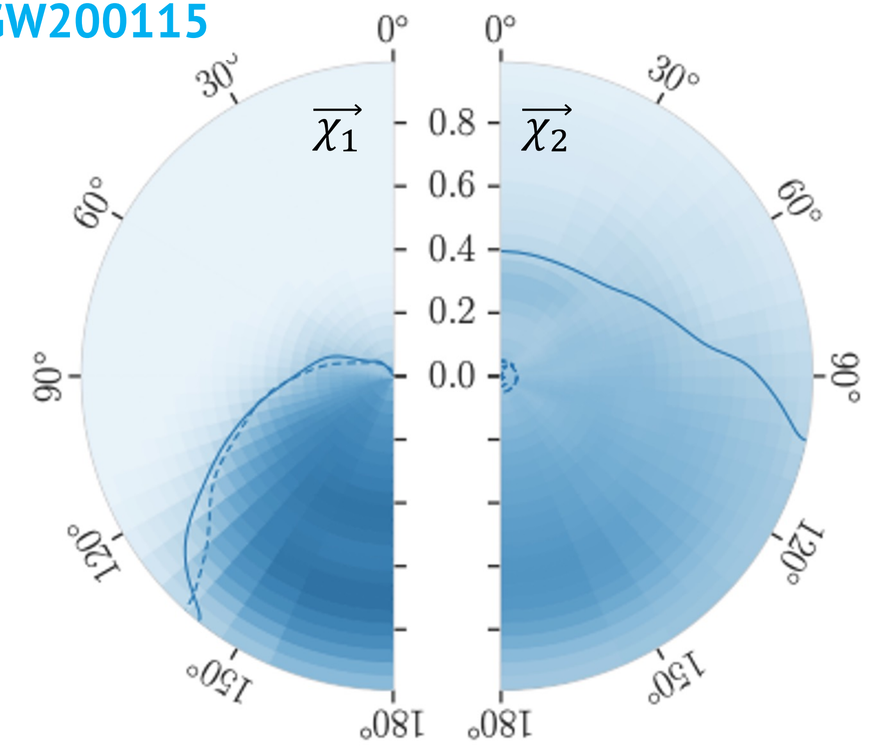

	GW200105	GW200115
$\vec{\chi}_1$	$\lvert\vec{\chi}_1\rvert < 0.23$ (90% confidence)	$\chi_{1,\parallel} = -0.19^{+0.24}_{-0.50}$ $P(\chi_{1,\parallel} < 0) = 88\%$
$\vec{\chi}_2$	Unconstrained	Unconstrained

Expected stochastic GW background

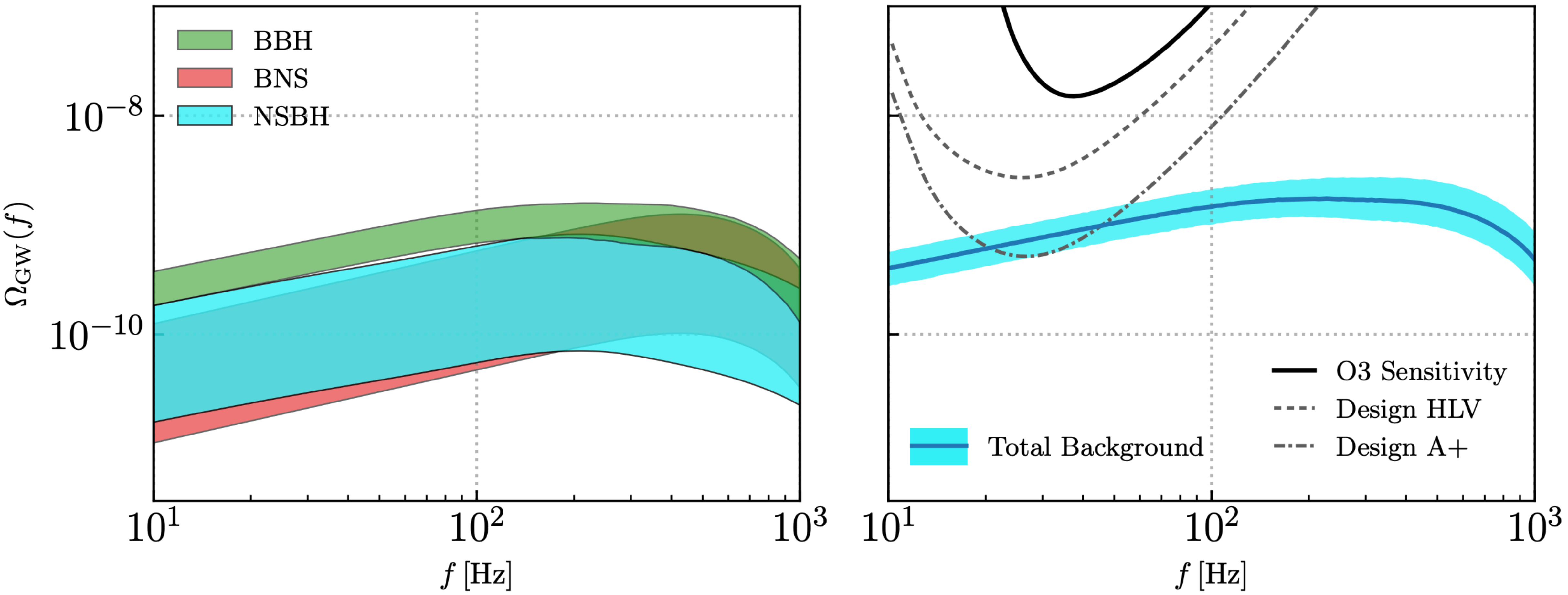

Figure: Expected stochastic gravitational-wave background (Taken from R. Abbott et al., arXiv: 2111.03634).

KAGRA in O3 and O4

Reference: Uchiyama-san's presentation at ASJ Spring Annual Meeting 2024

- KAGRA observations
  - O3: April 7 to 20 in 2020 with GEO600
  - O4: from May 24 to June 21 this year with LIGO (The first LIGO-KAGRA joint observation)
- Binary neutron star range: 0.66 Mpc (O3GK) → 1.3 Mpc (O4a)
- Duty cycle: 53% (O3GK) → 80% (O4a)

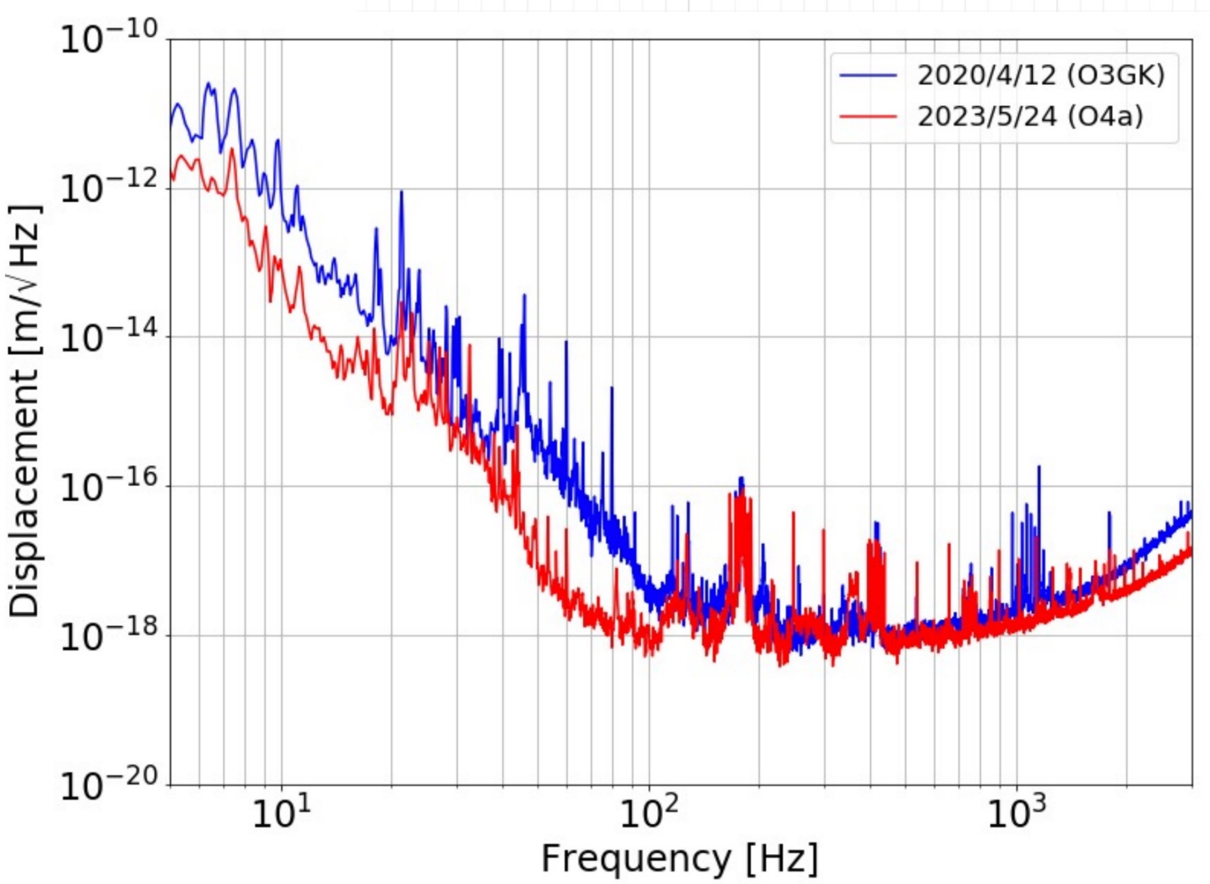

Figure: sensitivities in O3GK (blue) and O4a (red)

O3 GEO600-KAGRA

Reference:
R. Abbott et al., PTEP **2021**, 05A101 (2021).

- Joint observation of KAGRA and GEO600 from April 7 to 20 in 2020 (“O3GK”).

- Searches
  - All-sky CBC and burst searches
  - GRB-targeted searches

- No detections, but they demonstrate that analysis framework is ready.

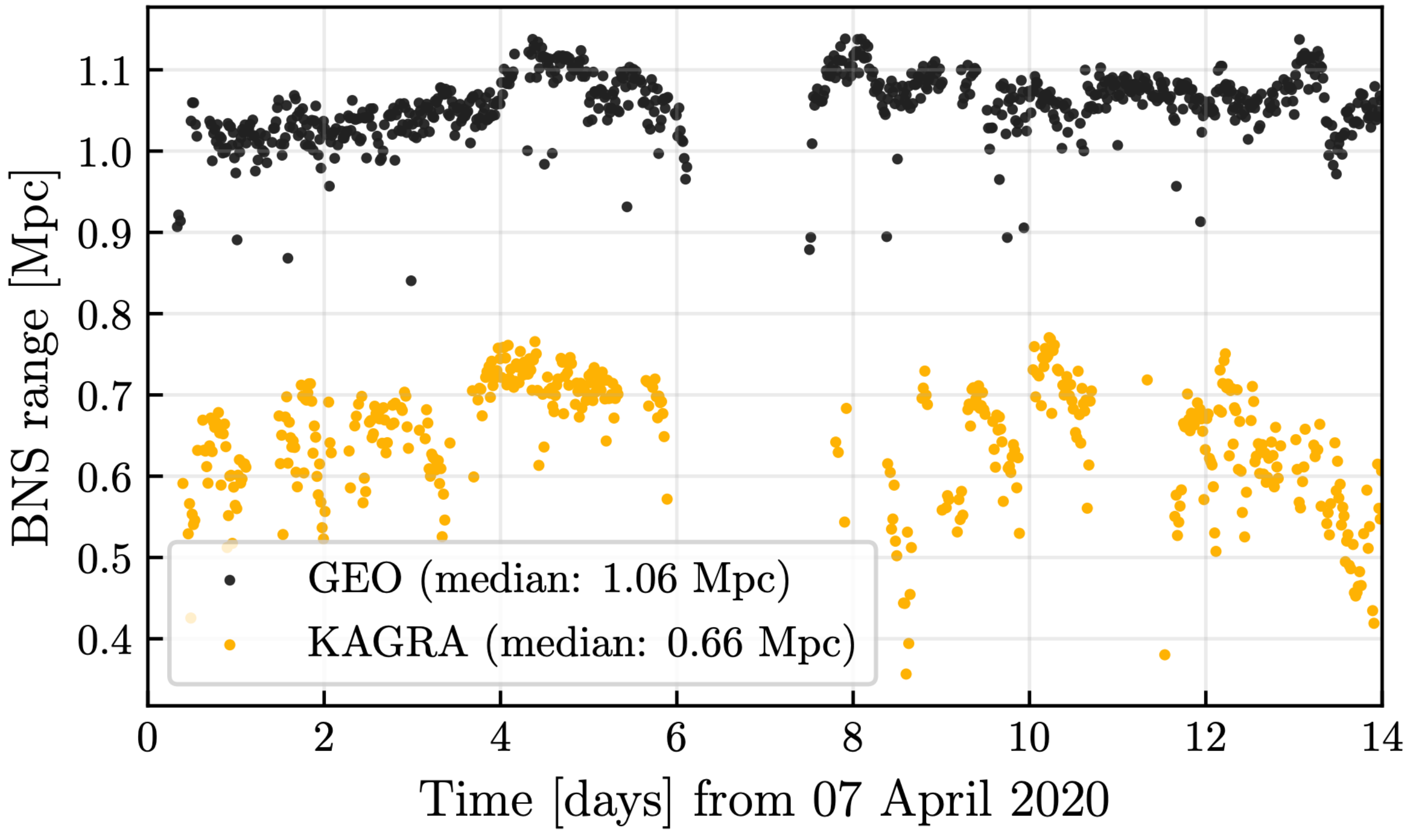

Figure: Binary neutron star range of GEO and KAGRA in O3GK

O3GK results

GRB Name	Data Source	Type	Analysis
200412A	*Fermi*-GBM	Long	`X-Pipeline`
200415A	*Fermi*-GBM, IPN	Short	`X-Pipeline` & `PyGRB`
200418A	*Fermi*-GBM	Long	`X-Pipeline`
200420A	*Fermi*-GBM	Short	`X-Pipeline` & `PyGRB`

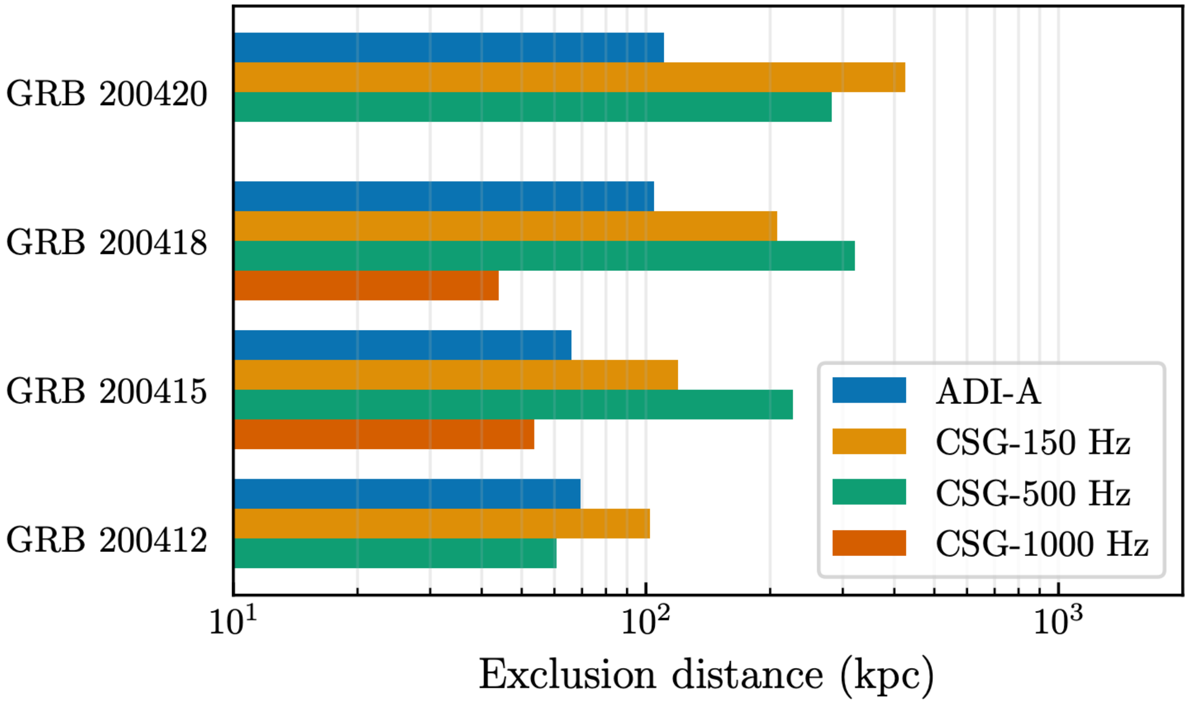

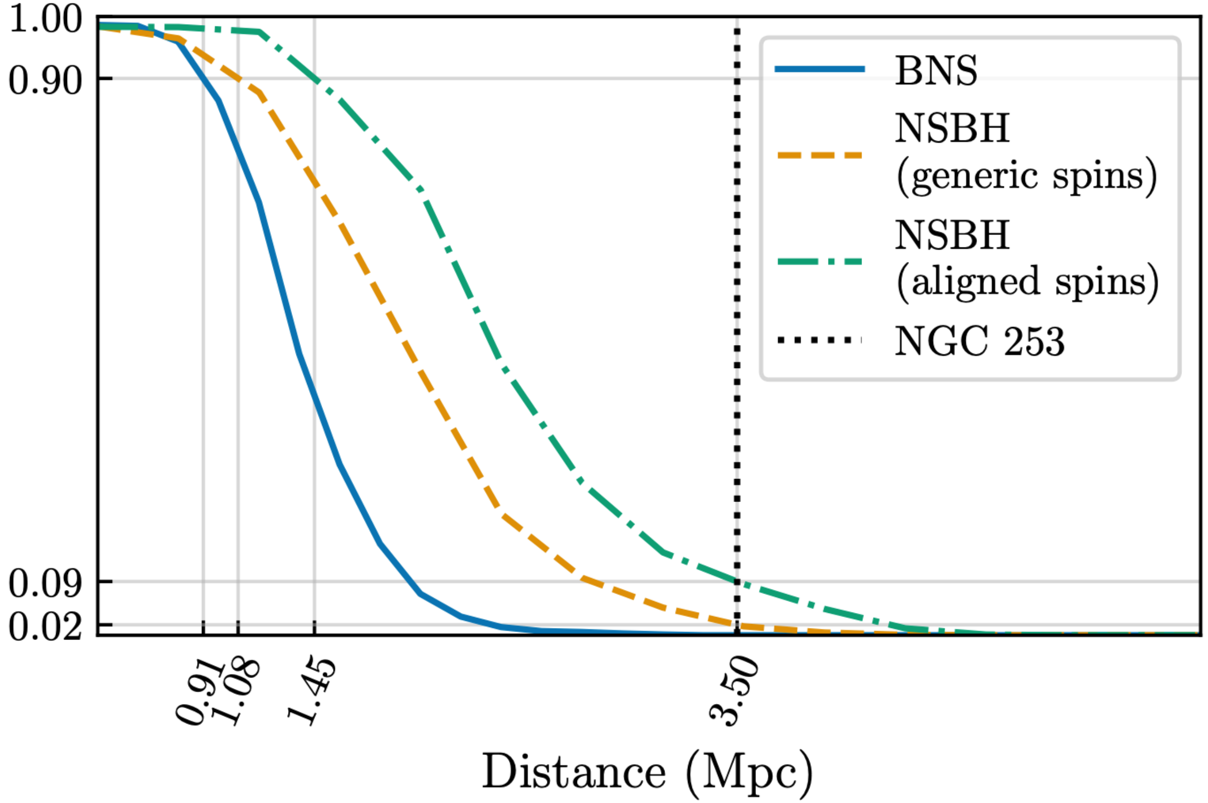

Figure: Exclusion distance for GRB200415A

Other types of signal: Null results

See LVK publications:
https://pnp.ligo.org/ppcomm/Papers.html

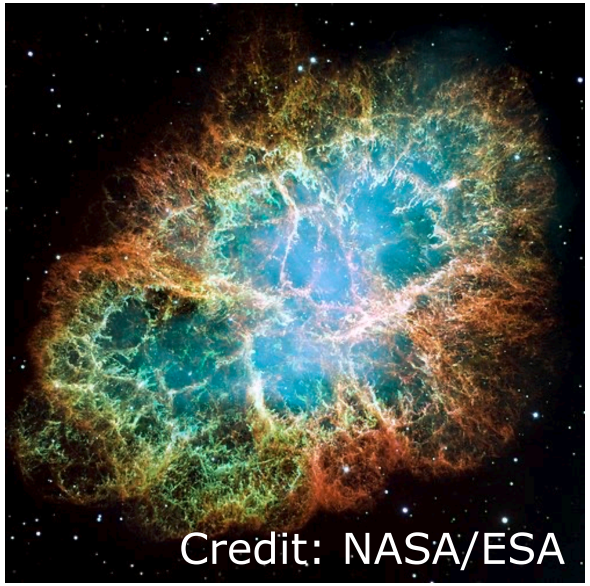

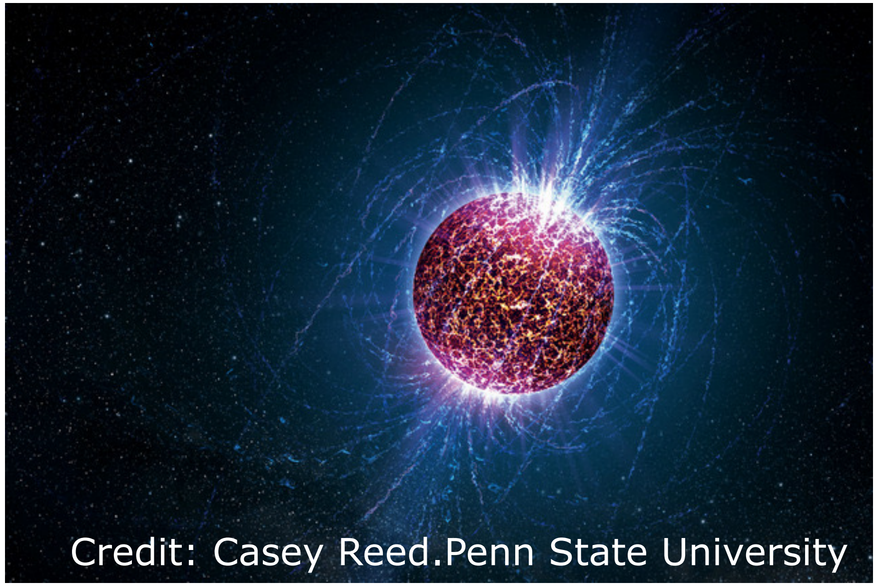

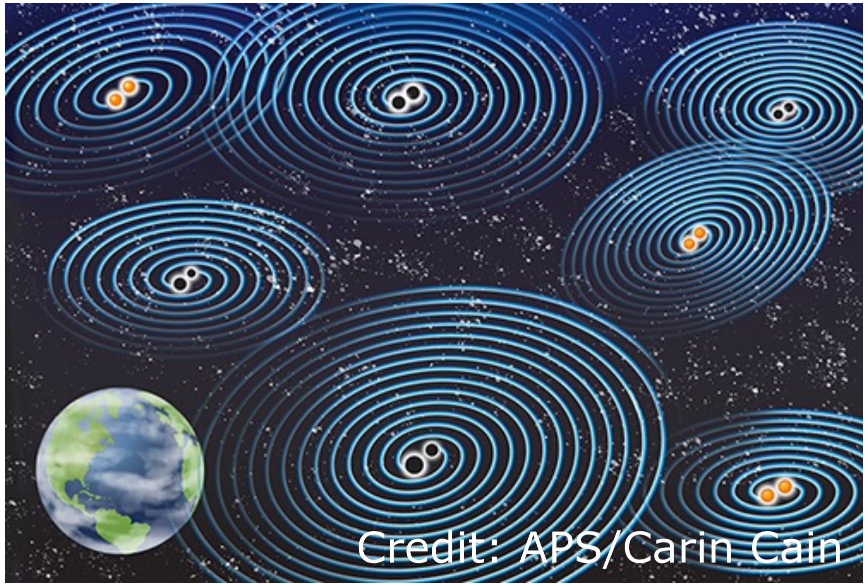

Unmodeled burst

- Short (<1s) (supernova, Pulsar glitch etc.)
- Long (>1s) (eccentric BBH etc.)

Continuous waves

- Rotating NS (Targeted, All-sky)
- Ultralight bosons (Direct coupling with mirrors, superradiance)

Stochastic backgrounds

- Superposition of CBCs
- Cosmic strings
- Anisotropic backgrounds

Others

Pulsar timing array

- Multiple pulsar timing array collaborations found evidence for a stochastic GW background in $1\ \mathrm{nHz} \lesssim f \lesssim 100\ \mathrm{nHz}$.

<u>References</u>
NANOGrav: Agazie+ ApJL **915**, L8 (2023).
EPTA + InPTA: Antoniadis+ A&A **678**, A50 (2023).
PPTA: Reardon+ ApJL **951**, L6 (2023).
CPTA: Xu+ RAA **23**, 075024 (2023).

- NANOGrav reports evidence with $p = 10^{-3}$ ($\simeq 3\sigma$) with a Bayesian search method.

Pulsar timing array

- (Power spectral density) $\propto f^{-\gamma}$, consistent with $\gamma = 13/3$ predicted by supermassive binary black holes evolving with GW emission.

- The observed correlation of timing residuals between pulsars is consistent with expectation from isotropic GW background ("Hellings-Downs curve").

Image credit: Agazie+ ApJL **915**, L8 (2023).

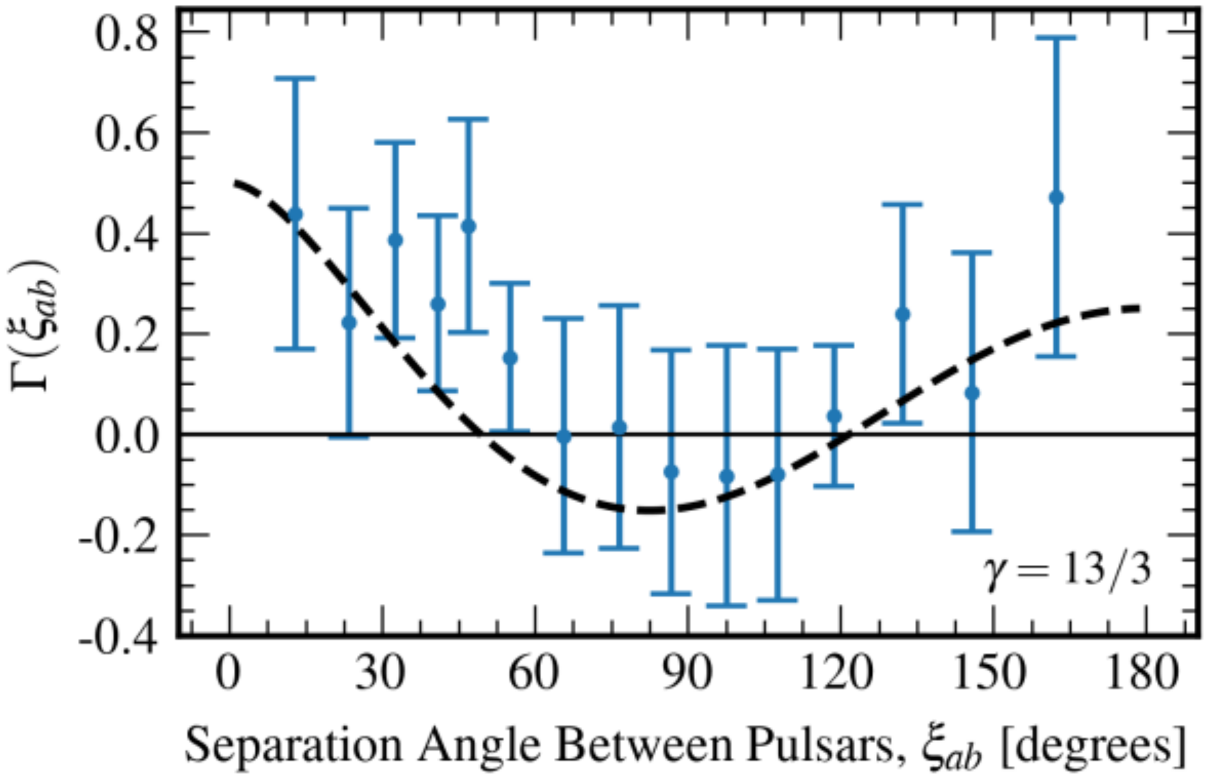

Figure: Observed correlation between pulsars (blue bars) and expectation from isotropic GW background (black dashed)

04 status

Online searches

- CBC search pipelines
  - GstLAL
  - MBTA
  - PyCBC Live
  - SPIIR

- Unmodeled burst search pipelines
  - cWB
  - oLIB

- See [LIGO/Virgo/KAGRA Public Alerts User Guide]() and references there for their details.

Credit: Ryan Magee

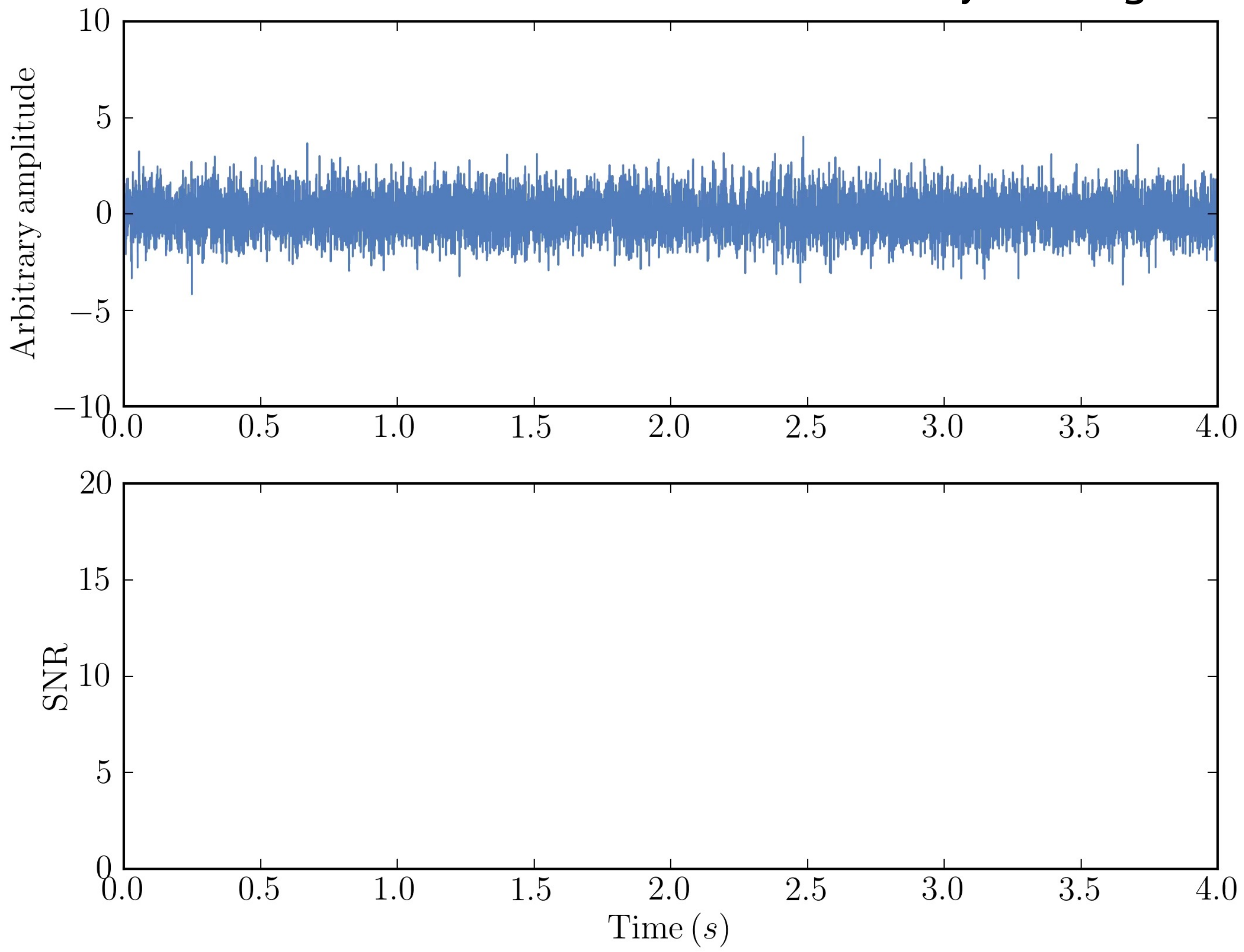

Figure: Matched filtering for modeled CBC search

Significance is quantified by False Alarm Rate (FAR). Lower FAR ⟷ Higher significance.

O4 event candidates

Event candidates with $\mathrm{FAR} < 2/\mathrm{day}$ are public at GraceDB. (Expected noise rate: 14/day)

CBCs with $\mathbf{FAR} < \mathbf{1/(5\ months)}$ and **bursts with $\mathbf{FAR} < \mathbf{1/(4\ years)}$** are considered **significant** and followed up by human vetting and detailed parameter estimation. (Expected noise rate: 1/month and 1/year respectively)

68 significant CBC candidates (66 BBHs, 2 can contain NS) as of Nov. 22.

O4 Significant Detection Candidates: **68** (79 Total - 11 Retracted)

O4 Low Significance Detection Candidates: **1376** (Total)

Show All Public Events

Page 1 of 6. next last »

SORT: EVENT ID (A-Z)

Event ID	Possible Source (Probability)	Significant	UTC	GCN
S231119u	BBH (95%), Terrestrial (5%)	Yes	Nov. 19, 2023 07:52:48 UTC	GCN Circular Query Notices | VOE
S231118an	BBH (74%), Terrestrial (24%), NSBH (1%)	Yes	Nov. 18, 2023 09:06:02 UTC	GCN Circular Query Notices | VOE
S231118ab	BBH (99%), Terrestrial (1%)	Yes	Nov. 18, 2023 07:14:02 UTC	GCN Circular Query Notices | VOE

Figure: Public Alerts at GraceDB (https://gracedb.ligo.org/)

Low-latency alert system in O4

- Alerts are automatically sent with latencies $\lesssim 30$ s.
- We also send alerts even before coalescence for loud BNS signals ("Early Warnings").
- See Sharma-Chaudhary & Toivonen et al., arXiv: 2308.04545 for more details.

Table: Latencies from mock data challenge (MDC)

Latency Measure	Description	50% (s)	90% (s)
Superevents	$t_{\text{superevent}} - t_0$	9.4	18.1
CBC Events	$t_{\text{event}} - t_0$	12.3	41.4
Burst Events	$t_{\text{event}} - t_0$	72.3	671.3
Early Warning Events	$t_{\text{event}} - t_0$	−3.1	2.9
GW Advocate Request	$t_{\text{ADV\_REQ}} - t_0$	12.7	40.1
GCN Preliminary Sent	$t_{\text{GCN\_PRELIM}} - t_0$	29.5	171.4
Coincidence with GRB Found	$t_{\text{EM\_COINC}} - t_0$	32.9	44.4
RAVEN Alert Triggered	$t_{\text{RAVEN\_ALERT}} - t_0$	35.3	48.4

Public data products: Coase-grained mass-spin information

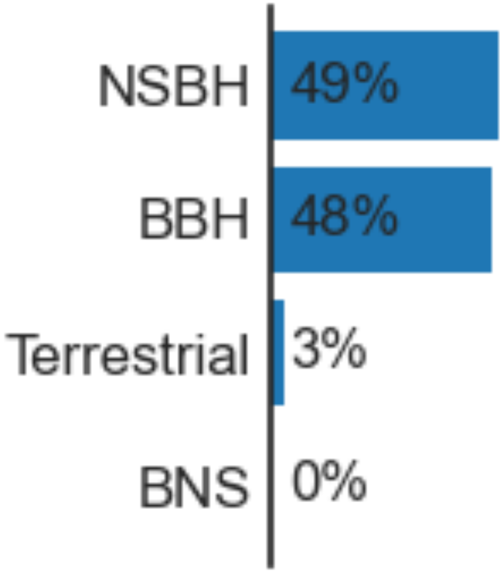

Figure: source classification

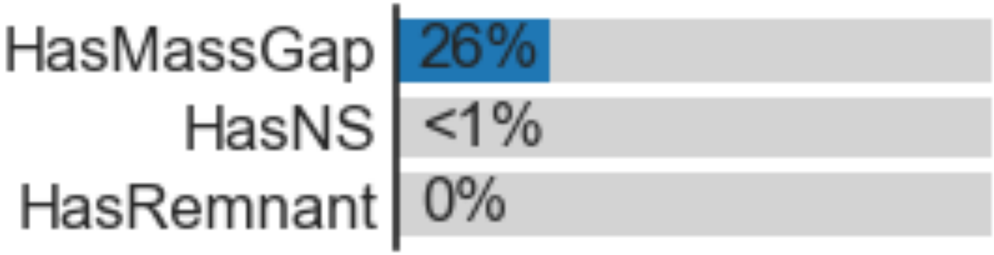

Figure: EM-Bright classification

Source classification based on masses, expected astrophysical event rate and FAR.

- **BH** = object with $m > 3M_{\odot}$
- **NS** = object with $m < 3M_{\odot}$
- **Terrestrial** = instrumental noise

EM-Bright probs based on masses and spins.

- **HasRemnant**: The prob. of source forming a nonzero mass outside the remnant BH.
- **HasMassGap**: The prob. of one of the colliding objects is in the mass gap between $3M_{\odot}$ and $5M_{\odot}$

Coincidence with External Triggers

- RAVEN (Urban 2016): temporal (and spatial) coincidence between LVK GW and **gamma-ray bursts/galactic supernova alerts from SNEWS**.

- LLAMA (Bartos+ 2019, Countryman+ 2019): coincidence between LVK GW and **IceCube High Energy Neutrino**.

Table: Time window employed by RAVEN

Event type	Time window (s)
GRB (*Fermi, Swift, INTEGRAL, AGILE*)	[-1, 5] (CBC), [-60, 600] (Burst)
SubGRB (*Fermi*)	[-1, 11]
SubGRBTargeted (*Fermi*)	[-1, 11]
SubGRBTargeted (*Swift*)	[-10, 20]
Low-energy Neutrinos (*SNEWS*)	[-10, 10]